RESILIENT MODULI OF FLEXIBLE PAVEMENT MATERIALS

RESILIENT MODULI OF FLEXIBLE PAVEMENT MATERIALS

by

ANDREW Y.-K.M. LAM, B.Sc.

A Thesis

Submitted to the Faculty of Graduate Studies

in Partial Fulfilment of the Requirements

for the Degree

Master of Engineering

McMaster University
Hamilton, Ontario
Canada

April, 1982

MASTER OF ENGINEERING (1982)
(Civil Engineering)

McMASTER UNIVERSITY
Hamilton, Ontario

TITLE: RESILIENT MODULI OF FLEXIBLE PAVEMENT MATERIALS

AUTHOR: Andrew Y. - K.M. Lam, B.Sc.
(National Cheng-Kung University)

SUPERVISOR: Dr. John J. Emery

NUMBER OF PAGES: (xii), 132

ABSTRACT

The behaviour of asphaltic concrete, granular base and subbase materials, and subgrade soils in repeated dynamic loading is best represented by their resilient moduli in rational flexible pavement designs. The recoverable, or resilient, strains in pavement structures due to repetitions of moving traffic loads can be predicted through the use of appropriate material parameters in analytical or numerical models of pavement response. It appears that the repeated-load triaxial test offers the most promising means of applying simulated field loading conditions to representative samples of flexible pavement components. This testing of laboratory or field prepared samples provides a good estimate of the material's overall dynamic behaviour and the desired resilient modulus and Poisson's ratio for design analyses. The purpose of this research was to simulate field loading conditions for a range of typical Southern Ontario granular base and subbase materials by means of repeated-load, variable and constant confining pressure, triaxial tests using laboratory research equipment readily adaptable to regular design use. The pavement materials were characterized in a condition corresponding to optimum density and moisture content with repeated loadings representative of field stress conditions of 0.1 second pulse duration at a frequency of 20 cycles per minute. In addition to determining the resilient modulus and Poisson's ratio for four basic conditions - unsaturated drained, unsaturated undrained, partially saturated drained, partially saturated undrained - the results were examined for

significant trends. The characterization of typical base, subbase and subgrade materials for Southern Ontario, coupled with previous work on asphaltic concrete, allows the use of representative moduli for all flexible pavement components in Ontario pavement design systems such as OPAC.

ACKNOWLEDGEMENTS

I wish to thank my advisor Dr. John J. Emery for his insight and encouragement during the course of this research. I am especially grateful for his critical reading of the manuscript.

I also want to thank Mr. Michael A. Lee (Research Engineer) for his useful discussions and assistance; Mr. W. Sherriff and Mr. R. Winterle for their help in the construction of the equipment; and Mrs. M. Lupton for typing the thesis.

I wish to acknowledge the financial and technical support provided by the Ontario Ministry of Transportation and Communications during this study. The technical input by Mr. W. A. Phang of the Ministry was particularly helpful.

Finally, a special thank you to my family for their encouragement and support throughout my education at McMaster University.

TABLE OF CONTENTS

LIST OF TABLES

LIST OF FIGURES

TABLE OF CONTENTS - Cont'd

LIST OF FIGURES- Cont'd

TABLE OF CONTENTS - Cont'd

LIST OF FIGURES- Cont'd

TABLE OF CONTENTS - Cont'd

LIST OF FIGURES - Cont'd

LIST OF FIGURES - Cont'd

CHAPTER 1

INTRODUCTION

1.1 PURPOSE AND SCOPE

Traditionally, the design of flexible pavements has been based on experience and accumulated design performance information. These empirical and semi-empirical methods, commonly employed in current designs, have evolved through the statistical analysis of past and existing field data to the use of integrated serviceability-performance concepts. Designers adopted this approach since flexible pavement materials are inherently more complex and variable in engineering properties than concrete and steel. Pavement materials are generally nonlinear and time dependent at traffic applied stress levels, with behaviour dependant on factors such as temperature, nature and rate of loading, density, stress history, stress state, and degree of saturation. The performance of a pavement is greatly influenced by the applied traffic loadings and environmental effects which are also variable and difficult to determine. The design process is further complicated by the fact that user serviceability governs design rather than pavement structural failure. A user typically considers a pavement to be in a poor or failed condition long before the cumulative effects of traffic loading and environment lead to structural conditions requiring reconstruction.

Over the past two decades, there has been a move towards designing flexible pavements by the "rational" or "mechanistic" method. The idealized layered system model adopted to represent the flexible pavement structure is analyzed using numerical techniques (simplified closed form, finite difference, finite element, etc.) for strain, stress and fatigue at critical points within the pavement structure, for representative material properties, anticipated loadings, and environmental conditions [1-4]. This approach was developed since highway engineers have long recognized that traditional design methods are of limited use to incorporate new construction materials, changing traffic conditions (heavier truck loadings and changed axle configuration, for instance) and different environmental conditions. While the rational appraoch is both more realistic and has predictive capabilities, it does require improved characterization of flexible pavement component materials (asphaltic concrete, base, subbase and subgrade), typically as resilient moduli (resilient modulus M_R and resilient Poisson's ratio ν_R typically) as basic input parameters along with realistic load and environment conditions. Typical computerized approaches are based on elastic theory, even though in reality, pavement materials are typically nonlinear, temperature dependent in the case of asphaltic concrete, and highly dependent on the field environment. However, while simplified, the rational approach when coupled with the empirical methods and designer experience has led to much improved designs and a far better understanding of flexible pavement behaviour including key fatigue aspects. On a more practical note, it is very important that the materials characterization methods developed at a research level can ultimately be readily applied during regular pavement design activities. This issue of practicality has been an important consideration during the study reported herein.

This study is concerned primarily with the laboratory measurement of the resilient modulus (M_R), resilient Poisson's ratio (ν_R), and permeability coefficient (k) of granular aggregates typically used as flexible pavement base and subbase materials in Southern Ontario. Similar measurements for a range of subgrades typical to the area were also completed. Measurements of M_R and ν_R for asphaltic concretes have been completed in previous studies at McMaster University by Gonsalves (5) and Lee (6), sponsored by the Ontario Ministry of Transportation and Communications. The current study extends the work to include the important unbound layers and overall pavement structure.

The rational design process assumes that the granular base and subbase courses indefinitely maintain their original moduli. This holds reasonably well if the moisture conditions remain constant with time, but this is rarely the case given the variability of weather conditions typical to Ontario (from humid in August to deep winter frost penetration with severe spring thaw conditions).

A significant proportion of flexible pavements fail prematurely every year, especially during the spring thaw period, because of saturated base conditions. However, flexible pavements are generally designed under the assumption that the granular base and subbase courses (specified as less than 8 to 10% passing 75 μm) are permeable enough to provide adequate subsurface drainage during the wet seasons [7,8]. For granular aggregates not low in fines (less than about 5% passing 75 μm), this is not the case. Water can be trapped in the unbound granular layers if their permeability is too low, and this results in general "degrading" and a reduction in the layer's effective stiffness (M_R) under the repeated traffic loads. Selection of suitable base and subbase materials should be based on an engineering compromise (i.e., balance of costs and advantages) between permeability and stiffness, since higher permeabilities may be coupled with lower stiffnesses. Permeability coefficients have been measured during the resilient moduli characterization study to assess the typical range for materials commonly used in Southern Ontario.

The resilient moduli tests were completed in triaxial equipment designed to simulate loading stress conditions representative of those expected in the field. This also required the development of specimen preparation procedures. The anticipated stress levels were determined by using the Shell Bistro computer program [2] for typical Ontario pavements [9] under a standard 80 kN (18 kip) truck axle loadings.

Test specimen deformations in the triaxial cell under repeated axial and/or confining stresses were measured with non-contact eddy current probes which do not touch the specimen itself, but detect movements by differences in the magnetic field.

Permeability tests were conducted in specimens compacted in CBR (California Bearing Ratio) molds. The CBR molds were modified so that low gradient constant head permeability tests could be performed. These specimens were prepared under the same moisture and compactive energy conditions as for the M_R and ν_R test specimens. Detailed descriptions of the experimental apparatus for measuring M_R, ν_R and k are given in following chapters.

1.2 FLEXIBLE PAVEMENT DESIGN BY RATIONAL METHODS

Typical flexible pavements are layered structures comprised of an asphaltic concrete surface course overlying one or more layers of asphaltic concrete binder course and/or granular base and subbase layers (typically unbound), constructed over a prepared subgrade. The layered configuration is designed so as to "dissipate" the imposed truck loading surface stresses through the pavement layers to a much lower intensity that may be carried by the subgrade without permanent deformations.

The objective of any flexible pavement design procedure is to provide a layered pavement structure that will be suitable in a specific environment and be able to sustain the anticipated heavy traffic loadings (typically in some equivalent form) for a given design period. It is generally considered that flexible pavements and rigid pavements (not considered here) deteriorate or lose serviceability with time, and a well-designed pavement should maintain an acceptable user performance level for the design period at a minimum overall cost.

According to the serviceability concept developed by Carrey and Irick [10], pavements display certain distress modes that can be placed in three main categories: fracture; distortion; and disintegration. Disintegration refers to distress in the asphaltic concrete layers caused by factors such as low stability, loss of fines, poor asphalt cement-aggregate bonds, etc. The problem of disintegration will not be considered here since it is not part of the structural design, but rather a function of appropriate asphaltic concrete mix designs.

Fracture and distortion take the following forms:

1. Permanent deformations (distortion mode);
2. Load-induced fatigue cracking (fracture mode); and,
3. Thermal-induced cracking (fracture mode).

Permanent deformation is also a fatigue related distress mode which is caused by the accumulation of inelastic permanent deformations due to repeated wheel loadings. The loading repetitions to fracture and level of permanent deformation can usually be estimated as part of the design theory which is considered in the rational design process. During the design process, the pavement structure is analyzed and modified as necessary to ensure that the critical distress modes will either be precluded or their effects reduced to tolerable functional levels for the selected design period.

The road use is of course the ultimate judge of the designer's success, and generally a harsh critic long before structural problems develop. For this reason, it is critical that maintenance strategies are available, and adopted following construction.

Most rational design approaches assume that a flexible pavement structure consists essentially of three main layers:

1. an asphaltic concrete surface layer or layers;
2. a granular base unbound layer or layers; and,
3. the subgrade.

The granular unbound layer(s) is absent for full depth asphaltic concrete pavements (pavements consisting essentially of a thick course of asphaltic concrete laid directly on top of the subgrade).

The two critical pavement conditions generally considered in the rational design methods are:

1. the horizontal tensile strain at the bottom of the lowest asphalt cement bound layer (asphaltic concrete or asphalt-stabilized base); and,

2. the vertical compressive strain at the surface of the subgrade.

These strains are controlled to limit the load-induced fatigue cracking and pavement deformation failure modes, respectively.

Pell's criterion [11,12] of maximum allowable tensile strain at the bottom of the lowest asphalt cement bound layer is supported by significant laboratory data. This can be summarized by the equation:

$$N_S = K \left(\frac{1}{\varepsilon_m}\right)^n$$

where: N_S = number of equivalent 80 kN (18 kip) load applications to initiate a fatigue crack;

ε_m = maximum induced tensile strain; and,

n and K = parameters depending on the composition of the asphaltic concrete mix.

Dormon and Metcalf [13] developed a limiting vertical subgrade strain criterion which is based on elastic layered system theory.

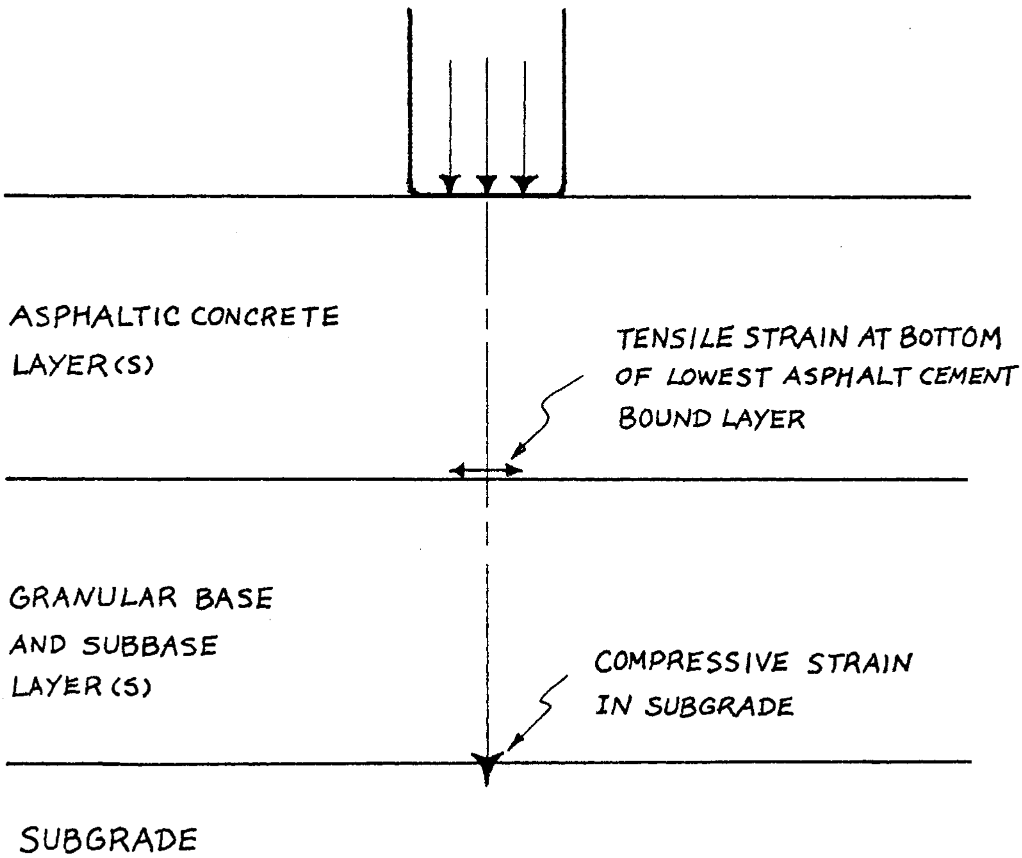

FIGURE 1-1 Diagram Showing the Governing Conditions of the Three-Layer Flexible Pavement System

The design process first entails the reduction of the predicted truck loading data to the design number of equivalent 80 kN (18 kip) standard axle load applications, with the use of charts such as those given by Sargious [14]. Limiting strains are then established from charts based on data such as that developed by Pell, Brown, Cooper, Dormon, Metcalf and others[11 to 13].

A layered pavement section with assumed thickness is then analyzed, typically using standard computer programs based on elasticity theory [1-4], for representative layer moduli (M_R and ν_R) to determine the strains and stresses at critical points. The computerized analysis is carried out using either a single or a dual wheel arrangement of the standard 80 kN (18 kip) axle loading shown in Figure 1.2. If the analysis indicates that the critical strains criteria are exceeded, changes are made in layer thickneses and/or materials until a satisfactory design is achieved. The ability to adjust layer thicknesses and materials enables the designer to make efficient use of available materials and to develop a cost effective pavement design.

1.3 SUMMARY OF OBJECTIVES

This study was concerned with the factors influencing the resilient modulus and resilient Poisson's ratio and permeability of typical Ontario granular materials used in road construction, and the M_R and ν_R for designing flexible pavements by rational methods

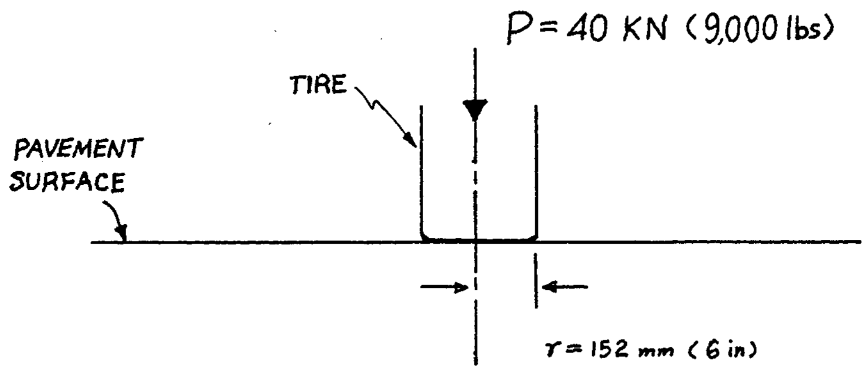

SINGLE WHEEL LOADING

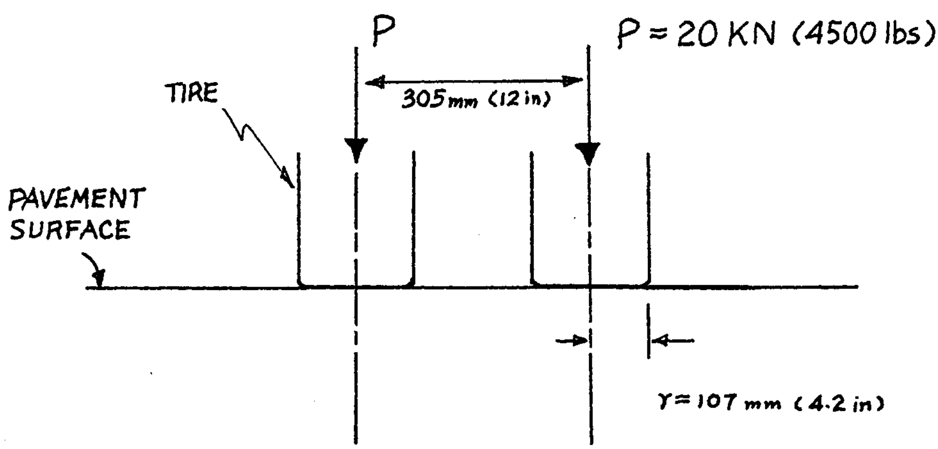

DUAL WHEEL LOADING

FIGURE 1-2 Wheel Loading Arrangements for Strain Analysis of Pavement in Ontario. In addition, the importance of permeability was considered to meet the study objectives of improved rational pavement design and performance.

in Ontario. In addition, the importance of permeability was considered to meet the study objectives of improved rational pavement design and performance.

CHAPTER 2

LITERATURE SURVEY

2.1 CONSTITUTIVE RELATIONSHIPS

The "laws" relating stresses and strains in materials are known as constitutive relationships. In general terms, strains and stresses in a material are dependent on location, temperature, rate of loading and other factors. Westmann [15], for example, used the following expression:

$$\varepsilon_{ij} = f_{ij}\,(\tau_{xx},\ \tau_{yy}\ldots\ldots\ldots\ldots\ldots\ldots\ldots X,Y,Z,t,T\,) \qquad (2\text{-}1)$$

where: ε_{ij} = strains;

τ_{ij} = stresses;

t = time;

T = temperature; and,

$X,Y,Z,$ = location.

It has been verified experimentally that unbound granular materials in general respond virtually independently of temperature and the rate of loading [16] in the case where the rate of loading corresponds to that of truck traffic. The response of granular materials may be further characterized as either linear rate-independent, or non-linear rate-independent. The non-linear response of granular materials has been well documented [17]. In addition, the general instantaneous and recoverable (elastic) nature of the strains in flexible pavement granular layers subjected to repeated loading had led most investigators to model granular base and subbase materials as non-linear, elastic materials [22]. Of course, the potential for initial traffic compaction, degradation, and permanent strains if overloaded is clearly recognized.

2.2 RESILIENT PROPERTIES

Yoder and Witizak [26] have summarized much of the available information on pavement material properties in their text, and this source plus the primary reference have been drawn upon in this section on resilient properties. The resilient modulus (M_R) of a material, a dynamic test response, is defined as the ratio of the repeated axial deviator stress (σ_d) to the recoverable axial strain(ε_a)[26]:

$$M_R = \frac{\sigma_d}{\varepsilon_a} \qquad (2\text{-}2)$$

Laboratory measurements of σ_d and ε_a can be completed on representative specimens in suitable loading and monitoring equipment to determine the M_R of various types of pavement materials ranging from cohesive subgrades to granular aggregates and asphaltic concrete. However, test conditions (stress state, strain levels, moisture content, temperature, etc.) influence the M_R responses of these materials in different ways. While repeated loading type tests have been used to characterize cohesive soils for some time, it is only recently that this type of test has been regularly used to study the resilient characteristics of granular pavement materials. These recent studies generally indicate that the response of granular materials to repeated loading is different from their response to static loading.

The applicability of the concept of a resilient response for granular materials in pavement design is now widely recognized (16,17,18,22). Basically, this approach seeks to formulate predictive equations for the resilient modulus and resilient Poisson's ratio of pavement materials through the use of repeated loading triaxial tests, or other appropriate test methods. By expressing these parameters as functions of the state of stress in the pavement layer, it is possible to account for the non-linear material response. The derived moduli may then be used to characterize the granular layer or subgrade in the numerical solution to transient pavement loadings and deflections.

2.3 FACTORS AFFECTING THE RESILIENT PROPERTIES OF GRANULAR MATERIALS

A literature survey of resilient moduli studies by other investigators indicates that the following factors have a significant effect on the resilient response of granular materials:

(1) stress level;

(2) degree of saturation;

(3) aggregate type and density;

(4) fines content (minus 75 μ_m (#200) material); and,

(5) stress duration and frequency.

These factors are discussed in following sections.

2.3.1 Stress Level

Previous investigators [16,17,18] have determined that stress level has the greatest effect on the resilient response of granular materials. The resilient modulus increases with confining pressure (cell pressure σ_3) and is relatively unaffected by the magnitude of the repeated deviator stress, so long as the repeated stress does not cause excessive permanent deformation. Two relationships have been used to describe the influence of confining pressure on the resilient modulus of granular materials[17]:

$$M_R = k_1(\sigma_3)^{k_2} \quad (2\text{-}3)$$

or

$$M_R = k_1'\theta^{k'_2} \quad (2\text{-}4)$$

where: M_R = resilient modulus;

σ_3 = confining pressure; and

θ = sum of principal stresses.

For triaxial test conditions:

$$\theta = \sigma_1 + 2\,\sigma_3;\text{ and,}$$

k_1, k_2, k'_1 and k'_2 = experimental constants from tests.

A typical plot of M_R versus stress state is shown in Figure 2-1 (from Hicks, 17). Extensive testing of granular materials has indicated that both the number of stress repetitions and the sequence of the applied stresses have little, if any, effect upon the M_R value. This implies that one specimen can be repeatedly used to derive the constants of Equation 2-3 or 2-4. In general, after "conditioning" the specimen with about 1000 repetitions, M_R values may be calculated after 150 to 200 repetitions at each stress state. In addition, the load duration and frequency have little effect upon granular aggregate M_R. In Hick's study [17], deviator stress loading was applied through haversine pulse loads with a load duration of 0.1 second applied at between 20 to 30 applications per minute. This loading is considered to be representative of trucks moving at creep speed.

Hicks [17] tested compacted samples of granular materials with the use of a conventional triaxial testing apparatus. He concluded that the resilient properties of granular materials were most significantly affected by stress level. Regression analysis of the results of tests conducted at various levels of confining stress yielded values for the constants in Equation 2-3 and 2-4. Hicks also modelled

Poisson's ratio as a function of the principal stress ratio:

$$\nu_R = A_o + A_1 \left(\frac{\sigma_1}{\sigma_3}\right) + A_2 \left(\frac{\sigma_1}{\sigma_3}\right)^2 + A_3 \left(\frac{\sigma_1}{\sigma_3}\right)^3 \qquad (2\text{-}5)$$

where the A constants were found by least squares techniques.

Hicks(17) concluded from repeated loading tests that the resilient properties of granular materials are greatly affected by the stress level. In all cases, the resilient modulus increased considerably as the confining pressure increased, but very slightly as the repeated axial stress increased. As long as shear failure does not occur, this stiffening effect is an important feature of the granular material response, and Equations 2-3 and 2-4 for M_R and Equation 2-5 for ν_R are valid. The resilient Poisson's ratio was found to increase as either the confining pressure decreased or the repeated axial stress increased. Figures 2-1 and 2-2 are typical representations of these equations.

Allen(22) completed a series of repeated loading tests on a variety of granular materials. The triaxial chamber confining pressure was varied simultaneously with the axial stress to simulate the actual stress pulse in flexible pavements. It was found that the applied state of stress significantly affected the resilient response of the granular specimens. Further, the effects of material type on the resilient response were small compared to the effects

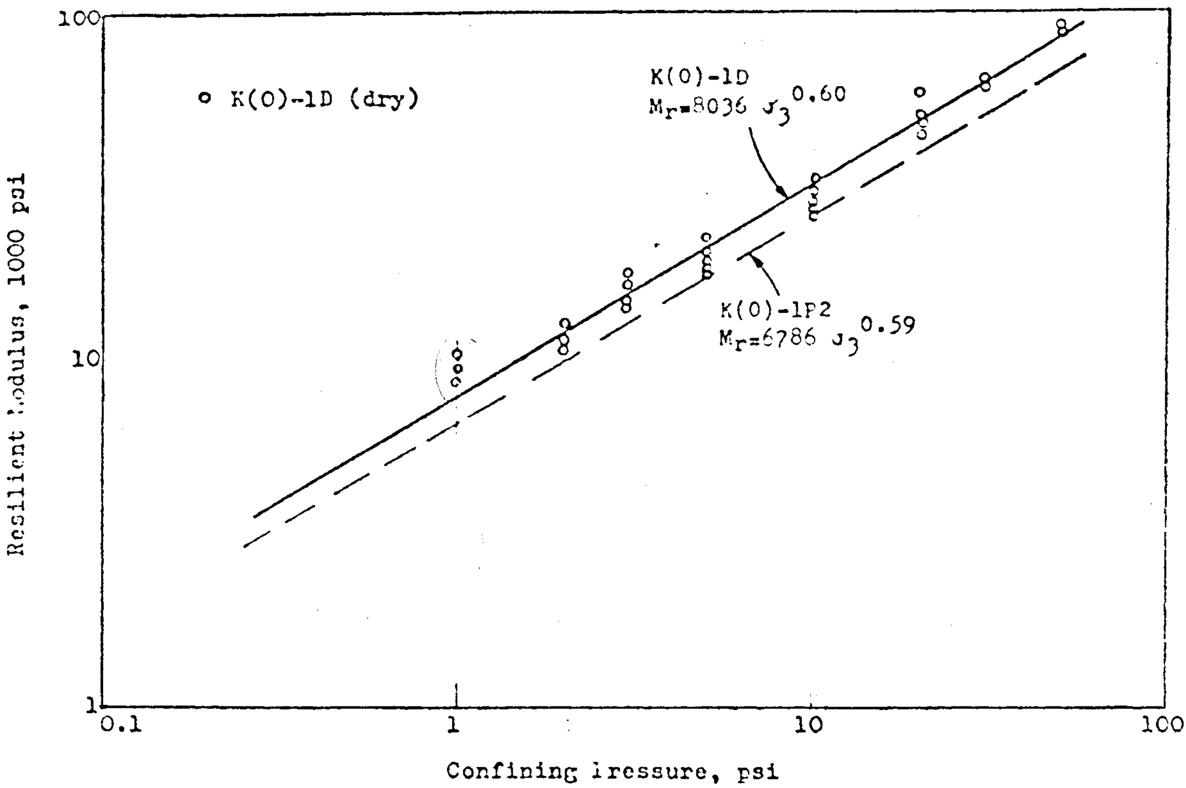

FIGURE 2-1 - Variation in Secant Modulus with Confining Pressure. Aggregate Base Sample Nos. K(O)-1D AND K(O)-1P2 (From Hicks,17)

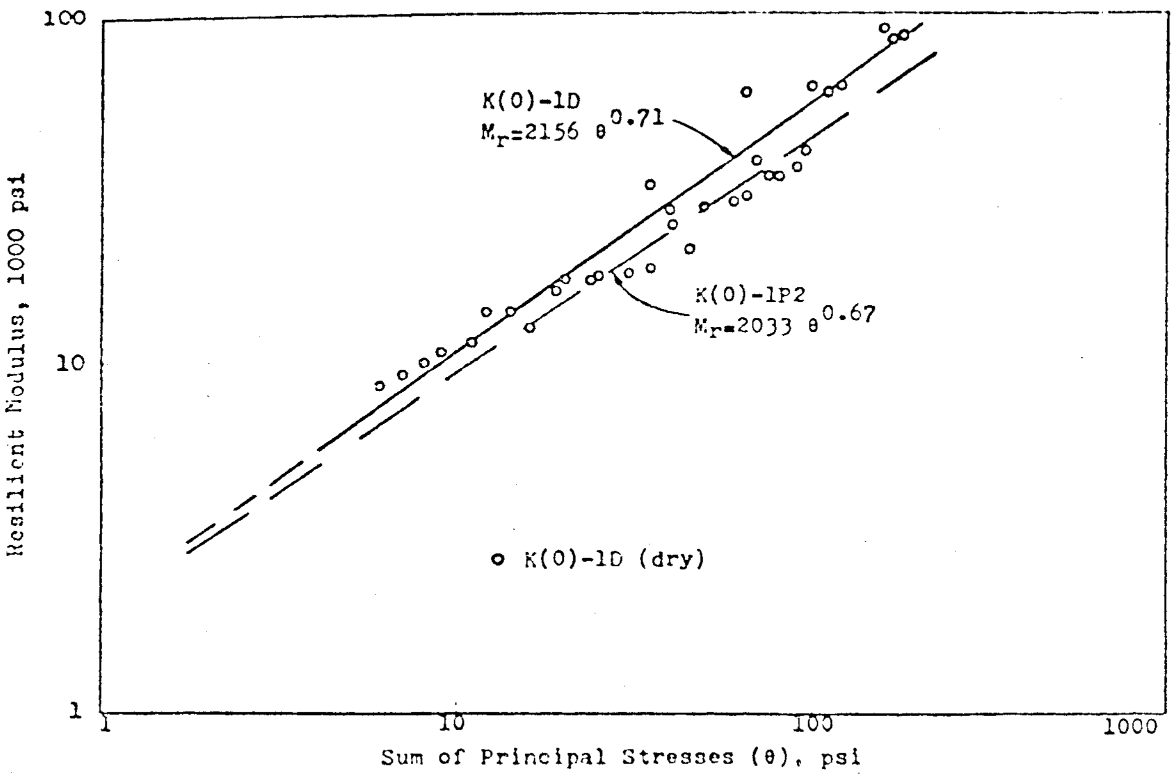

FIGURE 2-2 - Variation in Secant Modulus with Sum of Principal Stresses ($\theta = \sigma_1 + 2\sigma_3$). Aggregate Base Sample Nos. K(0)-1D and K(0)-1P2 (From Hicks, 17) of changes in the state of stress. Allen concluded that crushed stone yielded a slightly higher value of resilient modulus than natural gravel that tends to be rounded. The M_R of a blend of natural gravel and crushed limestone was usually found to be between the moduli of these two materials. Poisson's ratio varied only slightly from one material to another, with the values calculated for the natural gravel normally exceeding those for the crushed stone.

The dependence of granular aggregate resilient modulus on stress level was also observed in experiments conducted at the University of California and the Asphalt Institute[20]. Results obtained from repeated loading triaxial tests were expressed in terms of Equation 2-3.

2.3.2 Degree of Saturation

Studies concerned with the resilient properties of gravels at different degrees of saturation (or water content) have generally indicated that the resilient modulus decreases as the degree of saturation increases, as long as comparisons are made on the basis of the total confining pressure. Comparisons on the basis of effective stresses indicate that the resilient moduli for 100% saturated samples differ only slightly from those of dry samples. This finding is essentially in accord with the principle of effective stress, where the intergranular pressure is considered to govern shear and volumetric behaviour.

Haynes and Yoder[19] observed that the resilient moduli of natural gravels were more sensitive than crushed stone to an increase in the degree of saturation. Thompson[21] reported results of repeated loading triaxial tests on crushed stone that at high degrees of saturation showed resilient and permanent deformations, and monitored pore pressure increased substantially.

In general, it can be concluded from the technical literature that saturation of a granular material has an adverse effect on its undrained resilient modulus. This reduction in stiffness arises out of the development of pore water pressure under repeated loading, which reduces the effective confining stress unless drainage is rapid[24]. As shown by Hicks, the resilient ratio generally decreases as the degree of saturation increases[17].

2.3.3 Aggregate Type and Density

Hicks[17] found that the resilient modulus increased with increasing particle angularity or surface roughness. Figure 2-3 shows the effect of aggregate type and grading on the resilient modulus. For a given aggregate, varying the percentage finer than 75 μm (#200) has a small effect on the resilient response of the material for a range of fines from 6 to 10%[17]. These fines levels should be contrasted with a desirable fines level of less than about 5% for adequate base and subbase drainage.

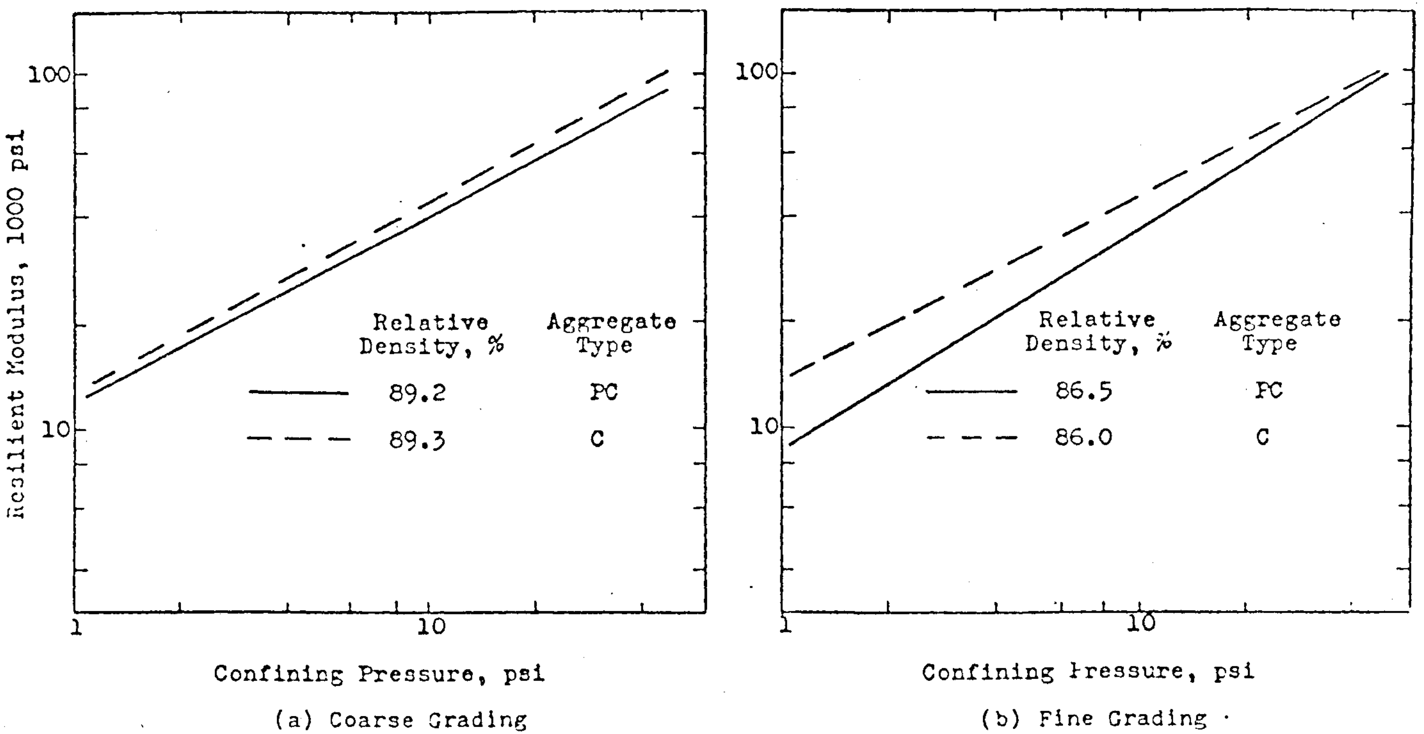

FIGURE 2-3 - Effect of Aggregate Type (Partially Crushed vs. Crushed) on the Relationship Between Resilient Modulus and Confining Pressure (σ_3). Dry Test Series (From Hicks, 17)

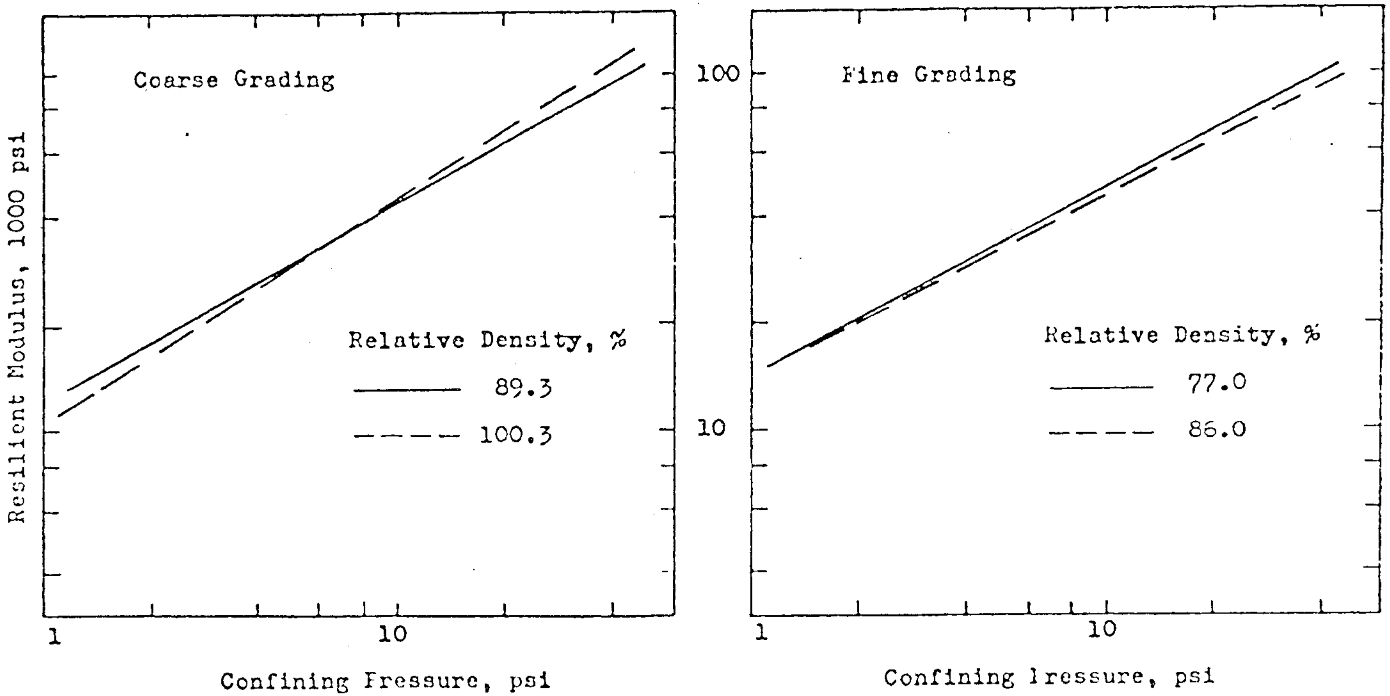

FIGURE 2-4 - Effect of Density on Relationship Between Resilient Modulus and Confining Pressure (σ_3). Crushed Aggregate. Dry Test Series (From Hicks, 17)

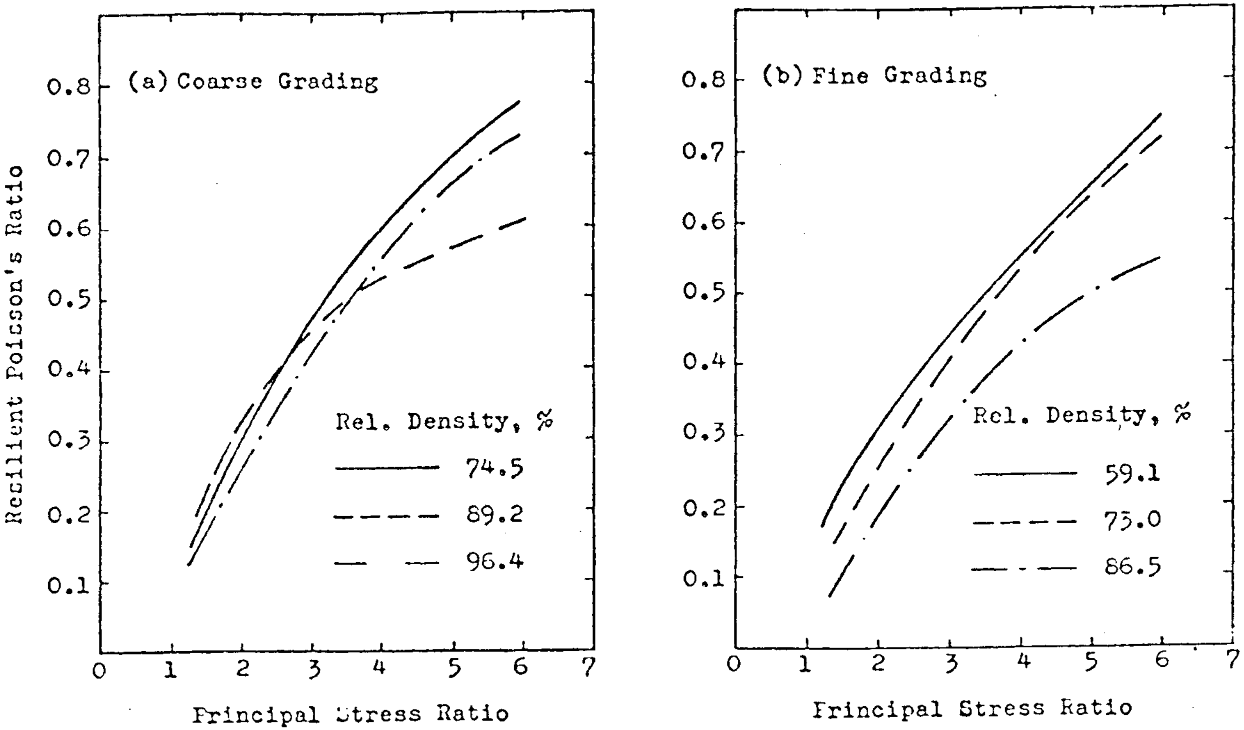

FIGURE 2-5 - Effect of Density on the Relationship Between Resilient Poisson's Ratio and Principal Stress Ratio (J_1/J_3). Partially Crushed Aggregate. Dry Test Series (From Hicks, 17)

There are only a limited number of studies on the effect of density (compaction) on the resilient properties of granular materials. However, the general view is that density has a significant effect. Hicks[17] indicated that the resilient modulus was greater for samples compacted to higher relative densities when subjected to identical stresses. Figures 2-4 and 2-5 from Hicks show the influence of density on M_R and ν_R.

Allen[22] also found that the resilient parameters are affected by variations in the density of the specimen. Generally, the resilient modulus increased as density was increased. However, the resilient Poisson's ratio showed no consistent variation with changes in density. The values of ν_R were similar for all specimens at corresponding values of stress ratio (σ_1/σ_3) in variable confining pressure tests.

It should be noted that the overall density effect appears to be relatively small when compared with the large influence of confining pressure. This is an important observation since the density of base and subbase courses in a pavement structure changes during the pavement's service life.

2.3.4 Fines Content (percentage passing 75 μm (#200)).

Studies of the variation in response of granular materials subjected to repeated axial stresses indicate the fines content can also affect the resilient behaviour. Haynes and Yoder[19] presented results of repeated loading triaxial tests on a natural gravel and crushed stone for a range of minus 75 μm (#200) material. Typical results indicated that for a given state of stress, the resilient modulus was only slightly affected by the grading, and that it increased moderately as the amount of fines increased. However, the resilient modulus of crushed stone was essentially the same regardless of the grading. Results of laboratory repeated load tests conducted by Hicks[17] showed the resilient Poisson ratio's was also influenced by fines content. He found that the resilient Poisson's ratio generally decreased, while the resilient modulus increased, with increasing fines content.

2.3.5 Stress Duration and Frequency

From repeated loading triaxial tests with both variable and constant confining chamber pressure, Allen[22] reported that the resilient response of well-graded granular materials is independent of stress pulse duration. Therefore, any pulse duration in the range of those applied by wheel loads moving at speeds of about 25 to 110 kph (15 to 70 mph) may be used in laboratory investigations. From repeated loading tests at stress durations of 0.1, 0.15 and 0.25 seconds, Hicks[17] found no change in the resilient modulus or Poisson's ratio. Although Seed et al[16] found the resilient modulus generally increases as the frequency of load application increases, there is little effect at frequencies in the range of those expected to occur in a pavement structure. Thus, most investigators have used testing frequencies in the order of 20 to 30 repetitions per minute[17,19].

2.4 FACTORS AFFECTING THE RESILIENT PROPERTIES OF SUBGRADE MATERIALS

For any given traffic and environmental conditions, the most important factor in flexible pavement design is the subgrade soil support. Researchers in recent years have indicated that the resilient deformation (rebound deformation under repeated load applications) of a flexible pavement structure is responsible for fatigue-type failure in the asphaltic concrete layers. Because of the importance of this potential failure mode, many design methods incorporate a "limiting deflection" criterion. For this reason, it is necessary to obtain representative subgrade materials layer coefficients for use in rational design methods.

Before undertaking the tests on subgrade materials reported herein, a literature survey was completed to gain insight into the experience of other researchers with similar materials. It was evident that the resilient modulus and resilient Poisson's ratio for fine grained soils are dependent on numerous factors, many of which are unpredictable and highly variable in both the field and the laboratory. It was also apparent that M_R varied over a very large range, and the results would have to be interpreted very carefully before they were used for design purposes.

From this literature survey [30,31,32,33,34] the following factors influencing the M_R and ν_R of fine grained soils were identified:

1. compacted density and moisture content;
2. method of compaction;
3. compaction energy;
4. degree of saturation;
5. state of stress (both confining and deviator stresses);
6. number of stress applications;
7. thixotropy of material;
8. changes in moisture content after compaction; and,
9. susceptibility to freeze-thaw action.

Each of these factors affects the resilient response to various degrees; however, the extent to which each of these influence the M_R is controlled by the combined effects of the other variables. Reference 31 gives an excellent summary of the background information, and a critical evaluation of the more important factors controlling M_R and ν_R of cohesive subgrade soils. These specific items were carefully considered before initiating the resilient modulus testing program, and will not be repeated here.

2.5 PERMEABILITY OF GRANULAR MATERIALS

A literature survey was also completed to determine typical ranges of the permeability coefficient (k) as a starting point for estimating drainage values for granular base and subbase materials.

TABLE 2-1

FACTORS AFFECTING PERMEABILITY OF GRANULAR MATERIALS (after Emery and Lee, 25)

VARIABLE	EFFECT
Temperature	Changes viscosity of water
Soil density	
Percent fines (minus 75 μm)	
Method of compaction	Affects the size,shape and orientation of voids between the aggregate particles
Shape and angularity of aggregate	
Gradation of aggregates	
Structure or arrangement of aggregate particles	
Plasticity of fines	Highly plastic fines form a barrier to flow due to the closely spaced, plate-like structure of particles which reduce the diameter of the conducting pores
Degree of saturation	Affects the continuity of flow path in voids

This review included a survey of methods and techniques by which permeability can be measured in the laboratory for conditions representative of the pavement structure. Some of the major factors influencing the permeability of granular materials are given in Table 2.1, based on research by Emery and Lee[25] to develop permeability prediction methods. The permeability of a granular aggregate material is quite a difficult property to determine due to the many variables involved, which each significantly influence k. However, precise determinations of k are probably not necessary, given the uncertain combination of variables encountered in both the laboratory and field.

CHAPTER 3

LABORATORY TESTING PROGRAM

3.1 TEST MATERIAL

3.1.1 Location of Materials

After selecting commercially available aggregates from several major sources of granular material in the Southern Ontario area, four representative types of granular base and subbase were considered: Ontario Ministry of Transportation and Communications Granular A, B and C, and a hybrid Granular A blend (a blending of natural gravel and crushed limestone). The sampling locations for these materials are given in Figure 3-1. The specifications for Granular A, B and C are given in Table 3-1.

Site A

Granular A: blended gravel (natural gravel and crushed limestone mix) - TCG Materials Co., Aberfoyle

Site B

Granular A, B and C: natural stone product - Consolidated Sand and Gravel Co., Paris

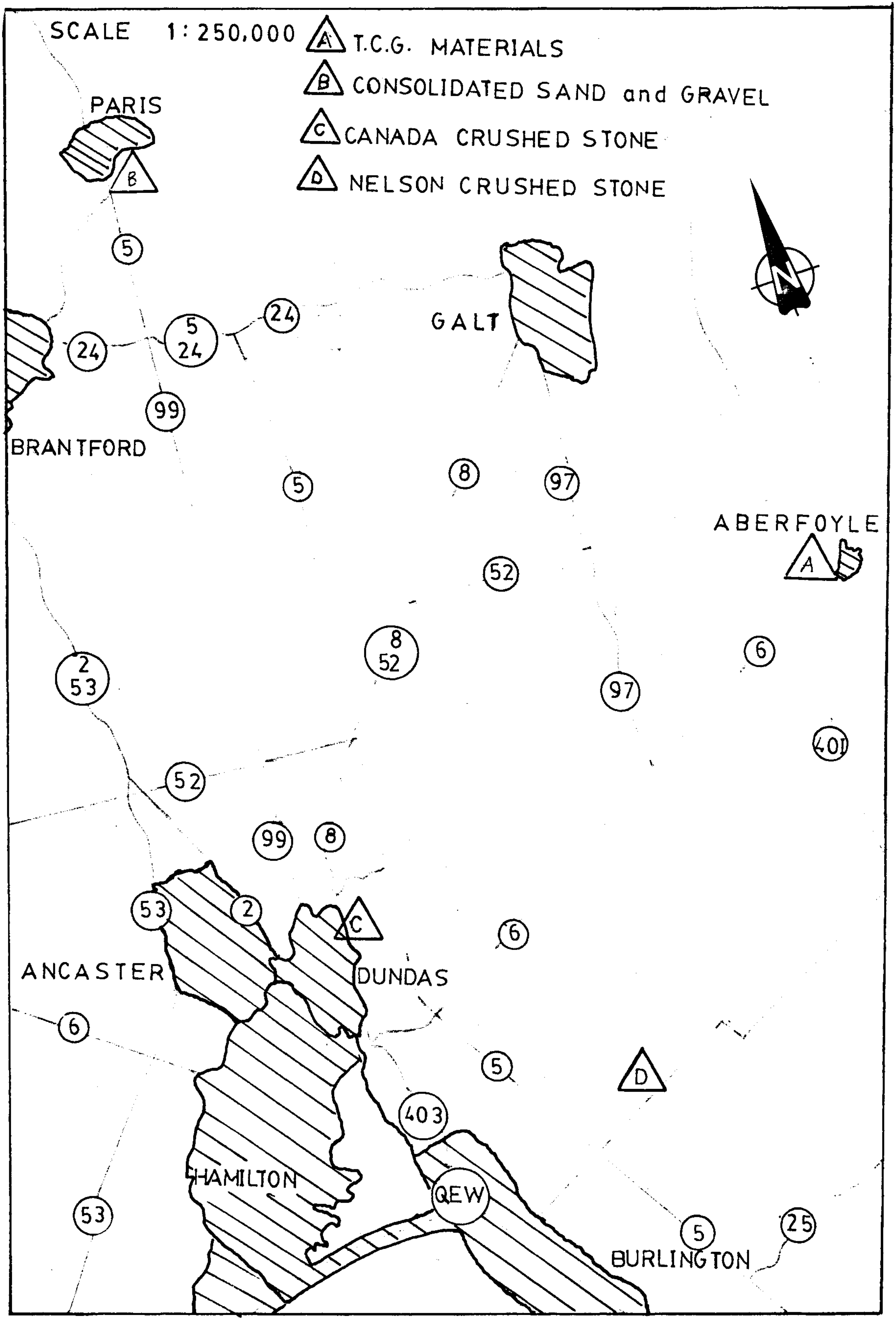

FIGURE 3-1 - Location of Test Materials

Testing of the Granular A was completed in four different tests based on fines (minus 75 μm) content. Test 1 involved the natural fines content of the material. Test 2 involved removing the natural fines from the material. Test 3 involved a 5% fines content and Test 4 involved a 10% fines content in the material.

Site C

Granular A and B: - Crushed Limestone

Canada Crushed Stone Co., Dundas

Site D

Granular A: - Upper level
- Lower level — Crushed Limestone

Nelson Crushed Stone Ltd., Burlington

Testing of both the upper level and lower level granular material was completed in four different tests based on fines (minus 75 μm) content as outlined above for the Site B Granular A.

In addition, Granular A air-cooled blast furnace slag from National Slag Ltd. in Hamilton was tested.

Since the findings of this study are to be applied in the Ontario Pavement Analysis of Costs program, the various subgrade soils used in the tests were supplied by the Ontario Ministry of

Transportation and Communications. These soils represent a wide range of typical Ontario subgrades. Approximately 92 kg (202 lbs) of each of the eight subgrade materials were received from the Ministry for evaluation:

1. sandy silt and clay loam till
   - (a) silt $< 40\%$
   - (b) $40\% <$ silt $< 50\%$
   - (c) silt $> 50\%$
2. Lacustrine clay
3. varved leda clay
4. tobacco sand
5. Welland slag
6. Hamilton steel cinders

The last two materials are not natural subgrade soils, but were being considered for fill applications.

3.1.2 General Properties of the Materials

A. Granular Materials

All granular materials used for the study meet the gradation requirements of the Ontario Ministry of Transportation and Communications given in Table 3-1.

TABLE 3-1

Gradation Requirements(Ontario MTC, #1010)

Ministry Sieve Designation	% Passing by mass					
	16 mm Crushed		Granular 'A'	Granular 'B'	Granular 'C'	Granular 'D'
	Type A	Type B				
150 mm	–	–	–	–	100	–
106 mm	–	–	–	100	–	–
26.5 mm	–	–	–	–	50 – 100	–
22.4 mm	–	–	100	57 – 100	–	–
16.0 mm	100	100	75 – 100	–	–	–
13.2 mm	75 – 95	75 – 95	65 – 90	–	–	–
9.5 mm	50 – 80	50 – 80	–	–	–	100
4.75 mm	25 – 50	25 – 50	35 – 55	25 – 100	20 – 100	50 – 100
1.18 mm	10 – 40	10 – 40	15 – 45	10 – 85	10 – 100	20 – 55
300 µm	2 – 20	2 – 20	5 – 22	5 – 40	5 – 90	10 – 30
150 µm	0 · 10	2 – 13	–	–	4 – 30	–
75 µm	0 – 5	0 – 8*	0 – 8*	0 – 8	0 – 10	0 – 12
53 µm	–	–	–	–	0 – 5	–

*Where Granular 'A' and 16 mm crushed Type 'B' is obtained from rock quarry sources, a maximum of 10% passing the 75 µm sieve will be permitted.

TABLE 3-2

PROPERTIES OF TEST SPECIMENS

Specimen Number	Site	Material	Density Wet kg/m³	Density Dry kg/m³	Optimum Moisture (%)	% Saturation	Gs
SC#4	D	"A" crushed limestone,Upper level, natural fines	2456	2310	6.3	73	2.85
SC#5	D	"A" crushed limestone,Upper level,without fines	2432	2246	8.3	78	2.86
SC#6	D	"A" crushed limestone,Upper level, 5% fines	2420	2284	6	77	2.85
SC#7	D	"A" crushed limestone,Upper level,10% fines	2419	2295	5.4	72	2.79
SC#8	D	"A" crushed limestone,Lower level,natural fines	2553	2420	5.5	68	2.85
SC#9	D	"A" crushed limestone,Lower level,without fines	2584	2444	5.7	71.2	2.85
SC#10	D	"A" crushed limestone,Lower level, 5% fines	2580	2440	5.8	77.0	2.85
SC#11	D	"A" crushed limestone,Lower level,10% fines	2576	2454	5	75	2.85
SG#12	B	"A" natural gravel, natural fines				74	2.79
SG#13	B	"A" natural gravel, without fines	2513	2358	6.6	78	2.77
SG#14	B	"A" natural gravel, 5% fines	2454	2331	5.3	77	2.78
SG#15	B	"A" natural gravel, 10% fines	2451	2326	5.4	75	2.77
SG#16	B	"A" natural gravel, natural fines	2512	2358	6.5	75	2.78
SG#17	B	"B" natural gravel, natural fines	2236	2098	6.6	58	2.76
SG#18	B	"C" natural gravel, natural fines	2395	2243	6.8	80	2.76
SC#19	C	"A" crushed limestone, natural fines	2419	2267	6.7	70	2.85
SC#20	C	"D" crushed limestone, natural fines	2468	2337	5.9	59	2.85
SC-G#21	A	"A" blend, natural fines	2435	2273	7.1	62	2.87
SS#22 (extra)	Dofasco	Air cooled slag	--	--	-	50	2.93

Each type of granular base and subbase material (crushed limestone, natural gravel, and blend) was air-dried and then screened into different sized fractions. The fractions were then recombined in such a way to meet the grading requirement for the MTC granular type involved. The pertinent properties of the test specimens are given in Table 3-2. It should be noted that the properties of each specimen were measured at a density corresponding with the maximum dry density and optimum moisture content as determined by the AASHO T-180 (ASTM D698) test.

Atterberg Limits tests (ASTM D423 and D424) were completed on the minus 420 μm (#40) portion of typical granular materials. As in Table 3-2, fines (minus 420 μm) from crushed limestone (Site D) had a lower plasticity index than fines from natural gravel (Site B). This behaviour is as anticipated, and is the reason for the higher allowable fines (minus 75 μm) content of 10% for crushed stone in the Ministry's specification compared to 8% for crushed gravel.

Field compaction is generally based on the achievement of a specified percent of standard (typically 100%) or modified (typically 95%) Proctor density and moisture content control. Compaction control tests were completed on the specimens using the AASHO T180 modified Proctor procedures (ASTM D1557-78). Typical results are presented in Figures 3-2 and 3-3 for crushed limestone (Site D) and natural gravel (Site B). The optimum moisture content for the crushed limestone was slightly greater than that for the gravel.

The overall purpose of this study was to observe the behaviour of granular materials in conditions closely approximating those found in the flexible pavement structure. Ideally then, the specimens to be evaluated for resilient properties should be taken from the base and subbase of inservice pavements because:

1. Specimens compacted in the laboratory often exhibit different structure properties from field specimens, due to the different compaction methods involved;
2. Construction difficulties in controlling field moisture conditions often result in the base and subbase being compacted appreciably wet of optimum; and,
3. The fines content of the granular material can result in behaviour completely different dry of optimum from that wet of optimum.

This is a recognized limitation of the study, but the testing is considered realistic in terms of providing the representative properties that must be available during design prior to construction. Further, it was considered desirable to develop laboratory equipment that could be produced at a reasonable cost for regular use during pavement materials evaluation for design purposes.

The modified AASHTO T180, ASTM D1557 (or standard AASHO T99, ASTM D698) laboratory compaction methods commonly used in North America are based on impact hammer techniques, even though field compaction methods differ from this laboratory approach, and between each other.

TABLE 3-2

Atterberg Limits Test

Material Type	Location	Liquid Limit	Plastic Limit	Plasticity Index	Specific Gravity
Crushed Limestone	D	20	13	7	2.85
Natural Gravel	B	26	16	10	2.78

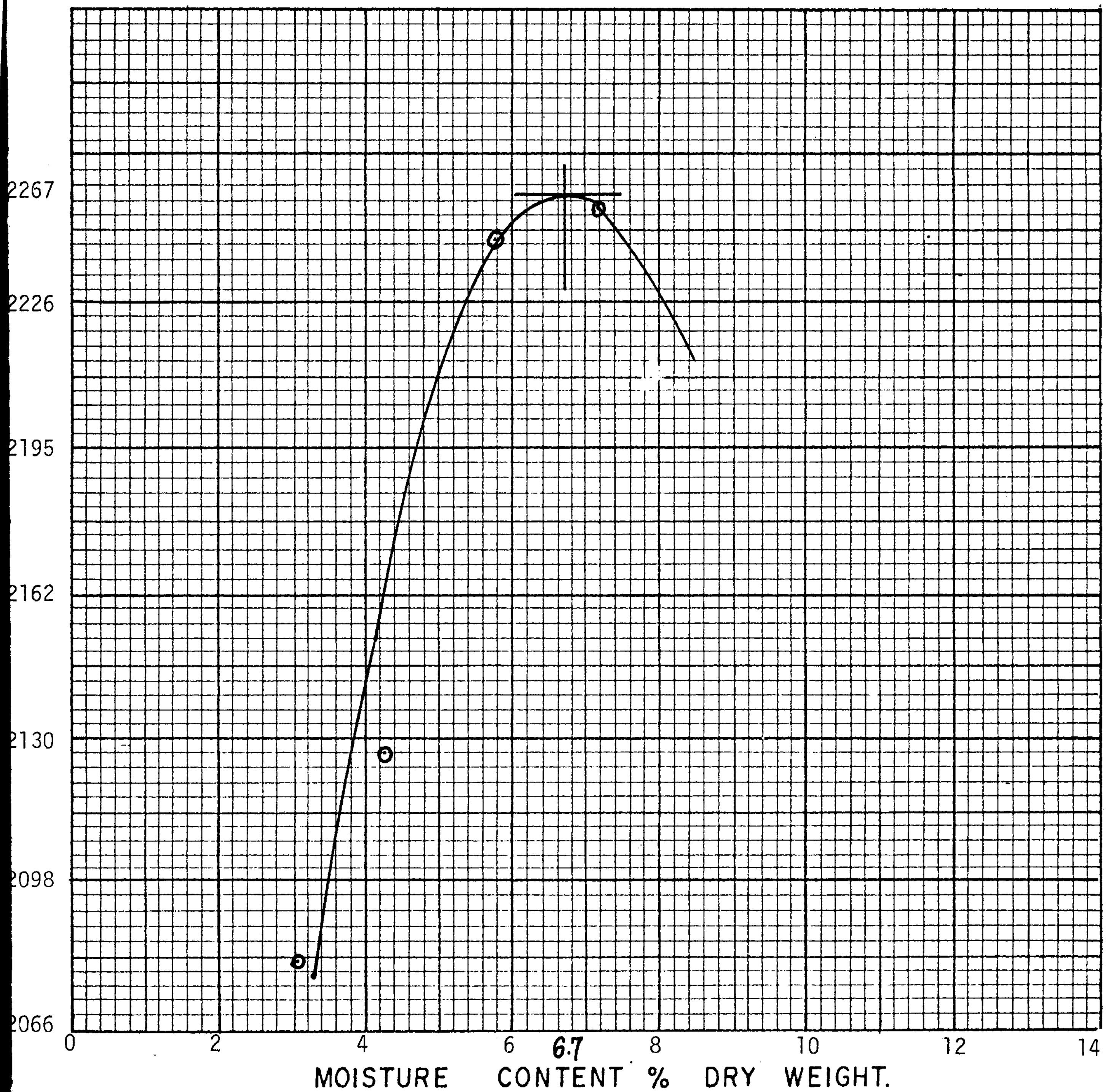

FIGURE 3-2 - Moisture-Density Curves For
Crushed Limestone Material (SC#19)

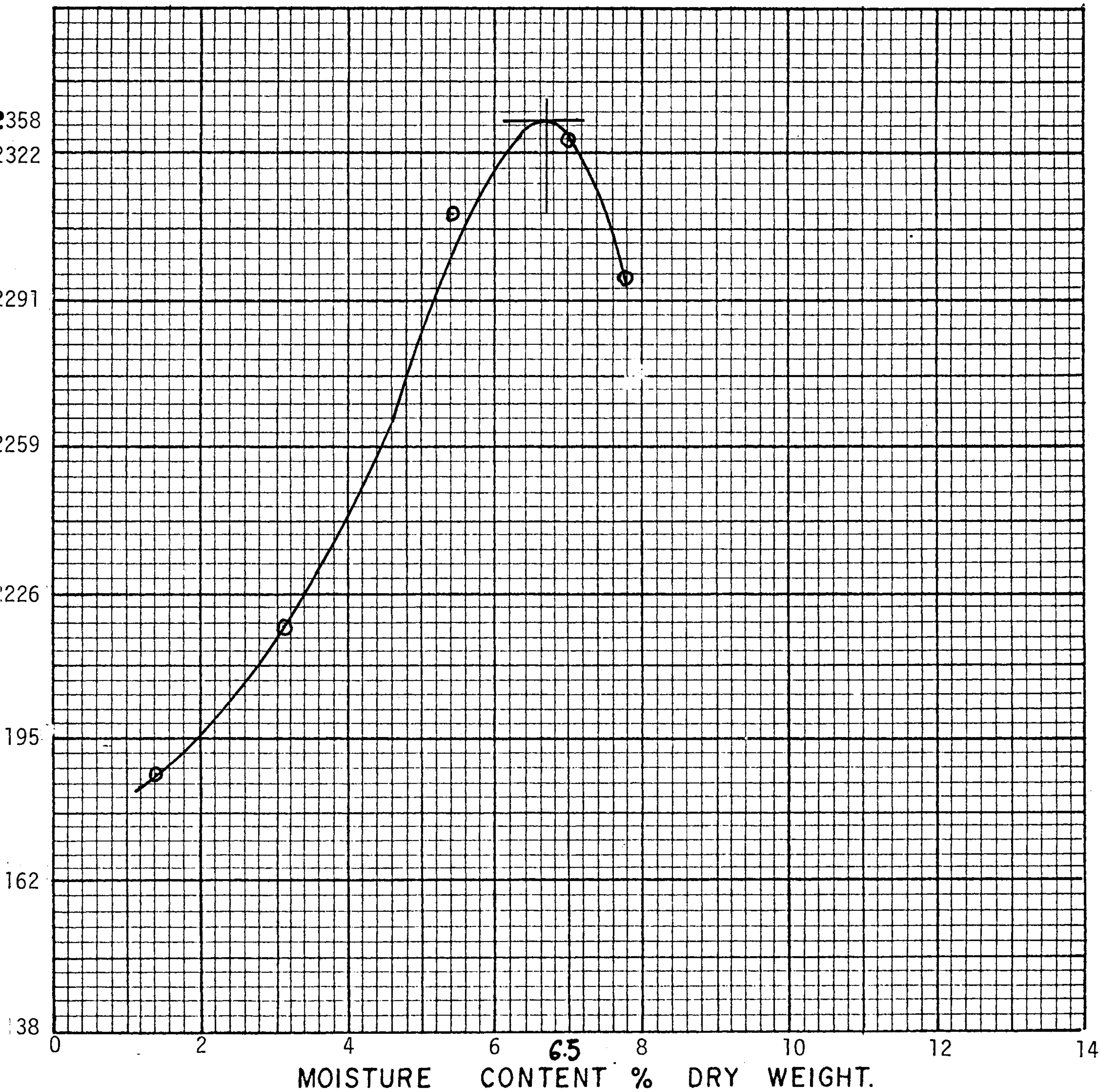

FIGURE 3-3 - Moisture-Density Curves for
Natural Gravel Material (SG#16)

Other laboratory compaction equipment is available that employs kneading, vibration, or static-action techniques. This equipment was developed in attempts to simulate various field compaction methods, however, they are only used in specially-equipped laboratories and probably suffer the same limitation of impact laboratory compaction techniques.

B. Subgrade Materials

The specimens of each subgrade soil type for resilient properties testing were prepared at:

1. 100% Standard Proctor compaction (AASHTO T99, ASTM D698) at optimum moisture content; and,

2. 2% below optimum moisture content, using Standard Proctor compaction (AASHO T99, ASTM D698).

To simulate low support values caused by very wet conditions associated with spring thaw, it was necessary that saturated specimens also be evaluated. However, compacted fine-grained soils do not readily saturate in the laboratory due to their characteristically low permeabilities.

To obtain relatively high saturated specimens, it was decided that the following specimens also be made for each subgrade soil type, in spite of the foregoing discussions:

3. 2% above optimum moisture content, using Standard Proctor compaction (AASHTO T99, ASTM D698).

All specimens for testing were compacted in a split mold (102 mm (4 inches) in diameter, 203 mm (8 inches) in height), which was also used with the granular materials. After compaction, the subgrade specimens were wrapped in plastic and placed in a constant temperature moist room to cure for a minimum of 7 days prior to resilient modulus testing. This curing period would minimize some of the thixotropic effects due to compaction.

3.2 TESTING EQUIPMENT

3.2.1 General Layout

The laboratory equipment developed for this study is basically an improved, advanced version of the equipment developed for previous resilient modulus studies by Gonsalves[5] and Lee[6], and permeability testing by Lee and Emery[25] at McMaster University. The previous work at McMaster University was concerned mainly with the development of resilient modulus and Poisson's ratio measuring devices for investigating asphaltic concrete properties under uniaxial, unconfined stress conditions and triaxial conditions. Temperature was the key factor influencing asphaltic concrete M_R and ν_R considered by Gonsalves[5] and Lee[6]. While temperature was not a concern for the base, subbase and subgrade materials, their low, if any, inherent strength required the development of special specimen preparation techniques.

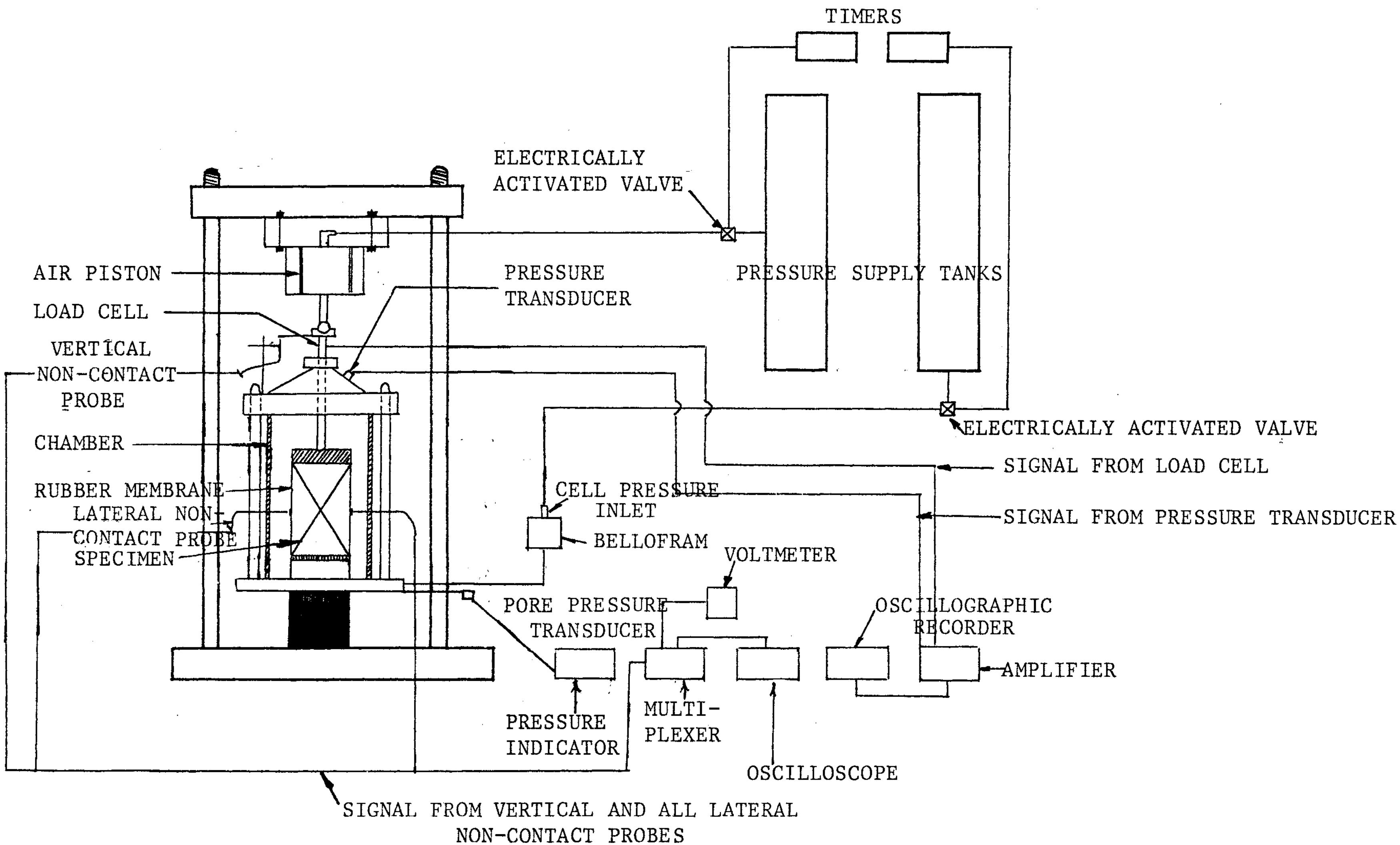

FIGURE 3-4 - GENERAL SCHEMATIC OF TESTING SYSTEM

A schematic of the general testing system is given in Figure 3-4 and described in following sections.

3.2.2 Resilient Modulus and Resilient Poisson's Ratio Measuring Equipment

Designed to determine the resilient modulus and Poisson's ratio, the triaxial equipment contains; a cylindrical specimen, 203 mm (8 inches) in height 102 mm (4 inches) in diameter, mounted within a standard 178 mm (7 inches) diameter triaxial cell as shown schematically in Figure 3-4. This larger size specimen generally yields more consistent experimental results, but most importantly, end restraint influences tend to be minimized, particularly when the length to diameter ratio is greater than two.

Compressive repeated loads are applied vertically along the axis of the cylindrical specimen during M_R and ν_R testing, with the resulting vertical deformations measured parallel to the load axis and the lateral deformations across the specimen diameter.

The vertical and horizontal specimen strains are calculated from the monitored vertical and lateral deformations, respectively. The experimental equipment has been specifically developed to determine the M_R and ν_r of granular base and subbase materials, and subgrade soils, when various confining pressures and repeated loading conditions are applied using controlled air pressure systems. This required care to not disturb the specimen during equipment set-up or deformation monitoring. Three non-contact eddy current probes fixed to the triaxial cell are spaced equi-distant around the circumference and located at mid-height to a prepared specimen, as shown in Figure 3-5. The probes are used for measuring specimen lateral deformations by detecting changes in the magnetic field when metal targets fixed to the specimen, as shown in Figure 3-6, move toward or away from the probes. A fourth probe of the same type is located on the top of the triaxial cell and is used to measure specimen axial deformations under repeated deviatoric stress. This probe system was modified from equipment designed by Emery and Lee[25]. The triaxial cell also contains an internal axial load cell to minimize friction influences (designed and built for equipment) and a pressure transducer for monitoring the applied deviator and confining stresses, respectively as shown in Figure 3-7.

3.2.3 Pulse Control System

3.2.3.1 Confining Pressure Control

The development of a simple pressure control system for applying a pulsed confining pressure (chamber pressure σ_3) to granular base or subbase specimens, and subgrade soils, was necessary. This was achieved through use of the equipment shown in Figure 3-8, which consists essentially of the following components:

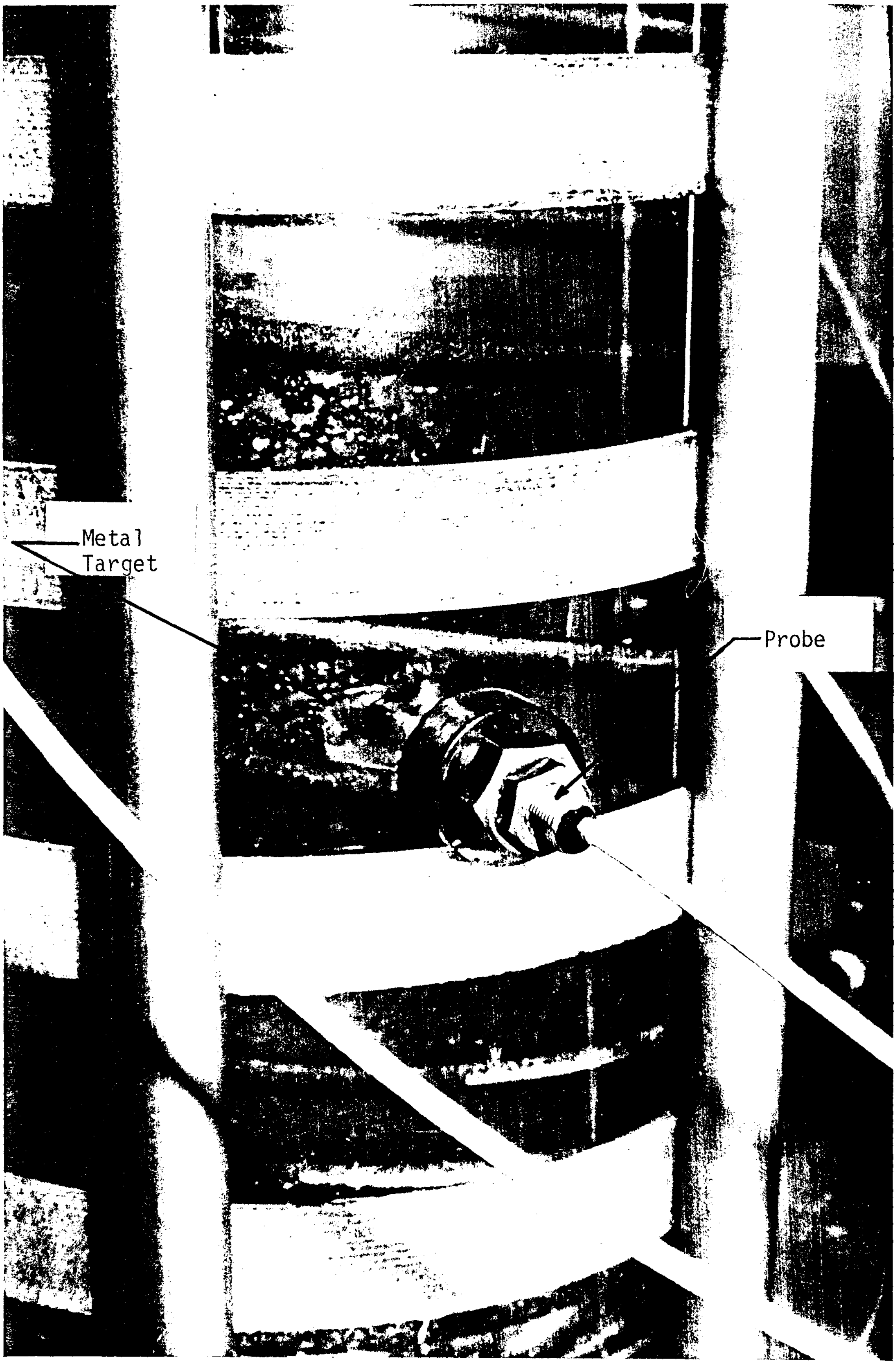

FIGURE 3-5 - Lateral Deflection Measurements
Using Non-Contact Eddy Current Probe

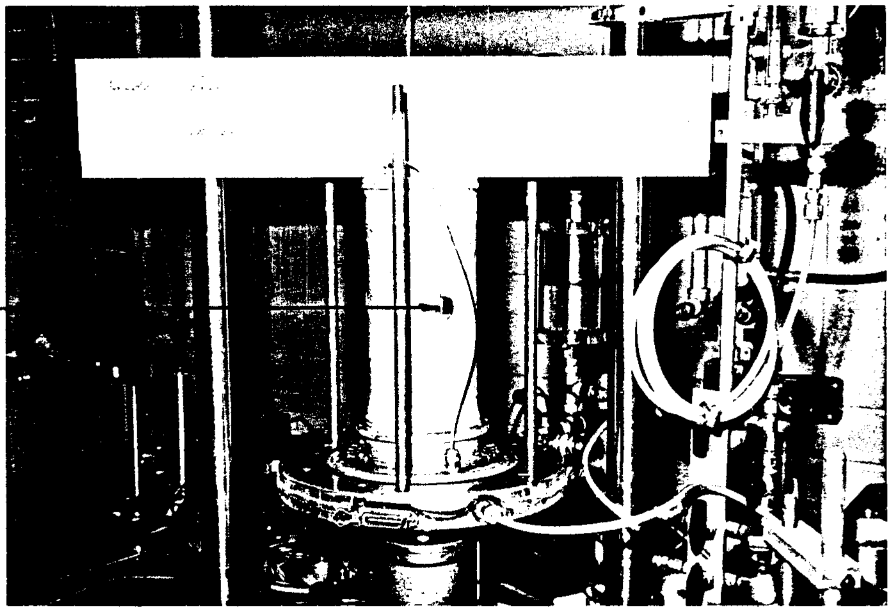

FIGURE 3-6 - Metal Target Affixed to the Specimen
For Lateral Deflection Measurement

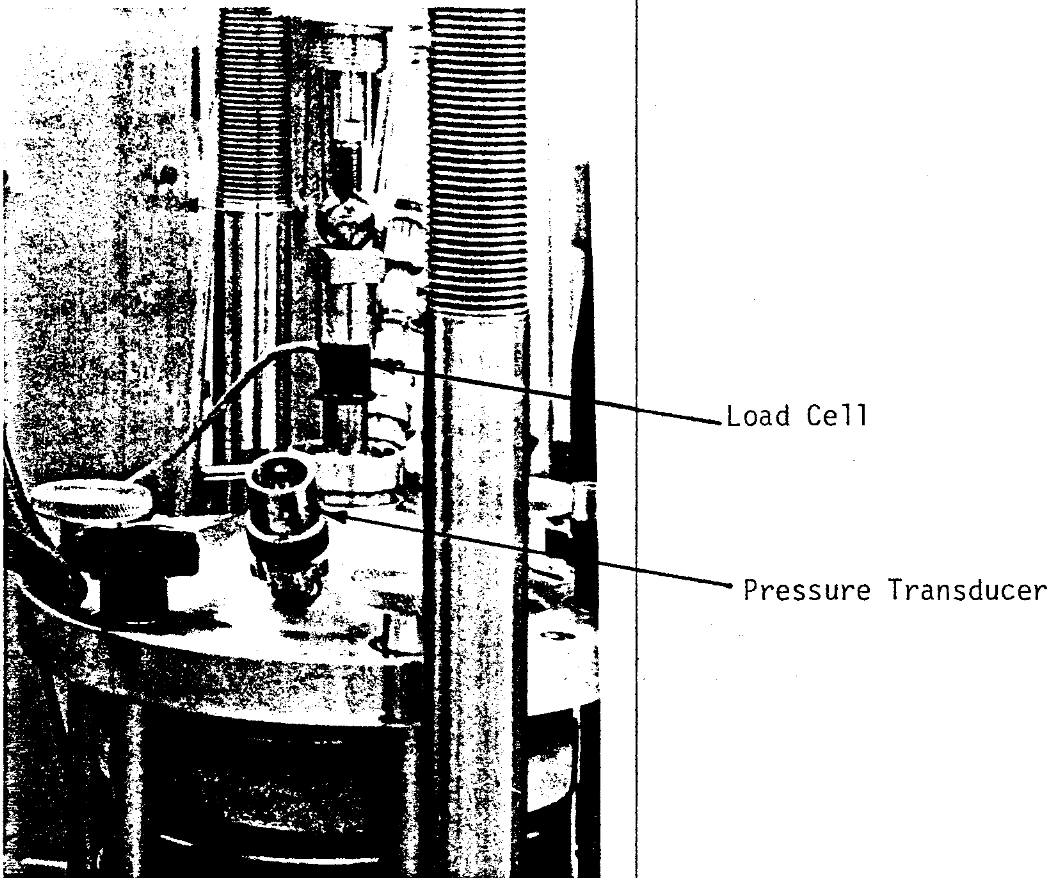

FIGURE 3-7 - Load Cell and Pressure Transducer for Measuring the Deviator and Confining Stresses

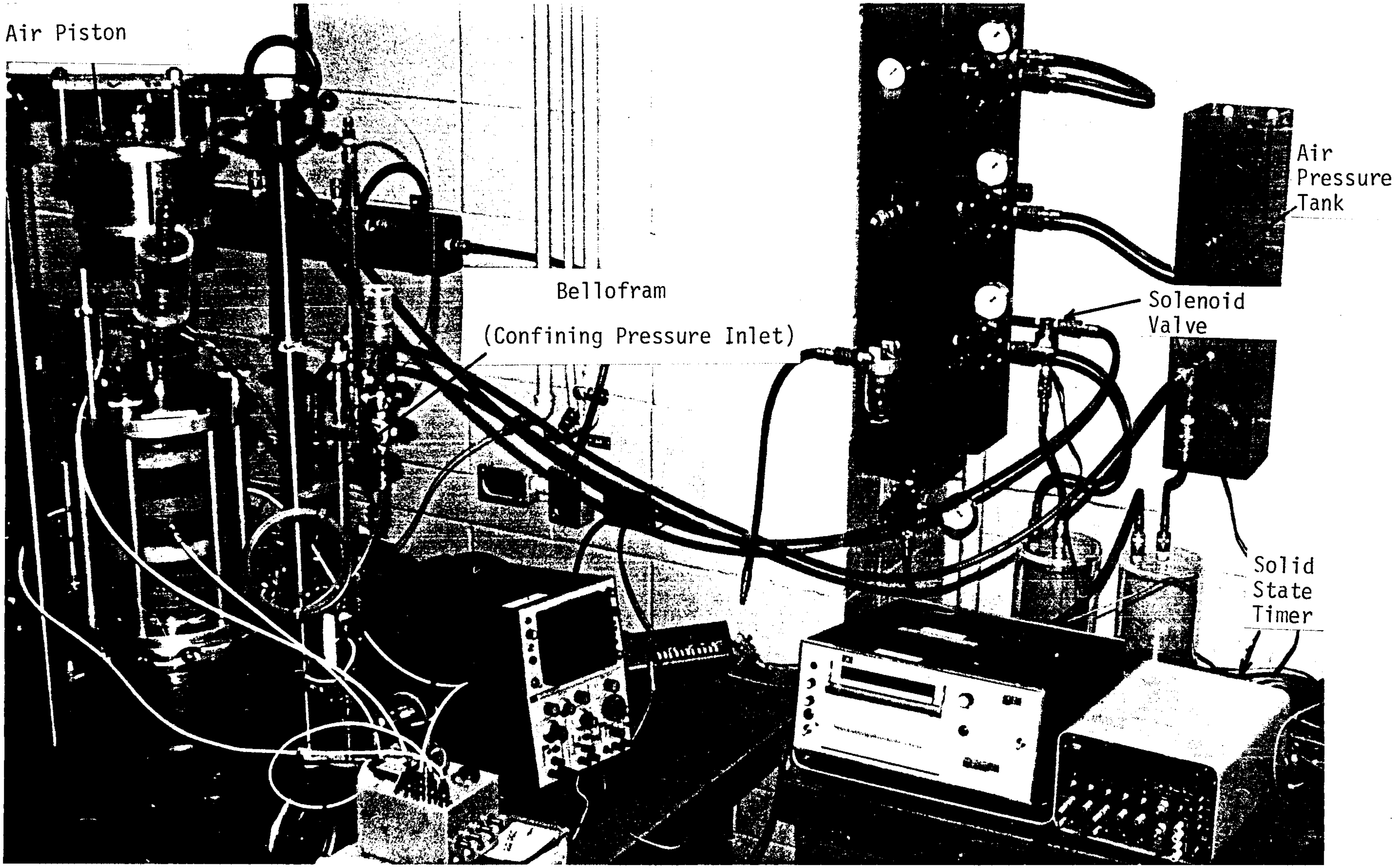

FIGURE 3-8 - Confining Pressure Control System

1. air pressure reservoir tank;
2. electrically triggered air valve;
3. Bellofram separating the air-water interface; and,
4. solid state timer for triggering the electrical air solenoid valves.

The timer was adjusted to open the valve for 0.1 second, twenty times per minute. Within this interval, the solenoid valve allows the air from the reservoir to flow to the flexible Bellofram, thereby transferring pressure to the water in the triaxial cell. As anticipated, there was appreciable "inertia" in the system which represents full pressure response in the cell. This inertia, besides depending on the dimensions of the apparatus (i.e., compliance) is also a function of the viscosity of the water which is temperature-dependent. Consequently, it was necessary to monitor the actual pulsating pressure within the cell using a pressure transducer (Statham Model PA 208TC-100-350, a strain gauge type) located at the top of the triaxial cell. This allowed close control of the peak pressure in the triaxial cell by adjusting the air pressure in the reservoir tank. The circuit diagram of the pulse timer is given in the Appendix Figure A-1. This timer is specially designed to minimize any electrical noise that might interfere with signals from the eddy current probes.

3.2.3.2 Axial Load Control

Repeated axial loading (vertical stress) at desired stress levels was produced by the air piston system shown in Figures 3-8 and 3-9. Basically, the system consists of the following components:

1. air pressure reservoir tank;
2. electrically triggered air valve;
3. 150 mm (6 inches) diameter air piston; and,
4. solid state timer for activating the electrical air solenoid valve.

The equipment is quite similar in principle and operation to the confining pressure control system discussed previously. The timer is adjusted to the same 0.1 second deviation at 20 cycles per minute. As a result, it triggers the valve to allow air to activate the piston. However, the axial loading system used a somewhat specialized timer in that it is triggered by the timer used in the lateral pressure equipment. The purpose of this triggering device was to provide an adjustable lag, so that the peak of both the axial loading (vertical stress) and the confining pressure were achieved at the same instant. This technique effectively compensates for any lag in developing full confining pressure for each load repetition, and is critical to ensure development of the desired repeated vertical and confining stresses. The circuit design of the phase-lag timer used for this equipment is shown in Figure A-1 of the Appendix.

Air
Pressure
Tank

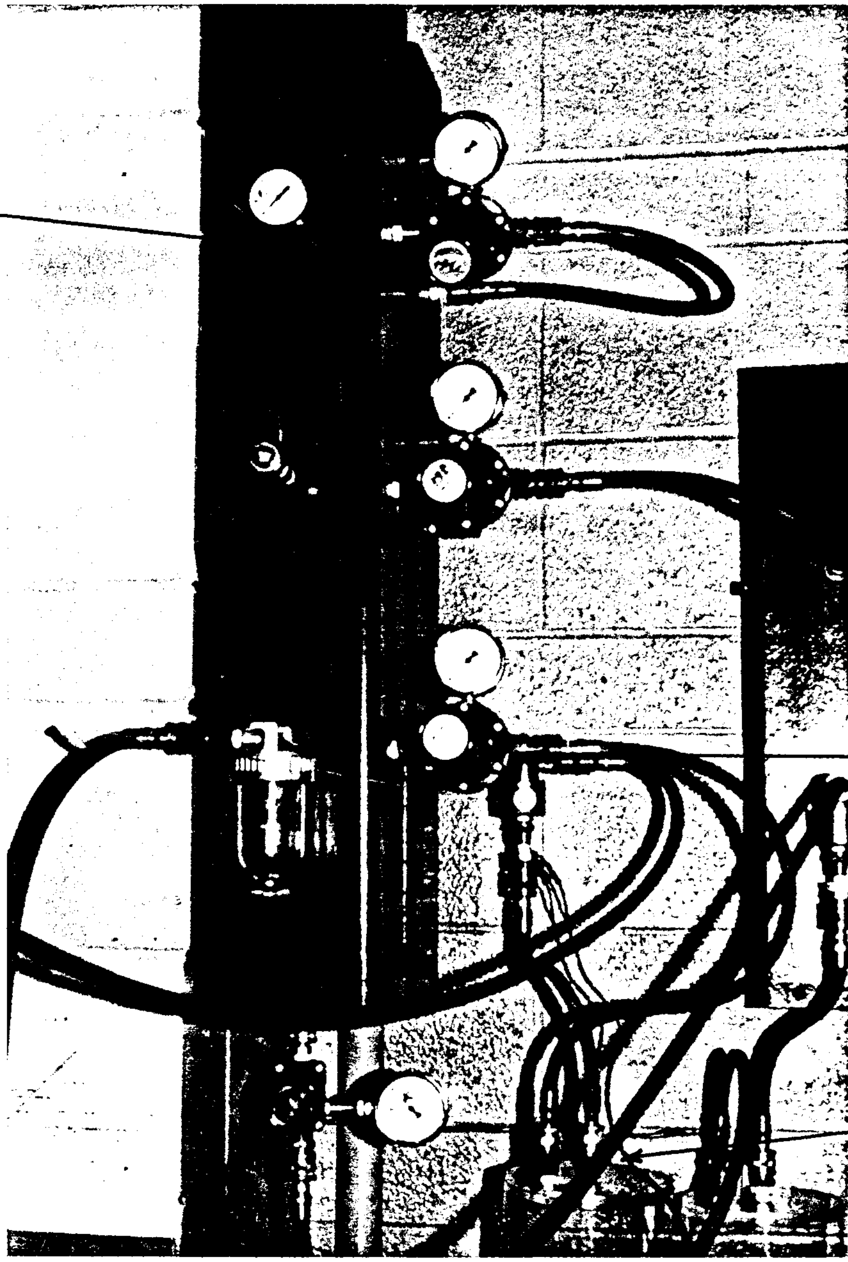

Air Solenoid
Valve

Leads to Solid
State Timer

FIGURE 3-9 - Air Pressure Control System

The axial load level is controlled by adjusting the pressure of the reservoir tank in a similar way to the confining pressure control system. Except for the timing sequence, both loading systems are completely independent of each other, and use separate air pressure reservoir tanks. This allows adjustment of pressure levels to obtain any combination of vertical stress and confining stress conditions during M_R and ν_R testing. The stress levels shown in Table 3-3 were determined by using the Shell Bistro computer program for typical Ontario pavements under a standard 80 KN (18 kips) truck axle loading. They were applied with a pulse duration of 0.3 second and a frequency of 20 cycles per minute, for the test types given in Table 3-4.

3.2.4 Monitoring and Recording of Output Signals

The determination of M_R and ν_R requires the accurate, dynamic monitoring of axial loading, confining pressure, axial deformation and lateral deformation for the various conditions of repeated triaxial loading.

Axial Load

Due to the potential friction between the vertical ram and the close fitting top seal of the triaxial apparatus shown schematically in Figure 3-10, it is necessary to monitor axial loads from within the cell (i.e., below the top seal) to obtain accurate vertical stress values. This was accomplished by using a bolt-type, strain-gauged load cell (2045 kg (4500 lbs.) capacity), which is mounted within the piston ram (Figure 3-10).

TABLE 3-3

TEST SCHEDULE

σ_3 kPa	σ_1 kPa	σ_1/σ_3
21	47	2.2
21	63	3
35	84	2.4
35	118	3.4
52	135	2.6
52	187	3.4
69	192	2.8
69	271	3.9

TABLE 3-4

TEST TYPES (For Every Specimen)

STATIC TEST (Constant Confining Pressure)	Unsaturated	Drained
		Undrained
	Saturated (not 100%)	Drained
		Undrained
DYNAMIC TEST (Variable Confining Pressure)	Unsaturated	Drained
		Undrained
	Saturated (not 100%)	Drained
		Undrained

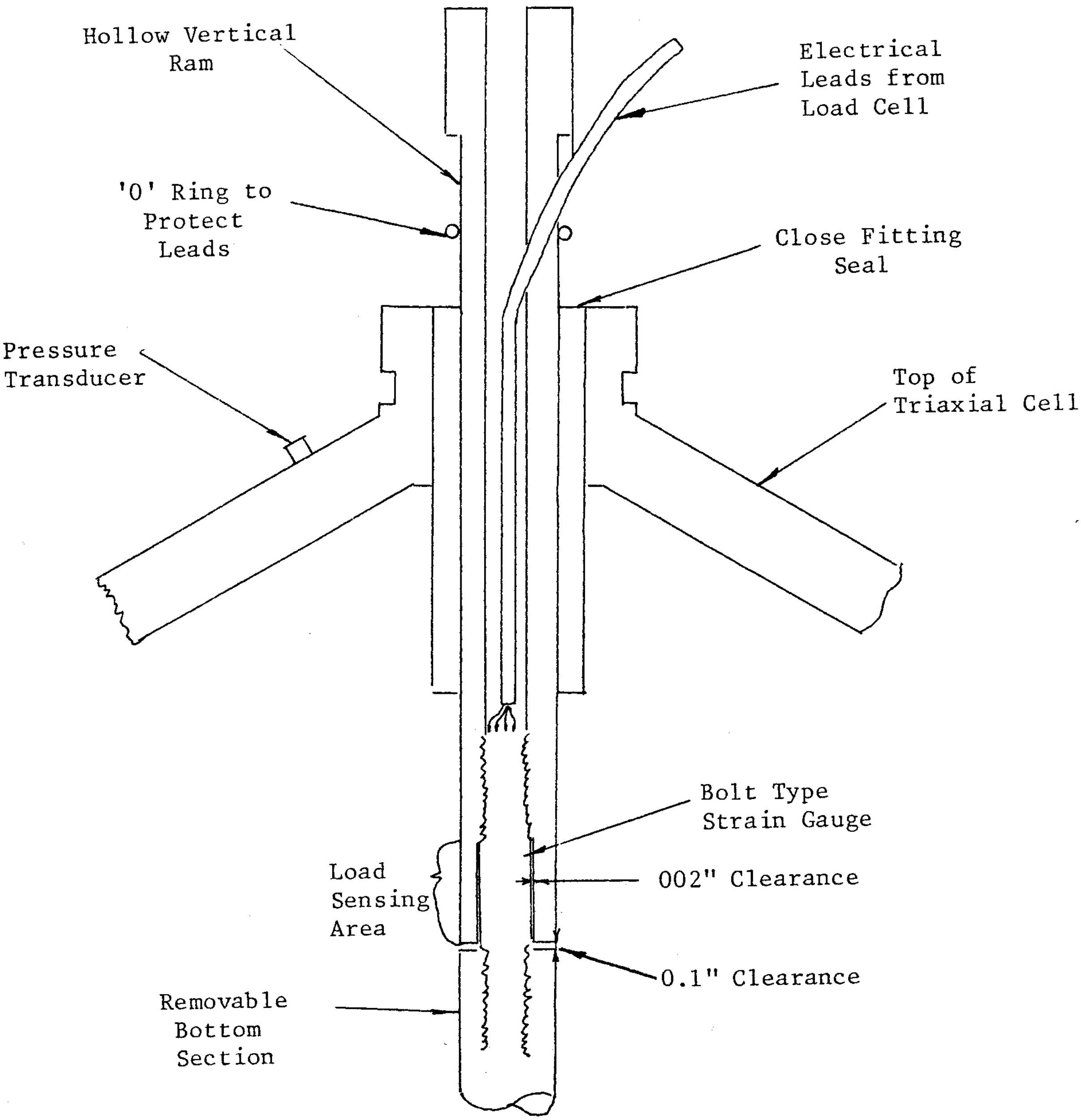

FIGURE 3-10 - Monitoring of Axial Load and Confining Pressure (After Lee, 6)

The wiring from the load cell is placed within the hollow piston rod and brought out above the top seal, thus allowing complete freedom of movement of the piston. Although their size is suitable for this particular application, both types of strain gauge generally lack low-level load monitoring sensitivity, and it is necessary to amplify the output signal prior to recording. Details of the amplifier used are presented in a later section.

Confining Pressure

As discussed in Section 3.2.3.1, accurate determination of applied confining pressure was essential because of compliance effects. Confining pressures (cell pressures) were measured using a Statham PA 208TC-100-350 pressure transducer, mounted in the top of the triaxial cell as shown schematically in Figure 3-10. For the 690 kPa (100 psia) range transducer used, the direct output signal level (i.e., sensitivity) was high enough for the monitoring equipment so that no amplification was needed in this case.

3.2.4.1 Data Acquisition Equipment

The data acquisition system consisted essentially of:

1. five channel amplifier/ balancing unit;
2. six channel light beam (SE 3006) oscillographic recorder;
3. digital voltmeter (Fluke 8000A);
4. oscilloscope recorder (Hewlett-Packard); and
5. junction box (multiplexer) for non-contact eddy current probes.

Amplifier/Balancing Unit

The signal amplifier/balancing unit was used to amplify low level signals to give readily measurable light beam deflections on the oscillographic strip recorder. In addition, the unit was designed to regulate the amplified signals to prevent oscillographic recorder damage. The amplifier system developed for this study is virtually "electronically noise free" and had excellent balancing capabilities. It was also free of channel interaction, despite the fact that a common 12 volt power source was used for all five channels. Details of the circuit design of this amplifier are given in Figure A-2 of the Appendix.

Oscillographic Recorder

The six channel light beam oscillographic recorder stores analogue data by printing directly on light sensitive strip paper, and produces its own grid with 2 mm (0.08 in.) divisions. Measurements of instrumentation response were made for each channel by counting the number of divisions created by a recorded deflection, and multiplying the result by the appropriate calibration constant for that channel.

Digital Voltmeter

The digital voltmeter provided a convenient and accurate readout display for balancing voltages from the amplifier system.

Oscilloscope

The oscilloscope used in this study was capable of storing a signal waveform indefinitely. Its function was to display the signal output (from non-contact probes and/or the load cell) against a time scale (selected by user). In this case, the resulting signal trace was stored until deliberately "erased" (where a permanent record was required, the oscillographic recorder was used).

Non-Contact Distance Measurement Probe Junction Box (Multiplexer)

The junction of one non-contact probe power supply, excitation source, and demodulator is shared (multiplexed) between four such probes. This eliminates the need for three extra (expensive) excitation and demodulator modules. The schematic diagram for this equipment is shown below.

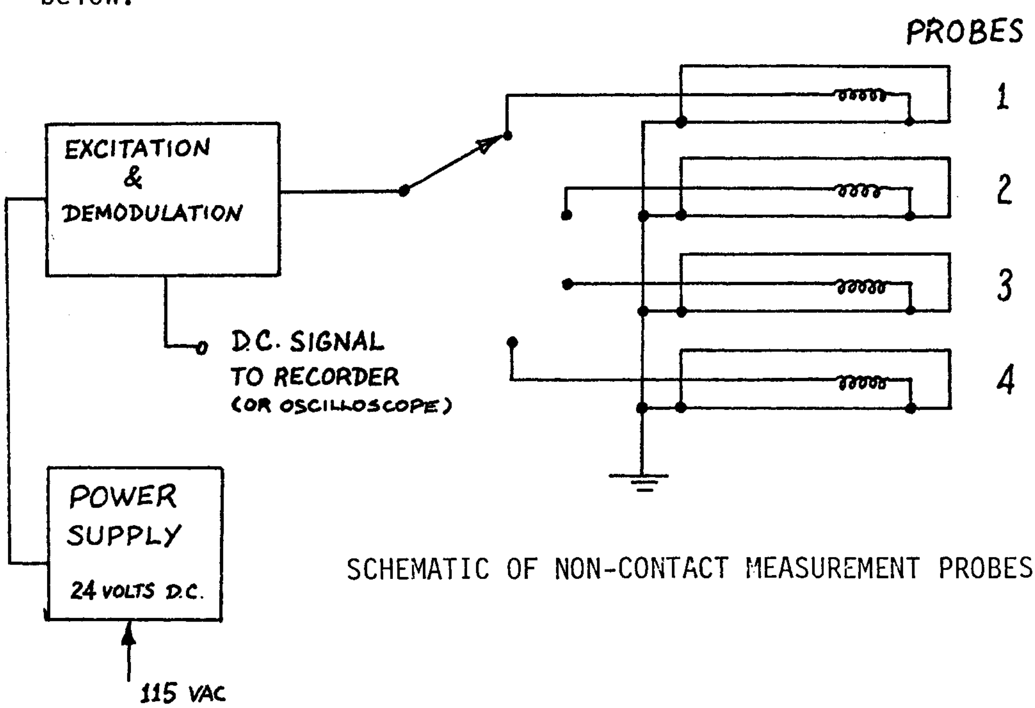

SCHEMATIC OF NON-CONTACT MEASUREMENT PROBES EQUIPMENT

A photograph of the data acquisition system is given in Figure 3-11, which shows the five major components.

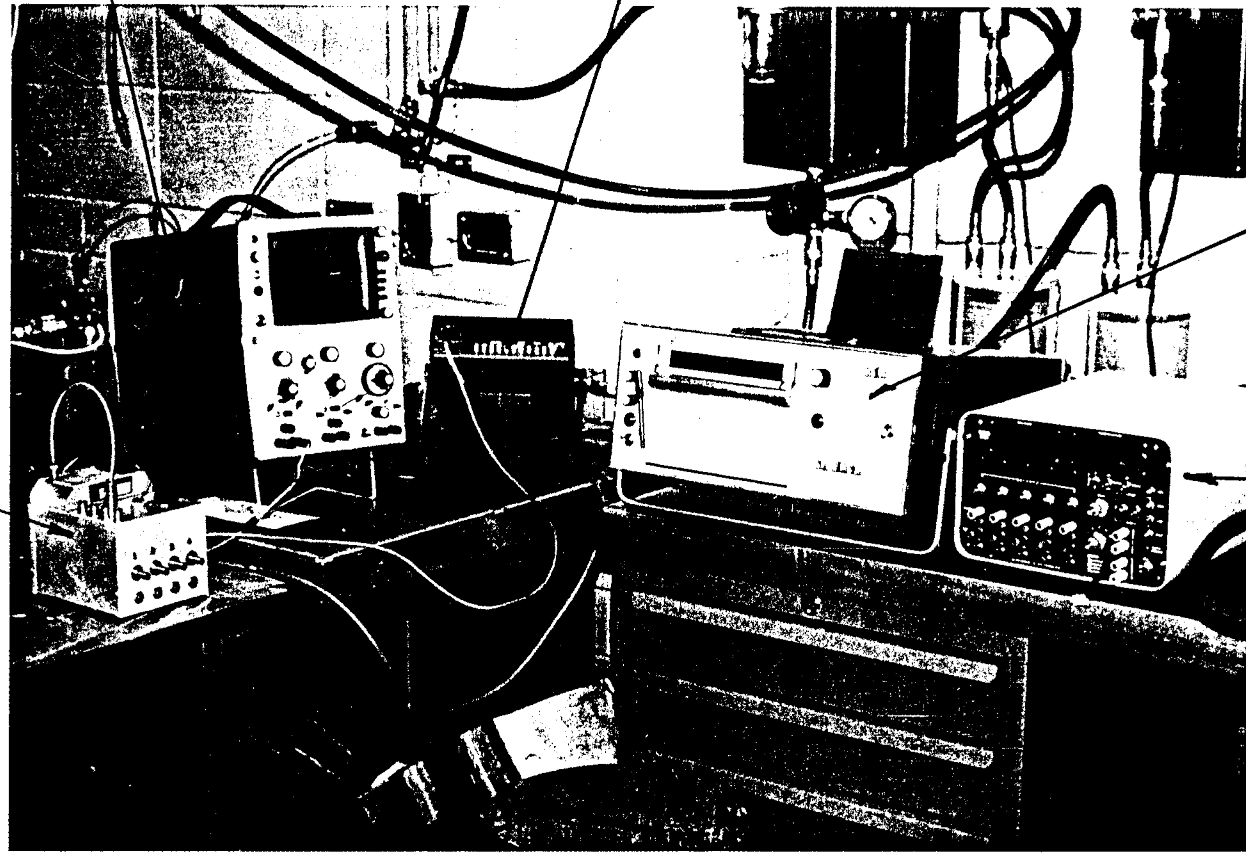

FIGURE 3-11 - Data Acquisition System

3.2.5 Monitoring Specimen Pore Water Pressure and Moisture Changes

The basic function of this part of the system was to monitor the internal porewater pressure response of the specimen under dynamic stresses. This pore pressure volumetric change equipment allows the sample to be changed from an unsaturated state at its compacted moisture content to a saturated state by channeling water into the base of the specimen through a drainage line.

In all of the triaxial tests performed, the monitoring of internal porewater pressure response was done electronically through the use of a pore pressure transducer and a portable strain indicator (P-350).

3.3 SAMPLE PREPARATION AND TESTING PROCEDURES

3.3.1 Resilient Modulus Test - Granular Material

Approximately 70 kg (155 lbs.) of each granular material were sampled from each source indicated earlier in Figure 3-1. The material was air-dried in the laboratory, then separated on a large sieve shaker to remove all particles which were larger than 19 mm (3/4 inches). The material which passed the 19 mm (3/4 inch) sieve was thoroughly mixed, and then split into several equal parts, each of which weighed approximately 7 kg (15 lbs.). The splitting was done by pouring the material through a standard riffle box.

Each material for resilient modulus or resilient Poisson's ratio testing was also tested to determine:

1. Atterberg Limits;
2. Grain Size Distribution;
3. Modified Proctor Density (AASHTO T180, ASTM D1557);
4. Specific Gravity of soil solids; and,
5. California Bearing Ratio.

All M_R and ν_R specimens were 102 mm (4 inches) in diameter and 203 mm (8 inches) in height. The larger diameter was chosen so that the full range of minus 19 mm (3/4 inch) aggregate sizes could be used. The standard two to one height to diameter ratio was necessary in order to minimize any end effects on deformations measured at the centre of each specimen.

After the maximum dry density and optimum water content were obtained from the modified Proctor test, all specimens were prepared in a 102 by 203 mm (4 by 8 inches) split mold with the same compactive energy per unit volume and optimum moisture content as the specimens that were prepared in the modified Proctor tests. The split mold containing the compacted granular specimen was then placed in a freezer at -35°C for approximately two hours. This was done so that the specimen could be readily handled and set up in the triaxial equipment, since the granular materials possess very little inherent strength (cohesive) properties. This freezing operation did not introduce any specimen disturbance.

Having prepared the specimens as described above, each specimen was set up and tested in the triaxial equipment using the following procedure:

1. The specimen was carefully extracted from the split mold and placed on the triaxial cell base containing a porous stone and filter paper. An aluminum loading cap was then placed on top of the specimen to produce an evenly distributed load over its 102 mm (4 inch) diameter.

2. Using conventional soil testing methods, a rubber membrane was placed around the specimen and sealed with rubber 'O' rings. This rubber membrane (shown in Figure 3-13) prevents loss of moisture and allows the application of confining cell pressure.

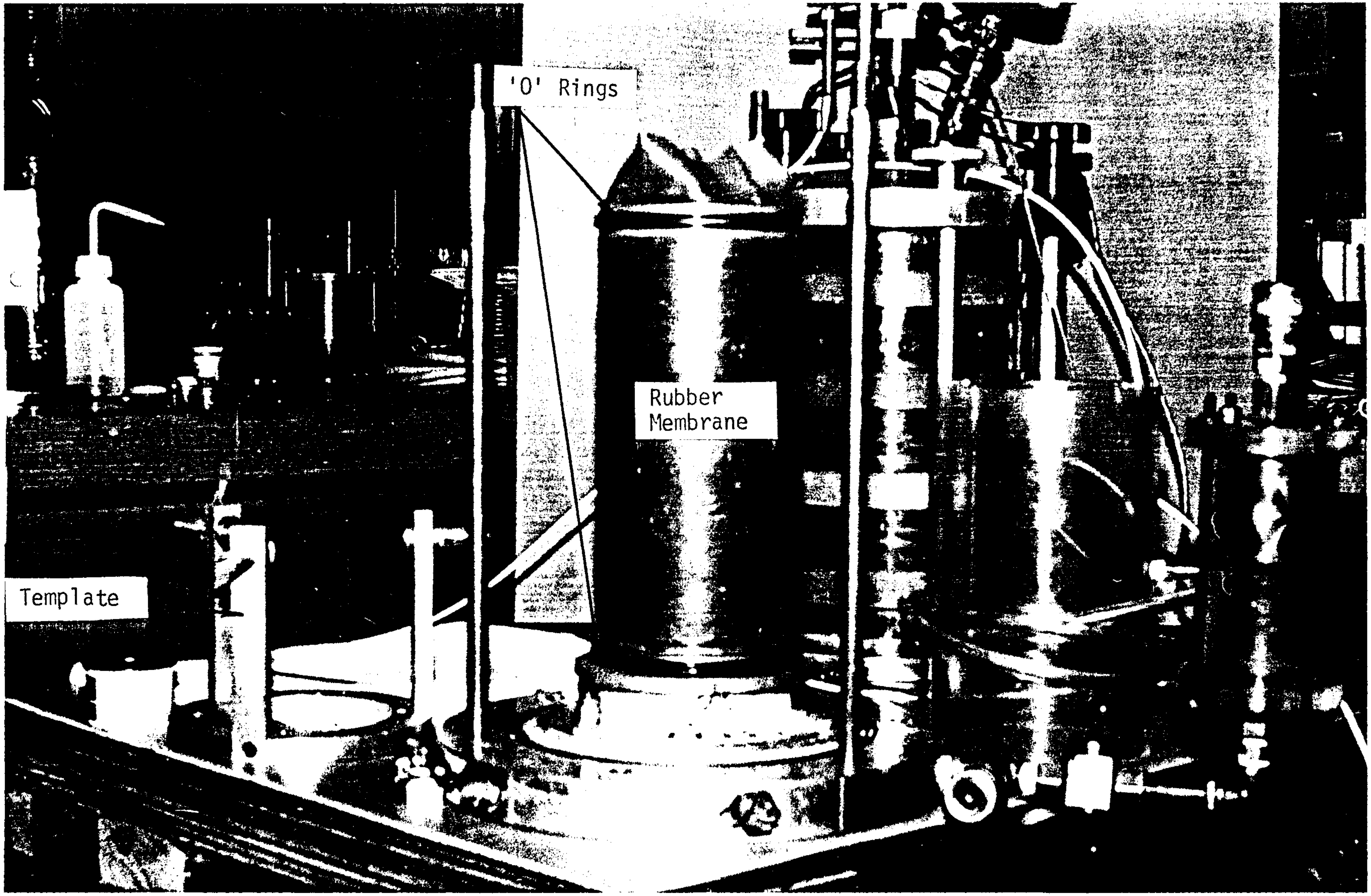

FIGURE 3-12 - Specimen Set-up and Rubber Membrane

3. Using a special template, (shown in Figure 3-12) the specimen was marked at three points (on the rubber membrane) spaced equidistant around the circumference and at mid-height on the specimen. The membrane was sanded lightly at the marked locations, and the area was thoroughly cleaned with acetone. Small stainless steel targets (about 0.025 mm (0.001 inches) thick) were glued with RTV Silicone glue at the prepared points around the specimen. The internal drainage tube between the top loading cap and the triaxial cell base was then connected.

4. The top of the triaxial cell was then placed on the base and securely fastened. The triaxial cell was positioned under the loading piston in the loading frame, and all necessary external connections were made as shown in Figure 3-13.

5. Next, the triaxial cell was filled with water at the inlet valve. The required channels of the oscillographic recorder were adjusted to approximately their respective positions on the strip chart grid. All electrical signal devices from the triaxial apparatus were then connected to the oscillographic recorder and the recorder light beam was focused on convenient grid locations.

6. All wires and air pressure hoses were connected, and the non-contact probes were adjusted to their optimum distance from the stainless steel targets through use of the digital voltmeter.

7. The specimen was subjected to a combination of typical confining and vertical (deviator) stresses for 15 minutes (σ_1 = 47 kPa, σ_3 = 21 kPa and σ_1 = 271 kPa, σ_3 = 69 kPa). This was done in order to "condition" the specimen, and to minimize any permanent deformation during actual measurements. During this 15 minute conditioning period, approximately 300 load pulses were applied.

8. Various combinations of confining and deviator stresses were applied to the specimen through the range of desired stress levels, and the resulting deformations, load and pressures were monitored and recorded.

A photograph showing the general arrangement of the overall system in use is given in Figure 3-14.

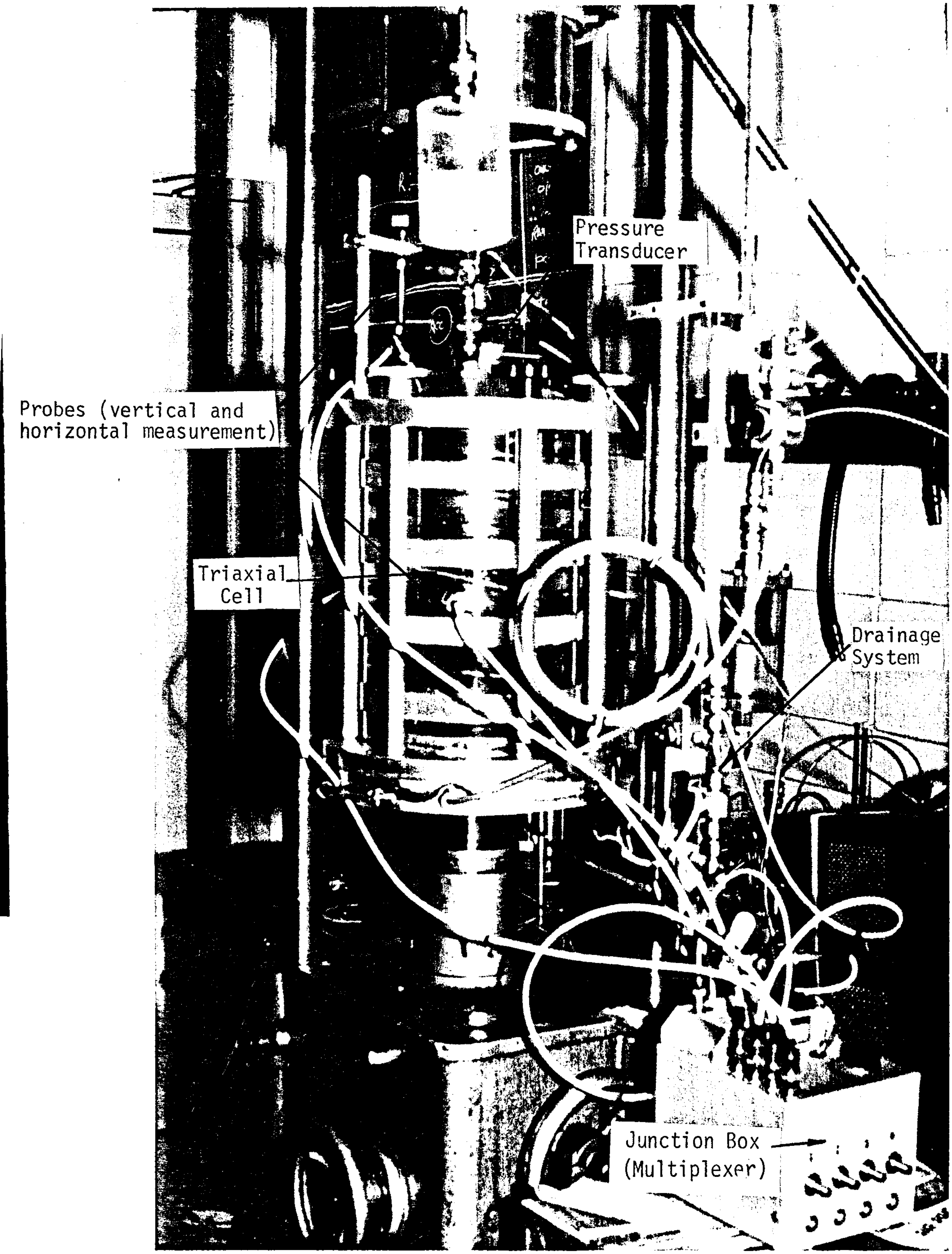

FIGURE 3-13 - Triaxial Apparatus Showing Final Connections before Testing

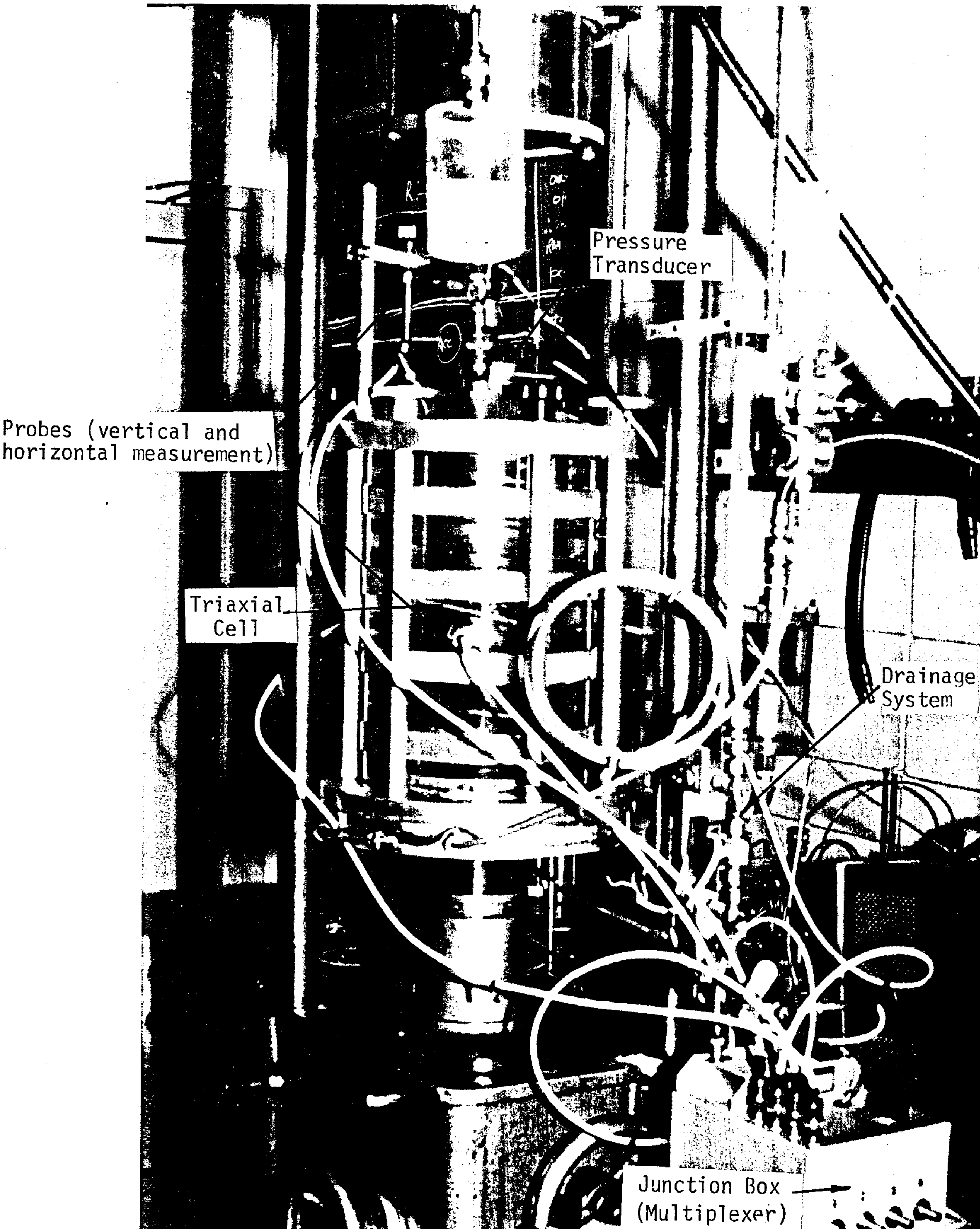

FIGURE 3-13 - Triaxial Apparatus Showing Final Connections before Testing

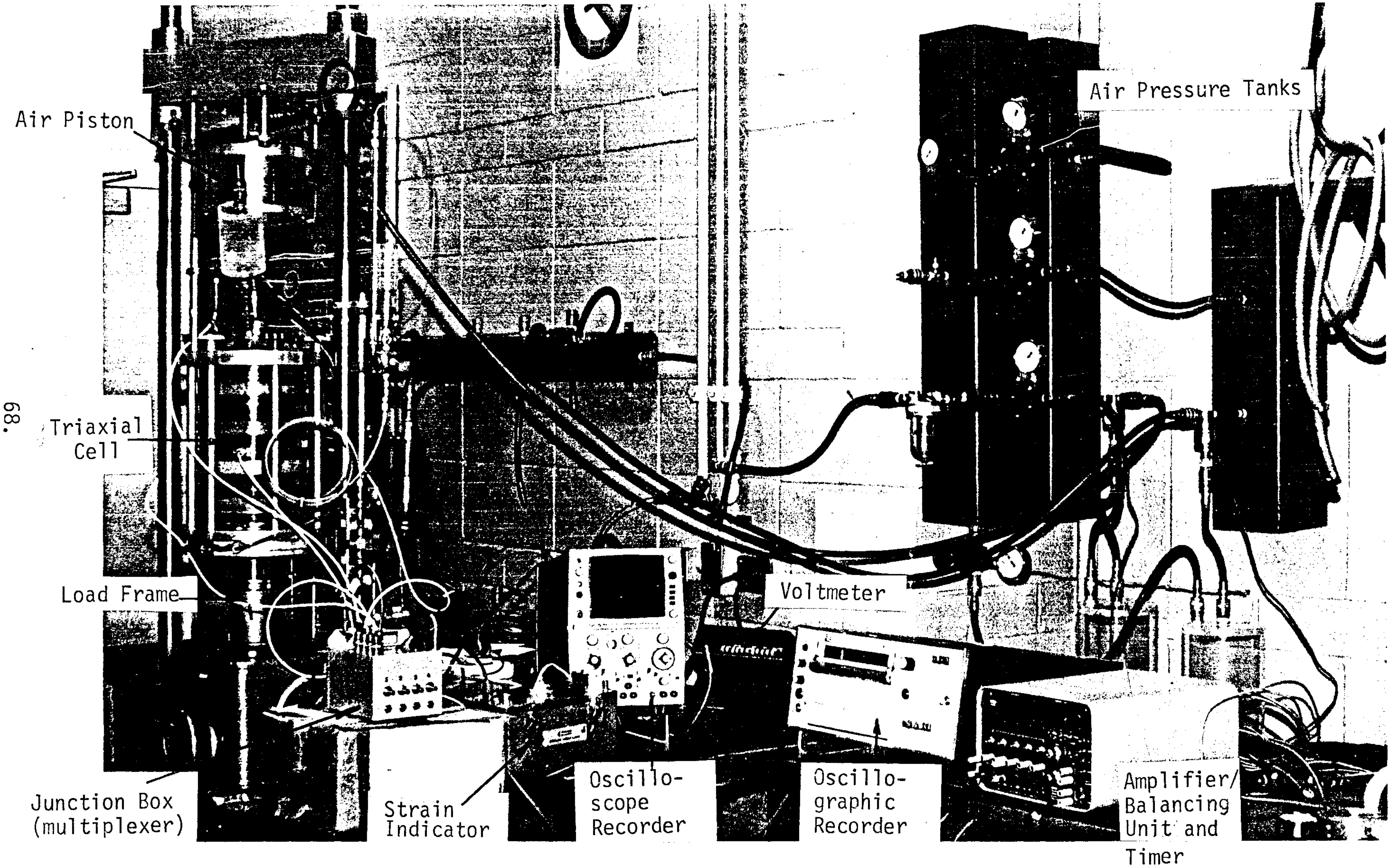

FIGURE 3-14 - General Layout of the Testing Equipment System with Specimen in Place

3.3.2 Resilient Modulus Test - Subgrade Soils

Each subgrade material for resilient modulus or resilient Poisson's ratio testing was tested to determine the following properties:

1. Grain Size Distribution;
2. Standard Proctor Density (AASHTO T-90, ASTM D698);
3. Specific Gravity of soil solids; and,
4. California Bearing Ratio.

Each specimen was set up and tested in the triaxial equipment using the following procedure:

1. The prepared specimen (Section 3.1.2) was carefully unwrapped, and was placed on the triaxial cell base containing a porous stone and filter paper. An aluminum loading cap was then placed on the top of the specimen to produce an evenly distributed load over a 10.16 cm (4 inch) circular area. Using conventional methods, a rubber membrane was placed around the specimen to prevent loss of moisture, and to allow for the application of confining cell pressures.

2. The top of the triaxial cell was then placed over the base and securely fastened. The complete triaxial cell was then put into position in the loading frame, and all necessary wires and pressure hose connections were made.

3. Using the stress levels discussed in Section 3.2.1, Item 7, the specimen was subjected to a combination of confining and deviator stresses for 15 minutes. This was done in order to "condition" the specimen, and to minimize the permanent deformation during actual measurements. For a 15 minute conditioning period, approximately 300 load pulses were applied to the specimen.

4. The triaxial cell was next removed from the loading frame, and the top was taken off. Using a special template, the specimen was marked, and small stainless steel (0.001 inches thick) targets were glued to the rubber membrane at mid-height. The triaxial cell was again put together as before, and placed into position on the loading frame. All wires and pressure hoses were reconnected, and the non-contact probes were adjusted to be at optimum distance from the steel targets using a digital voltmeter.

5. Various combinations of confining and deviator stresses were applied to the specimen, and the resulting deformations and loads were monitored and recorded.

3.3.3 Permeability Test - Granular Material

A brief description of the set up and testing procedure is as follows[25]:

1. After compaction, the CBR mold containing the specimen is carefully removed from the compaction base, inverted, and then seated in the permeameter base plate containing a porous plastic filter.

2. The spacer slug used for the CBR compaction procedure is removed, a porous plastic filter placed on top of the specimen, after which a 4.5 kg (10 lb) surcharge weight is placed on top of the filter.

3. The upper permeameter plate is secured on top of the mold, making sure the '0' ring seals at top and bottom are properly seated before tightening all nuts.

4. The water supply is connected (at the base plate end), and the base is de-aired through a second pipe connection at the base plate.

5. Water is allowed to seep through the specimen under about 250 mm (10 in) of head until flow occurs out of the upper plate connection.

6. All connections to the cell (upper plate - CBR Mold - bottom plate) are closed off, and a vacuum of 125 mm (5 in) of mercury is applied to the top of the specimen

until no further air bubbles are withdrawn (about 10 minutes), after which the vacuum is removed and water again allowed to flow through the specimen. The specimen is then left for additional saturation overnight.

7. Permeability measurements are made by collecting the outflow over a known length of time. For constant head tests, downward hydraulic gradients (i) representative of actual pavement conditions of approximately 0.3 are used for each specimen.

8. After permeability measurements are completed, the end plates are removed, and CBR tests performed on each specimen.

9. Samples are taken from each CBR specimen for density and saturation determinations (Emery and Lee,[25]).

The combination of tests described in this Chapter yielded the desired M_R, ν_R and K values, plus additional descriptive data, for each granular and subgrade material.

CHAPTER 4

RESULTS AND DISCUSSION

4.1 RESILIENT MODULUS, M_R, AND RESILIENT POISSON'S RATIO, ν_R

The resilient modulus is defined as the ratio of the repeated deviator stress, $(\sigma_d=\sigma_1-\sigma_3)$, to recoverable axial strain, ε_d[26]. The resilient Poisson's ratio is defined as the ratio of recoverable lateral strain, ε_ℓ, to recoverable axial strain, ε_a. This method of computation is the same as that which applies to an isotropic, linear elastic material under uniaxial stress conditions, and thus incorporates this idealization for any given repeated loading stress state. The specimen was allowed to consolidate under the new constant chamber pressure before the dynamic increment of stress was applied in the axial direction. This technique is widely used in determining resilient parameters.

As discussed in Chapter 2, when the stress-deformation relationships for granular materials are compared for a representative range of confining stress levels, the M_R is not constant but varies with the state of stress. Therefore, this nonlinear, stress dependent behaviour can be characterized by the regression line developed in the statistical analysis of the values of M_R calculated for the range of stresses. In such an analysis, the dependent variable is M_R, and the independent variable is some appropriate stress parameter such as σ_3 (cell pressure) or θ (the sum of the principal stresses).

The following discussion illustrates the necessity of applying the above procedure for calculating M_R. The data are taken from the static constant confining pressure test on Specimen No. 8.

σ_3 = 20.7 kPa ε_ℓ = .0003855

σ_d = 37.27 kPa ε_a = .0009637

Use of the uniaxial stress-strain relationship results in the following calculated values of M_R and ν_R for this data:

$$M_R = \frac{\sigma_d}{\varepsilon_a} = \frac{37.37}{.0009637} = 38.672 \text{ MPa}$$

$$\nu_R = \frac{\varepsilon_\ell}{\varepsilon_a} = \frac{.0003855}{.0009637} = 0.4$$

Considering another stress level:

σ_3 = 69 kPa ε_ℓ = .0005085

σ_d = 186.34 kPa ε_a = .0014251

$$M_R = \frac{\sigma_d}{\varepsilon_a} = \frac{186.34}{.0014251} = 130.755 \text{ MPa}$$

$$\nu_R = \frac{\varepsilon_\ell}{\varepsilon_a} = \frac{.0005085}{.0014251} = 0.37$$

4.1.1 Statistical Analysis of Data

Statistical analysis of the data gathered during the test series was necessary in order to develop predictive equations for the resilient parameters. The test data (static and dynamic) were analyzed using linear regression techniques to correlate the calculated value of M_R from each specimen with various stress parameters: σ_3;σ_1/σ_3; σ_d; and Θ, the sum of the principal stresses.

A comparison of the various stress parameters (models) made possible the selection of the models which most accurately fit the laboratory data. The following models were chosen to represent the resilient modulus-stress relationship:[17]

$$M_R = k_1 \, \Theta^{k_2} \tag{2-4}$$

or

$$M_R = k_1' \, \sigma_3^{k_2'} \tag{2-3}$$

where:

$\Theta = \sigma_1 + 2\sigma_3$,

σ_1 = major principal stress;

σ_3 = minor principal stress; and

k_1, k_2, k_1' and k_2' are material constants from regression analysis.

Table 4-1 summarizes the parameters developed for the resilient modulus-stress relationships. (The resilient modulus is presented as a function of the sum of the principal stresses, and as a function of σ_3).

Significantly, all further test data computations in this study are based on the observation that the resilient modulus of the base or subbase course material depends closely on the sum of the principal stresses, i.e., the relationship:

$$M_R = k_1 \Theta^{k_2} \tag{2-4}$$

From a theoretical point of view, there is an inherent weakness in the application of Equation 2-3 as the modulus determined in this equation is essentially for the axial direction only. In the lateral directions, the modulus depends on the axial stress as well as the lateral stress, so that the moduli are not the same in the three orthogonal directions. On this basis, it seems that the mean of the three principal stresses should be used to compute the modulus, rather than σ_3 alone[27].

Data collected from each test type (static and dynamic) yielded different material constants for the resilient parameters for the same specimen as shown in Table 4-1.

TABLE 4-1

REGRESSION EQUATIONS FOR M_R FROM PRIMARY TEST DATA

Site	Specimen	Material Type	Test* Type	$M_R=f(\Theta)$	Correlation Coefficient	Standard Error	$M_R=f(\sigma_3)$	Correlation Coefficient	Standard Error
D	SC-4	"A",crushed stone,upper	D	$2.181\ \Theta^{.63}$	.981	4.102	$6.699\ \sigma_3^{.617}$	.9012	8.9474
D	SC-8	"A",crushed stone,lower	D	$1.9409\Theta^{.6806}$	.9882	3.2206	$6.898\ \sigma_3^{.673}$	.9094	8.6186
B	SG-12	"A",natural gravel	D	$1.128\ \Theta^{.82}$	.9969	2.2328	$2.176\ \sigma_3^{.1.112}$	.9303	9.4168
B	SG-16	"A",natural gravel	D	$1.8238\Theta^{.6849}$	.9802	3.7756	$4.6913\sigma_3^{.775}$	.8947	8.6724
B	SG-17	"B",natural gravel	D	$1.618\ \Theta^{.6744}$	.9915	2.4346	$5.505\ \sigma_3^{.675}$	.9401	6.2432
B	SG-18	"C",natural gravel	D	$1.734\ \Theta^{.676}$	.981	4.4938	$6.399\ \sigma_3^{.64}$	.9074	9.4111
C	SC-19	"A",crushed stone	D	$2.558\ \Theta^{.655}$	.9839	3.9852	$7.6599\sigma_3^{.701}$	.8923	10.2394
C	SC-20	"B",crushed stone	D	$3.941\ \Theta^{.5893}$	.988	3.7521	$12.836\ \sigma_3^{.587}$	.9131	9.7393
A	SC-G-21	"A",blend	D	$2.8073\Theta^{.6193}$	.9891	3.3907	$8.5148\sigma_3^{.6233}$	.9256	8.3558
D	SC-4	"A",crushed stone,upper	S	$2.5379\Theta^{.6593}$	.992	3.2957	$7.293\ \sigma_3^{.674}$	.9807	7.0881
D	SC-8	"A",crushed stone,lower	S	$.7352\Theta^{.8677}$	.9963	2.155	$3.128\ \sigma_3^{.864}$	.9719	7.3067
B	SG-12	"A",natural gravel	S	$.806\ \Theta^{.87}$	.9975	4.6018	$3.648\ \sigma_3^{.854}$	.9674	10.7488
B	SG-16	"A",natural gravel	S	$1.1658\Theta^{.805}$	.9965	2.5856	$4.1566\sigma_3^{.8152}$	.975	8.0351
B	SG-17	"B",natural gravel	S	$.948\ \Theta^{.82}$	.9987	1.8099	$3.266\ \sigma_3^{.844}$	.9899	4.6374
B	SG-18	"C",natural gravel	S	$.988\ \Theta^{.785}$	.9971	1.7966	$2.027\ \sigma_3^{.961}$	.9702	7.9388
C	SC-19	"A",crushed stone	S	$1.132\ \Theta^{.824}$	.9966	2.7252	$3.7404\sigma_3^{.8629}$	.9738	8.7116
C	SC-20	"B",crushed stone	S	$1.472\ \Theta^{.8012}$	.9895	5.831	$5.3\ \sigma_3^{.812}$	.9655	10.478
A	SC-G-21	"A",blend	S	$1.414\ \Theta^{.7943}$	.9976	2.4054	$4.8739\sigma_3^{.811}$	.9774	8.9591

* D = Dynamic S = Static

4.1.2 Preliminary Testing

Before the primary test series was initiated, it was necessary to recognize factors such as stress duration and stress repetition that might influence the resilient response of granular materials. These effects govern the basic testing procedures in terms of the numbers of repetitions of each stress level to be applied and the duration of the applied stress pulse. With the completion of these preliminaries, it was then possible to proceed with the primary testing, and through this experience to minimize any errors that might occur in the course of the testing.

Figure 4-1 and 4-2 show the variation in resilient modulus with stress repetitions for crushed limestone (SC-1) and natural gravel (SG-2), respectively. Importantly, nowhere does a stress repetition influence appear to show up. Figure 4-3 from Hicks (17) leads support to this observation, as he also discovered that the resilient stress-strain characteristics of granular materials were virtually the same after 50 to 100 load repetitions as after 25,000 repetitions.

Since vehicles do travel on a pavement structure at various speeds,particularly the important truck loadings, it was necessary to subject specimens to a range of stress pulse durations in order to ascertain if appreciable error would be introduced by the use of only

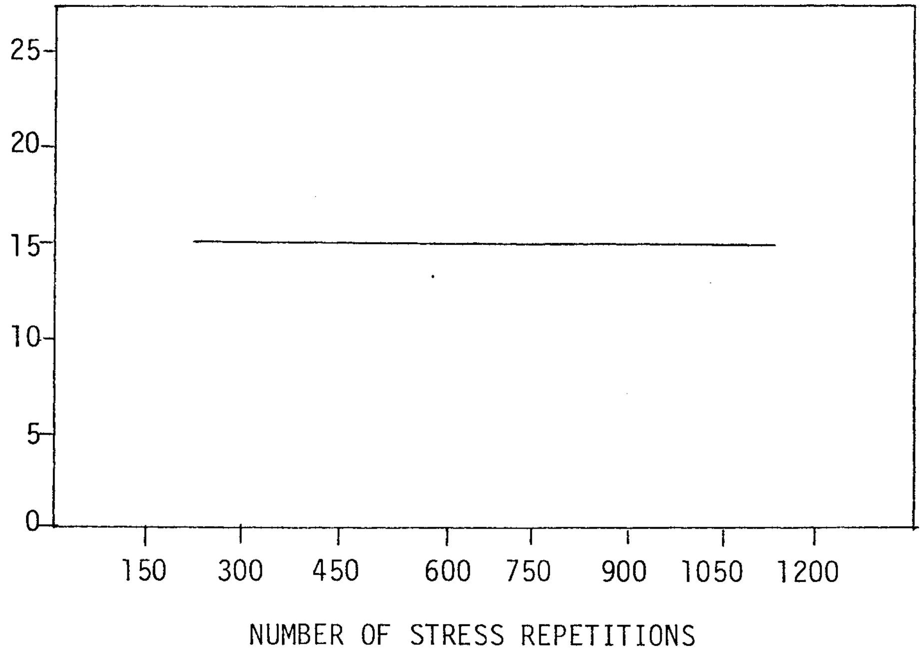

FIGURE 4-1 - Relationship of Resilient Modulus and Number of Stress Repetitions Crushed Limestone, SC-1, σ_1=85 kPa,σ_3=30 kPa

RESILIENT MODULUS, M_R, (MPa)

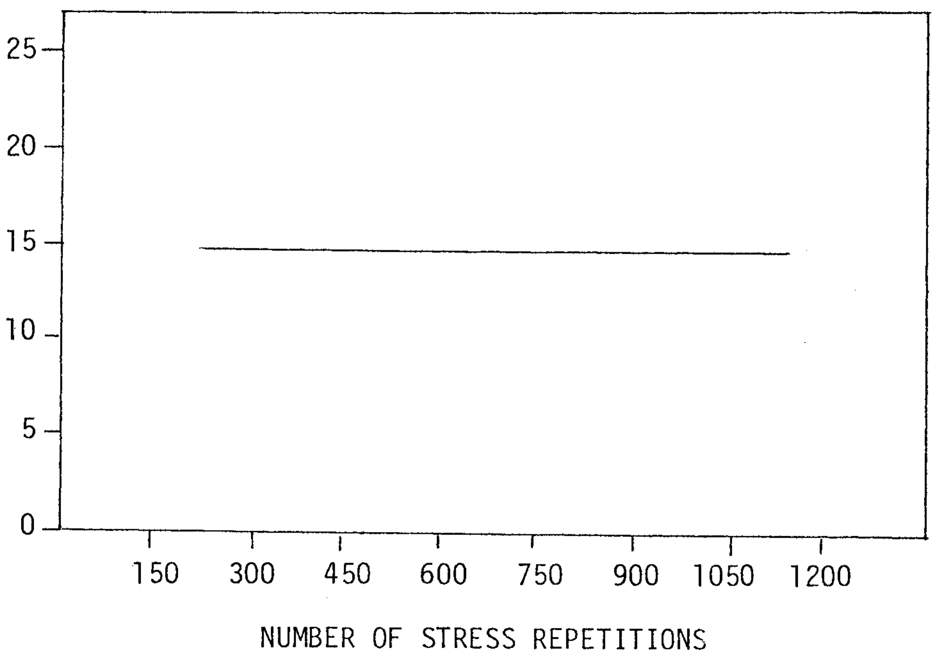

FIGURE 4-2 - Relationship of Resilient Modulus and Number of Stress Repetitions Gravel, SG-2, σ_1=85 kPa,σ_3=30 kPa

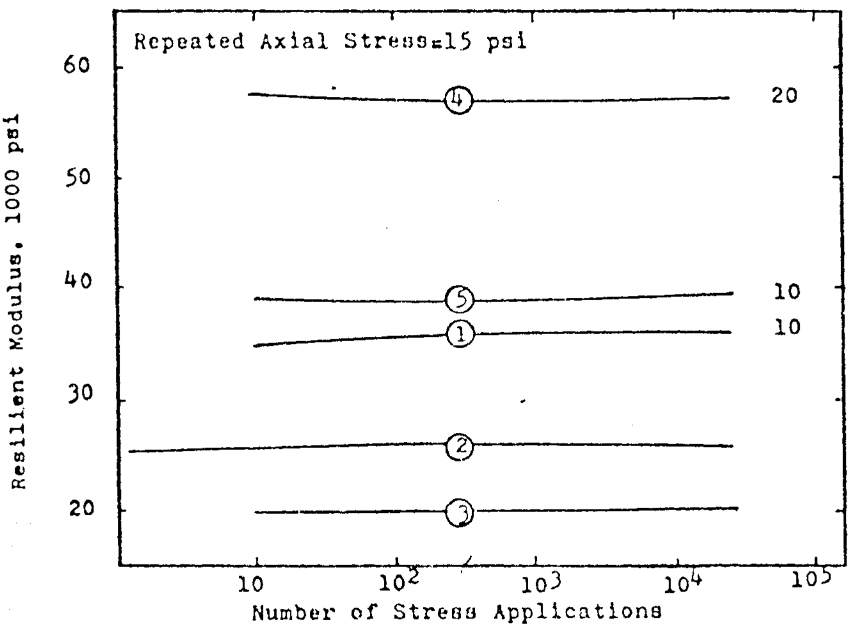

FIGURE 4-3 - Variation in Resilient Modulus and Poisson's Ratio with Number of Stress Repetitions. Dry Crushed Aggregate. Specimen No. C(00)-P1 (from Hicks, 17) one pulse time. Table 4-2 shows the variation in resilient modulus and Poisson's ratio for dynamic testing where the stress pulse duration varies from 0.1 second to 0.5 second. It can be seen that the resilient modulus of the crushed limestone specimen decreased by about 1 percent as the pulse duration increased to 0.5 second, and the variation in resilient Poisson's ratio was about 2 percent. Only slight changes were observed in the response of the natural gravel specimen. In general, it appeared that a single stress duration-one pulse time of 0.1 second could be used throughout the primary test series and each specimen could be tested over the whole range of stress levels, including both dynamic and static tests.

4.2 RESULTS OF PRIMARY TEST SERIES

4.2.1 Typical Test Results for Resilient Modulus and Resilient Poisson's Ratio

The primary test results prove that the resilient properties of granular material are much more significantly affected by changes in the state of stress than by changes in any other factors examined in the study.

The effects of confining pressure on the resilient modulus are illustrated in Figures 4-4, 4-5 and 4-6. These figures are typical of the entries in Table 4-3. The materials presented in these figures are crushed limestone, natural gravel and a blend of crushed stone and natural gravel. Figures 4-4 shows the data extracted from both the

TABLE 4-2

EFFECT OF STRESS DURATION ON GRANULAR MATERIALS

Location	Material Type	σ_3 kPa	σ_1 kPa	Test Type	Duration Sec.	M_R MPa	ν_R
Site D	Crushed Limestone	30	90	Dynamic	0.1	52.565	.34
	Crushed Limestone	30	90	Dynamic	0.3	52.307	.33
	Crushed Limestone	30	90	Dynamic	0.5	52.017	.323
Site B	Natural Gravel	30	90	Static	0.1	65.212	.28
	Natural Gravel	30	90	Static	0.3	65.210	.28
	Natural Gravel	30	90	Static	0.5	65.210	.28

Crushed Limestone, SC-1 (Dynamic Case)
Natural Gravel, SG-2 (Static Case)

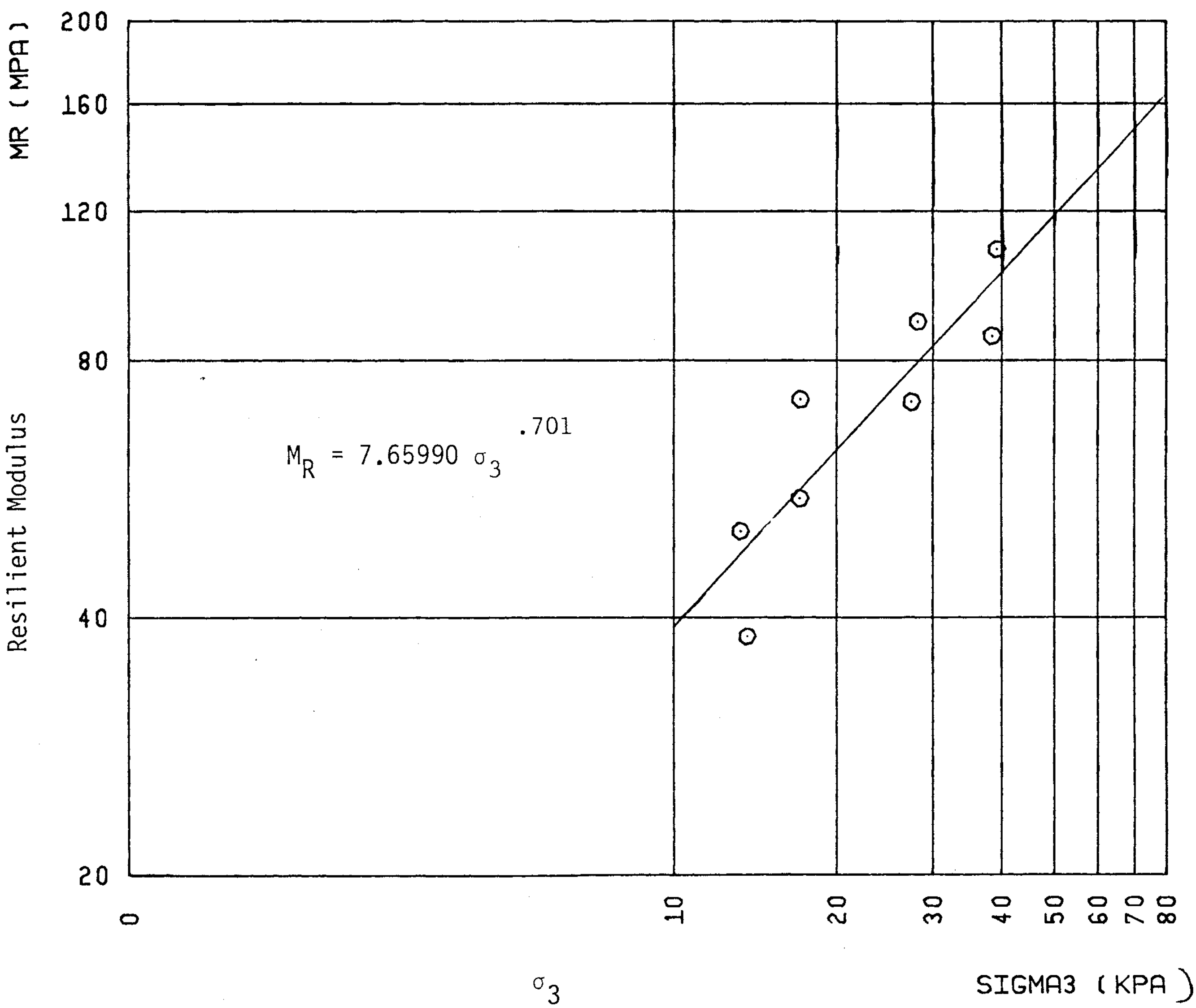

FIGURE 4-4a - Resilient Modulus (M_R) as a Function of σ_3 for Crushed Limestone (SC#19), Dynamic Case (σ_1 = 180 kPa)

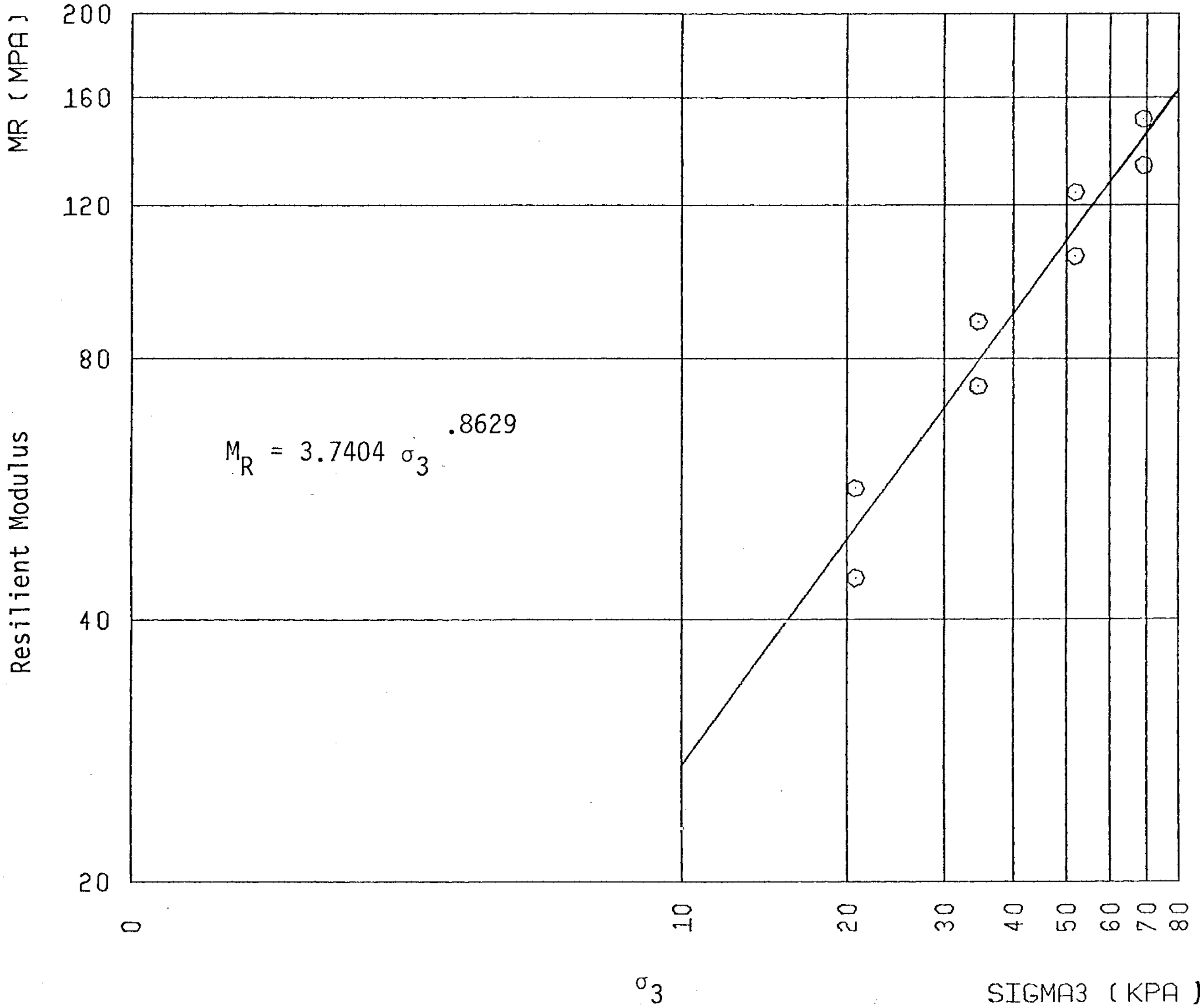

FIGURE 4-4b - Resilient Modulus (M_R) as a Function of σ_3 for Crushed Limestone (SC#19), Static Case (σ_1 = 180 kPa)

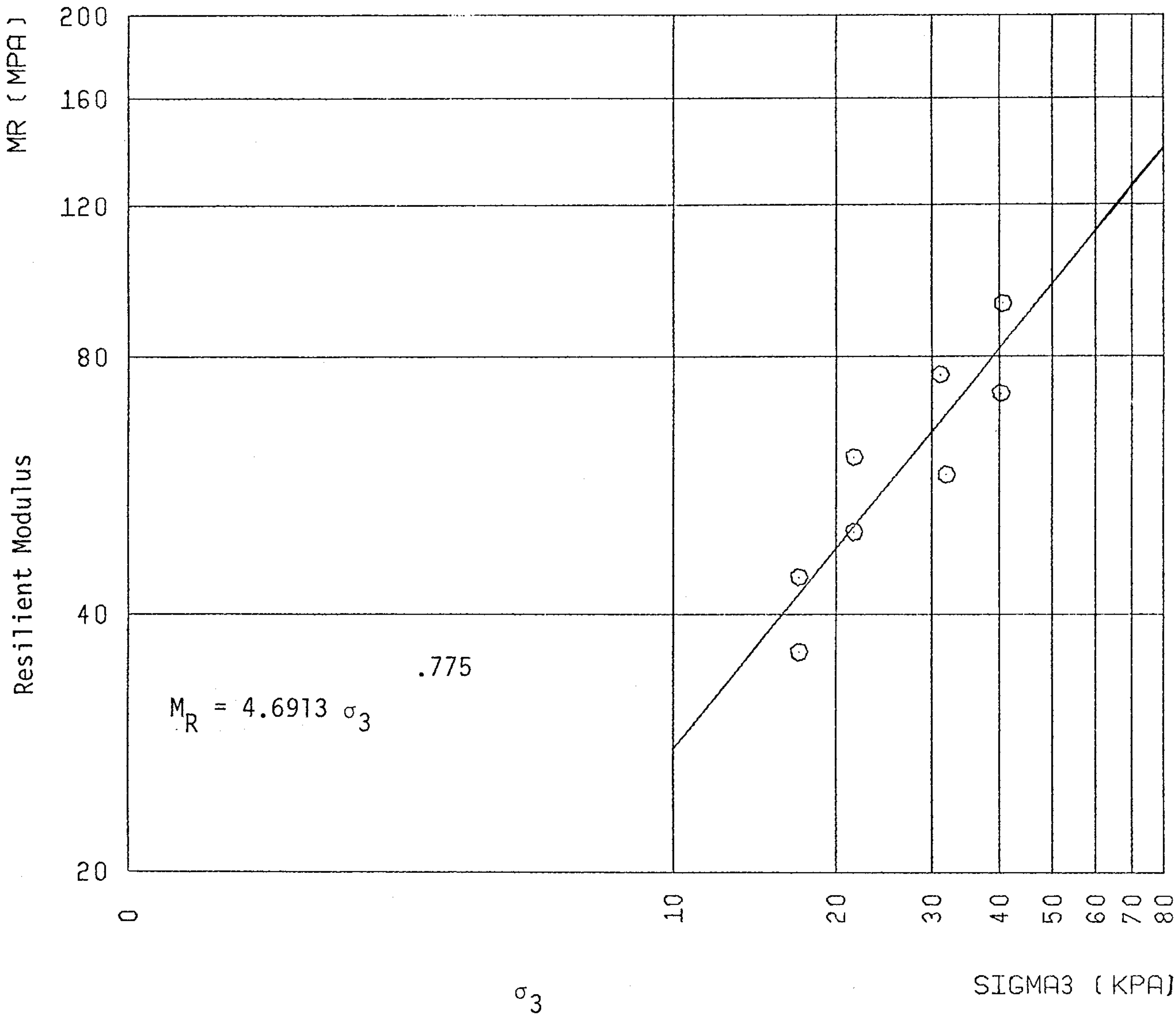

FIGURE 4-5a - Resilient Modulus (M_R) as a Function of σ_3 for Natural Gravel Specimen (SG#16), Dynamic Case (σ_1 = 180 kPa)

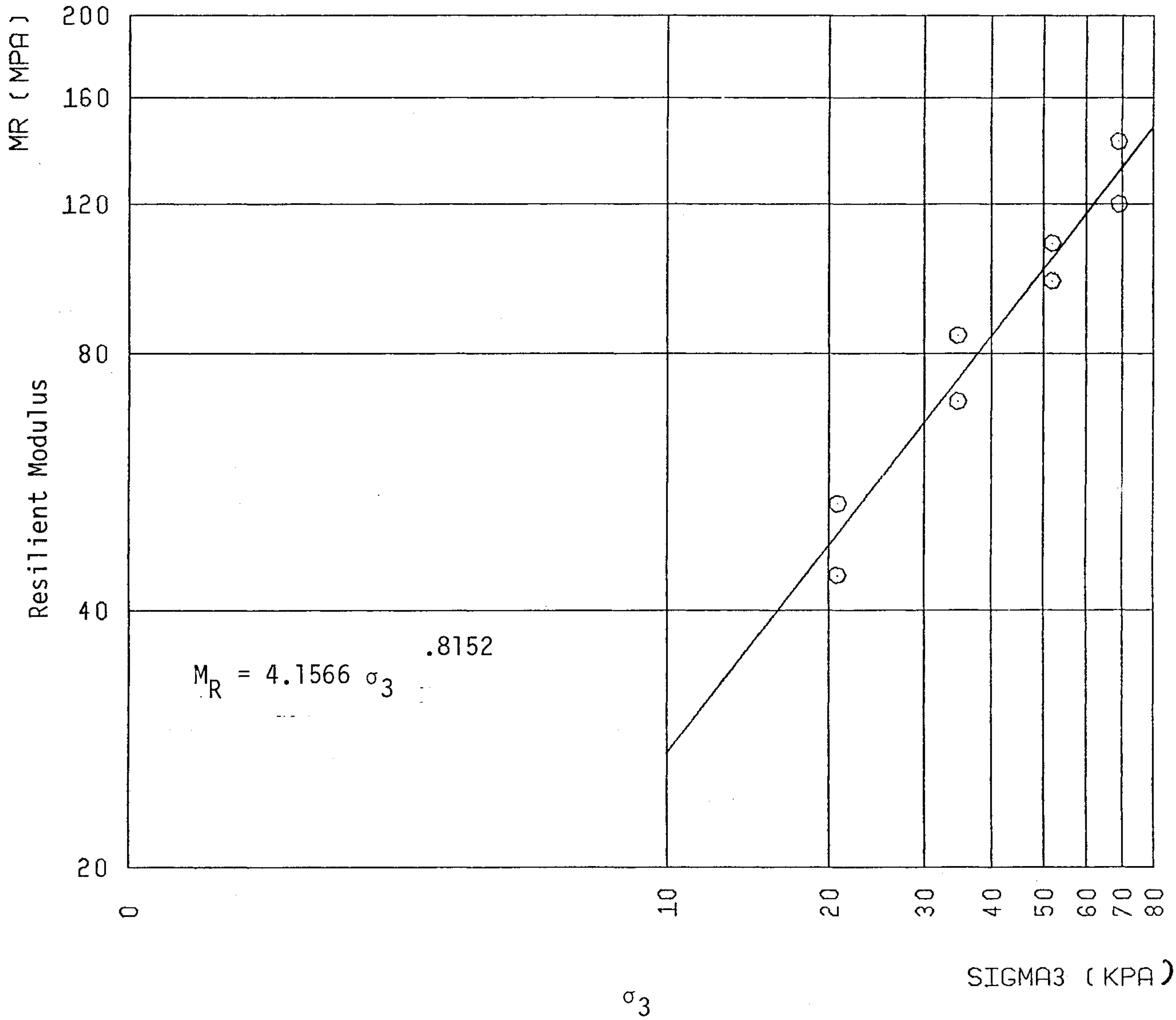

FIGURE 4-5b - Resilient Modulus (M_R) as a Function of σ_3 for Natural Gravel Specimen (SG#16), Static Case (σ_1=180 kPa)

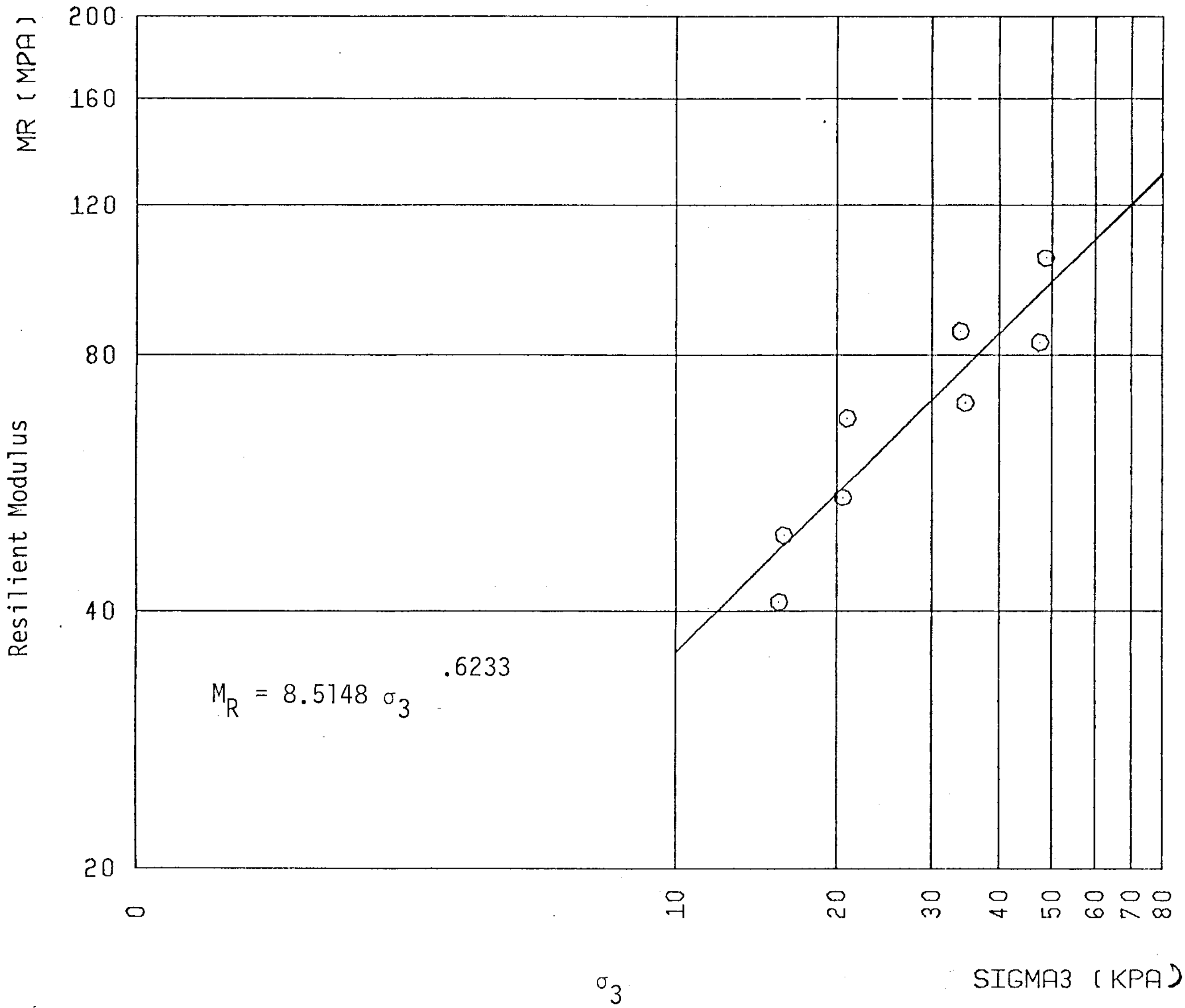

FIGURE 4-6a - Resilient Modulus (M_R) as a Function of σ_3 for Blended Specimen (SC-G#21), Dynamic Case (σ_1 = 180 kPa)

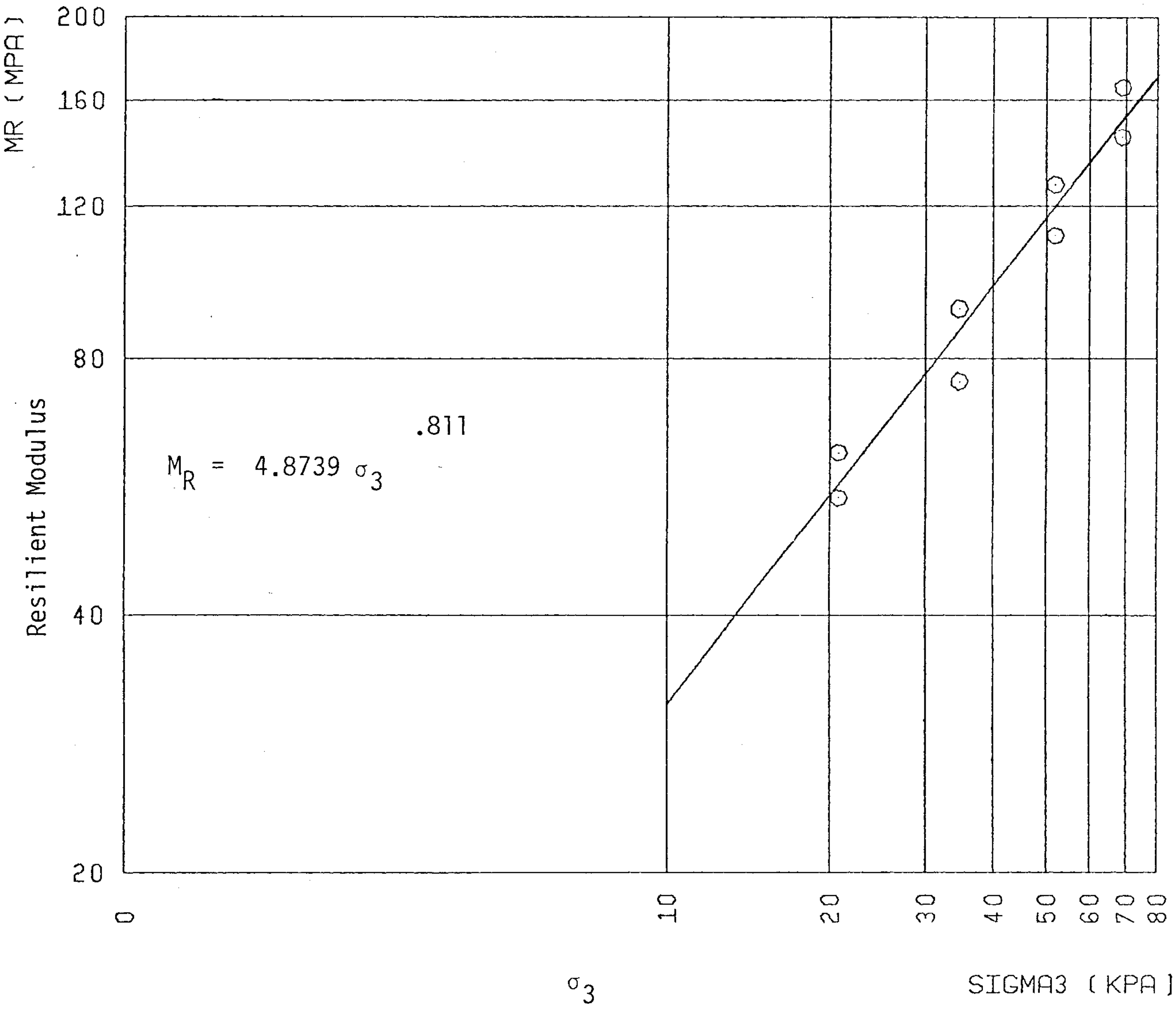

FIGURE 4-6b - Resilient Modulus (M_R) as a Function of σ_3 for Blended Specimen (SC-G#21),Static Case (σ_1 = 180 kPa) static and dynamic test results for the crushed limestone. In the dynamic test, the confining pressure, σ_3, increases from 13 to 40 kPa and the resilient modulus increases by around 270 percent. In the static test, σ_3, increases from 20 to 70 kPa and the resilient modulus increases almost about 300 percent. As regards to the natural gravel and the blended specimen, Figures 4-5 and 4-6 show a similar increase in the resilient modulus.

The variations in the resilient modulus at each value of σ_3 in Figures 4-4, 4-5 and 4-7 are indicative of the effects of axial stress, σ_1, on the resilient response, which is significant. Figures 4-7, 4-8 and 4-9 show the modulus versus σ_1 at various levels of σ_3 for the same three specimens illustrated in Figures 4-4, 4-5 and 4-6. Clearly, the major principal stress exerts a significant influence on the resilient modulus and this helps explain the scatter in the data shown in Figures 4-4, 4-5 and 4-6.

Figure 4-10 shows the variation in resilient modulus with principal stress ratio. The effect of the axial stress on the modulus is again clearly seen in this figure. At any σ_3 level, the M_R increases as the principal stress ratio increases, and at higher σ_3 levels, the effect is more obvious. In general, there is an increase in the resilient modulus of the samples as axial stress (or principal stress ratio) increases.

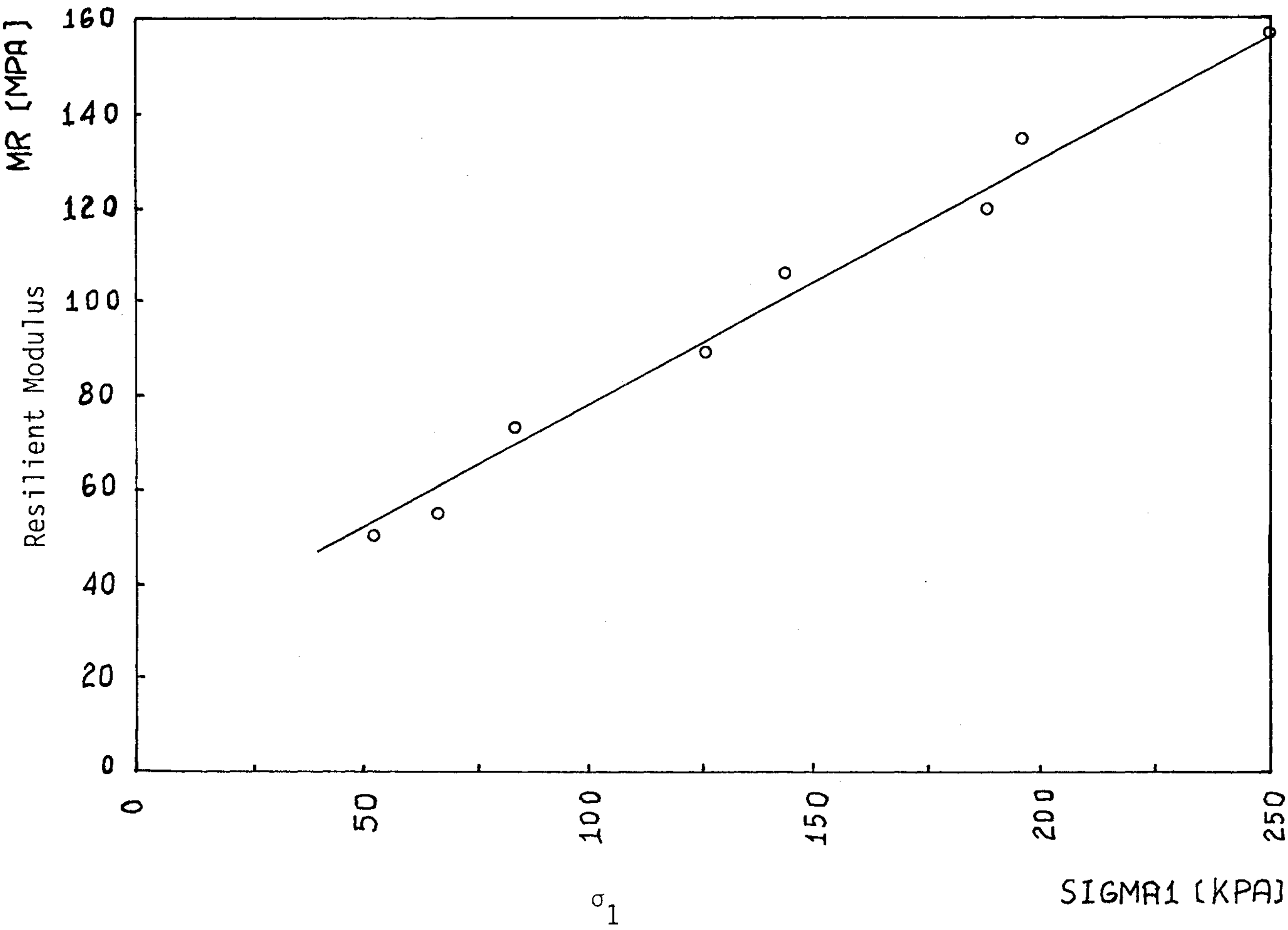

FIGURE 4-7 - Resilient Modulus vs. Major Principal Stress for Crushed Limestone (SC#19)

(σ_3 = 50 kPa)

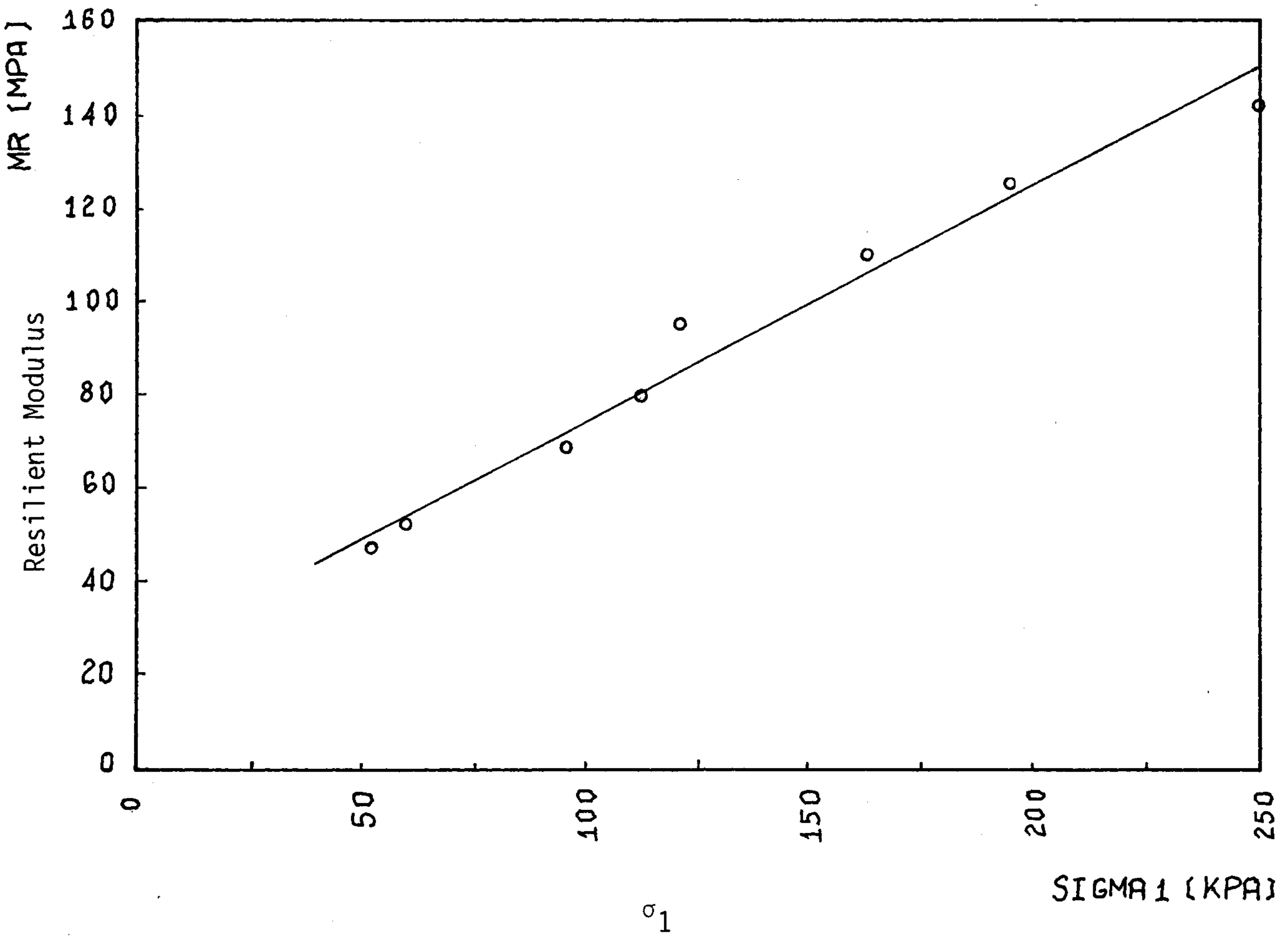

FIGURE 4-8 - Resilient Modulus vs. Major Principal Stress for Natural Gravel (SG#16)

(σ_3 = 50 kPa)

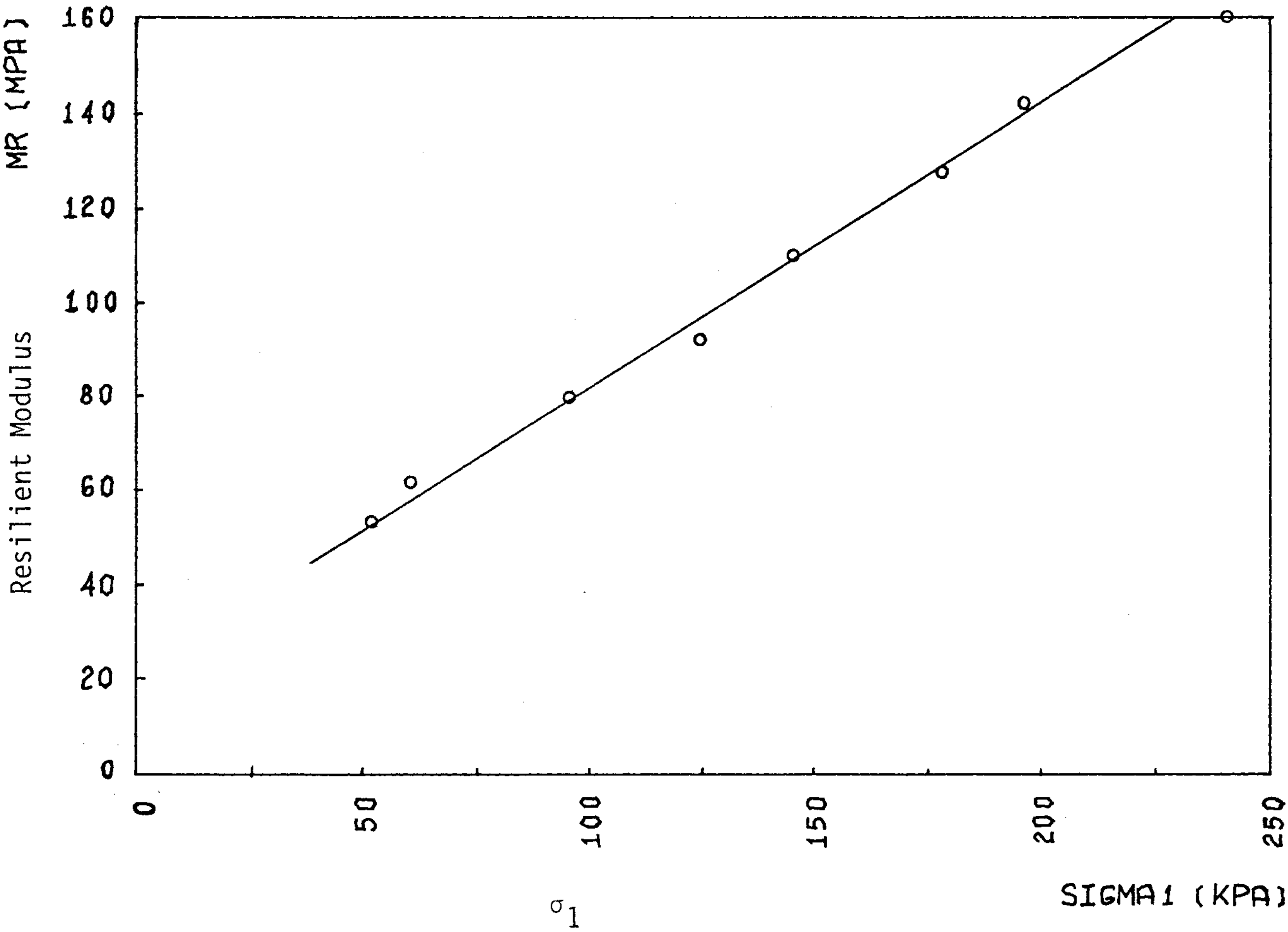

FIGURE 4-9 - Resilient Modulus vs. Major Principal Stress
for Blended Material (SC-G#21)
(σ_3 = 50 kPa)

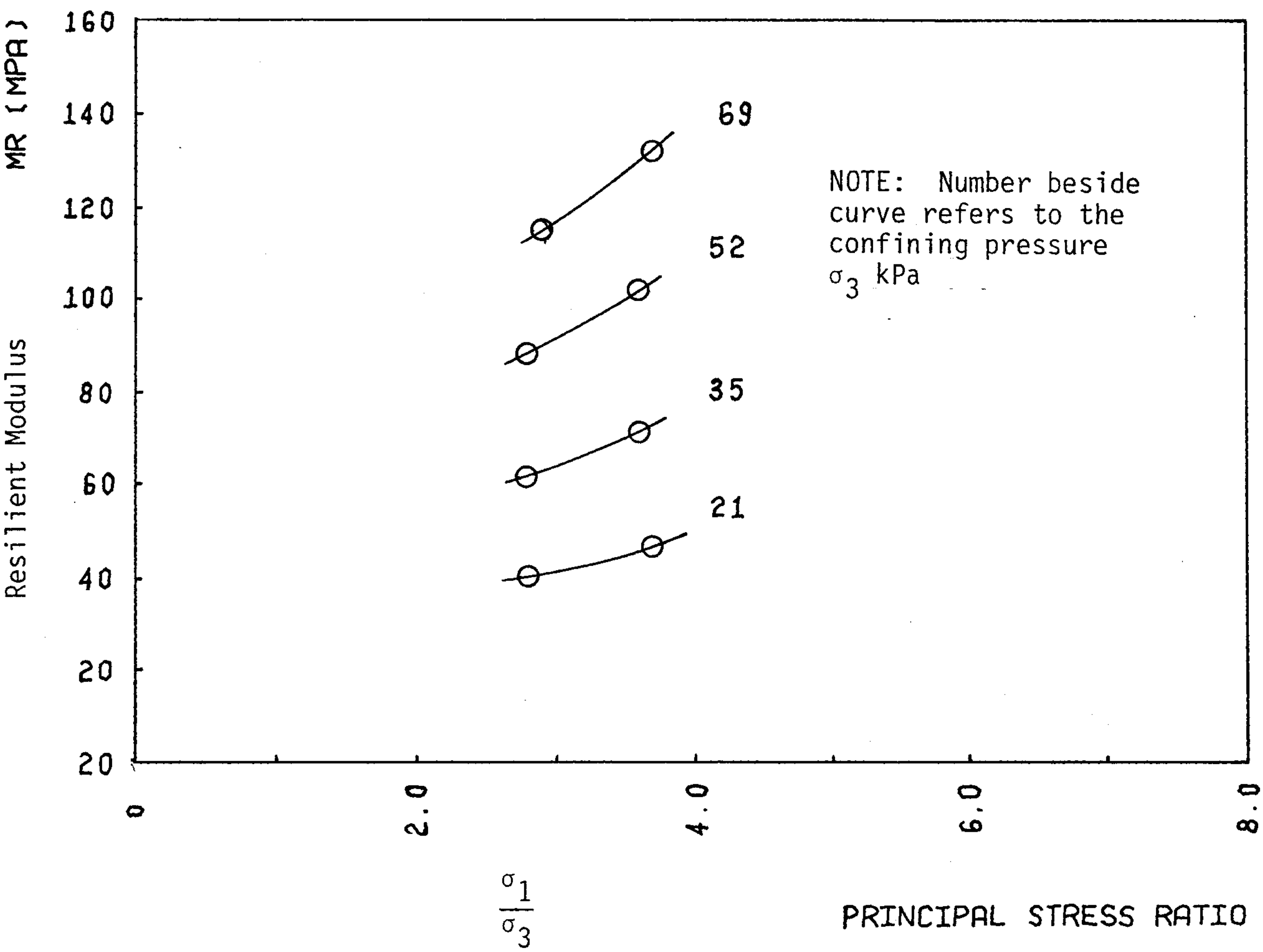

FIGURE 4-10 - Variation of Resilient Modulus with Principal Stress Ratio (Crushed Stone SC-8)

The effect of the sum of principal stresses on the resilient modulus is shown in Figures 4-11, 4-12 and 4-13 which indicates the relationship for the same three specimens discussed previously. The higher correlation coefficients and lower standard errors - indicating the clear advantage of the Θ model over the σ_3 model (Figures 4-4, 4-5, 4-6, 4-11, 4-12 and 4-13), are also seen from the testing of other specimens. It is clear that M_R increases as Θ increases from 70 kPa to 300 kPa. Although Figures 4-4 through 4-13 give data from just three typical specimens, the overall trend of the proportional increase in M_R to the increase in Θ still holds.

The stress-dependent nature of resilient Poisson's ratio is shown in Figure 4-14. The laboratory data collected from testing all of the specimens is best expressed by the formula shown on Figure 4-14 in which ν_R is a function of principal stress ratio (σ_1/σ_3). The figure shows this relationship for the dynamic test data obtained for a typical crushed limestone specimen. The flat slope of the curve falls in the range of σ_1/σ_3 of 2 to 7. This observation indicates that, since this range of stress ratios is typical of that found in pavement systems, pavement analyses based on a representative constant value of Poisson's ratio for a given aggregate in granular layers might be appropriate. The validity of this observation is strengthened by the fact that the dynamic test results for all specimens yielded values of Poisson's ratio very close to those shown in Figure 4-14 for the same range of σ_1/σ_3.

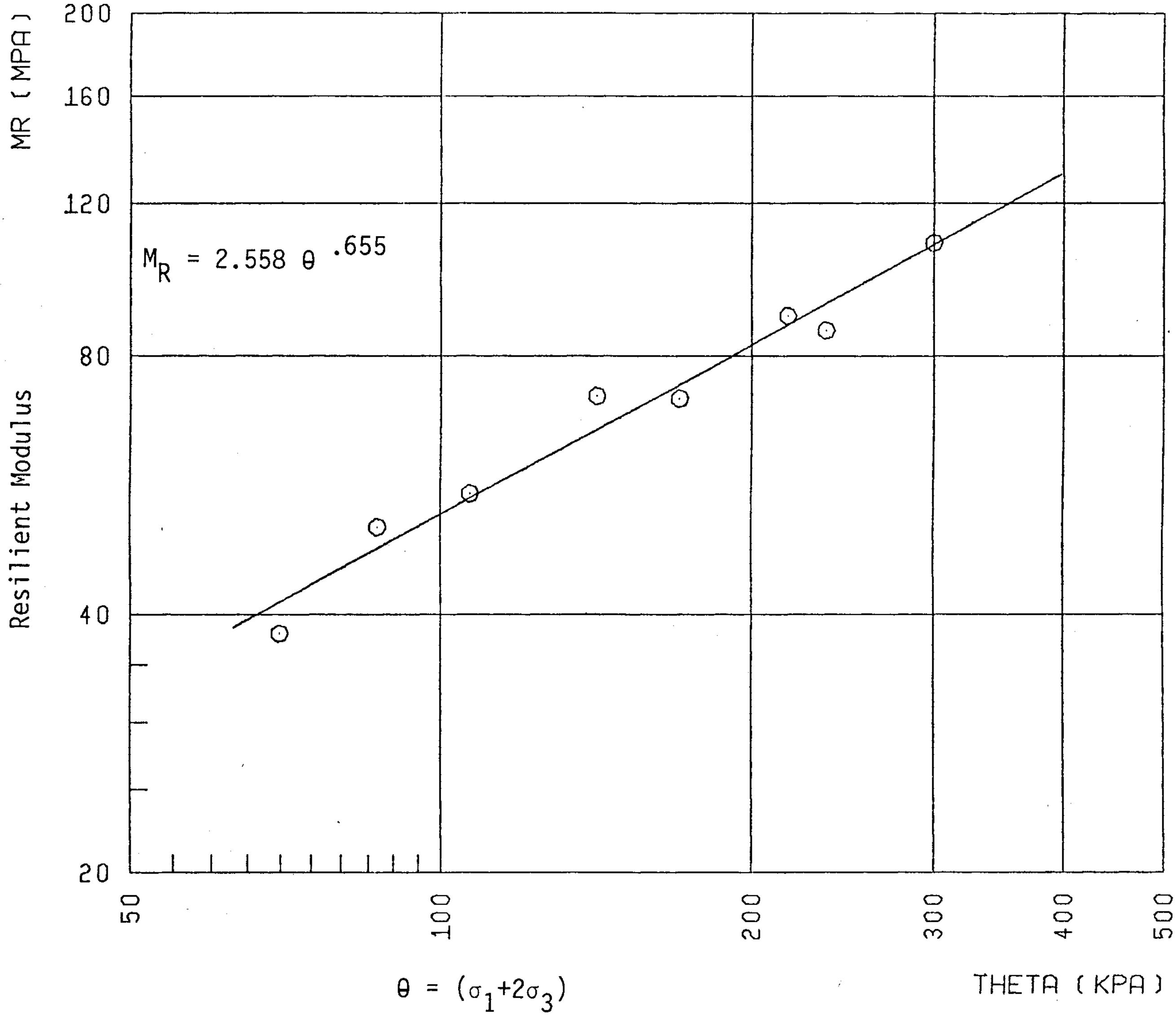

FIGURE 4-11a - Resilient Modulus (M_R) as a Function of the Sum of the Principal Stresses (Θ) Crushed Limestone Specimen (SC#19), Dynamic Case

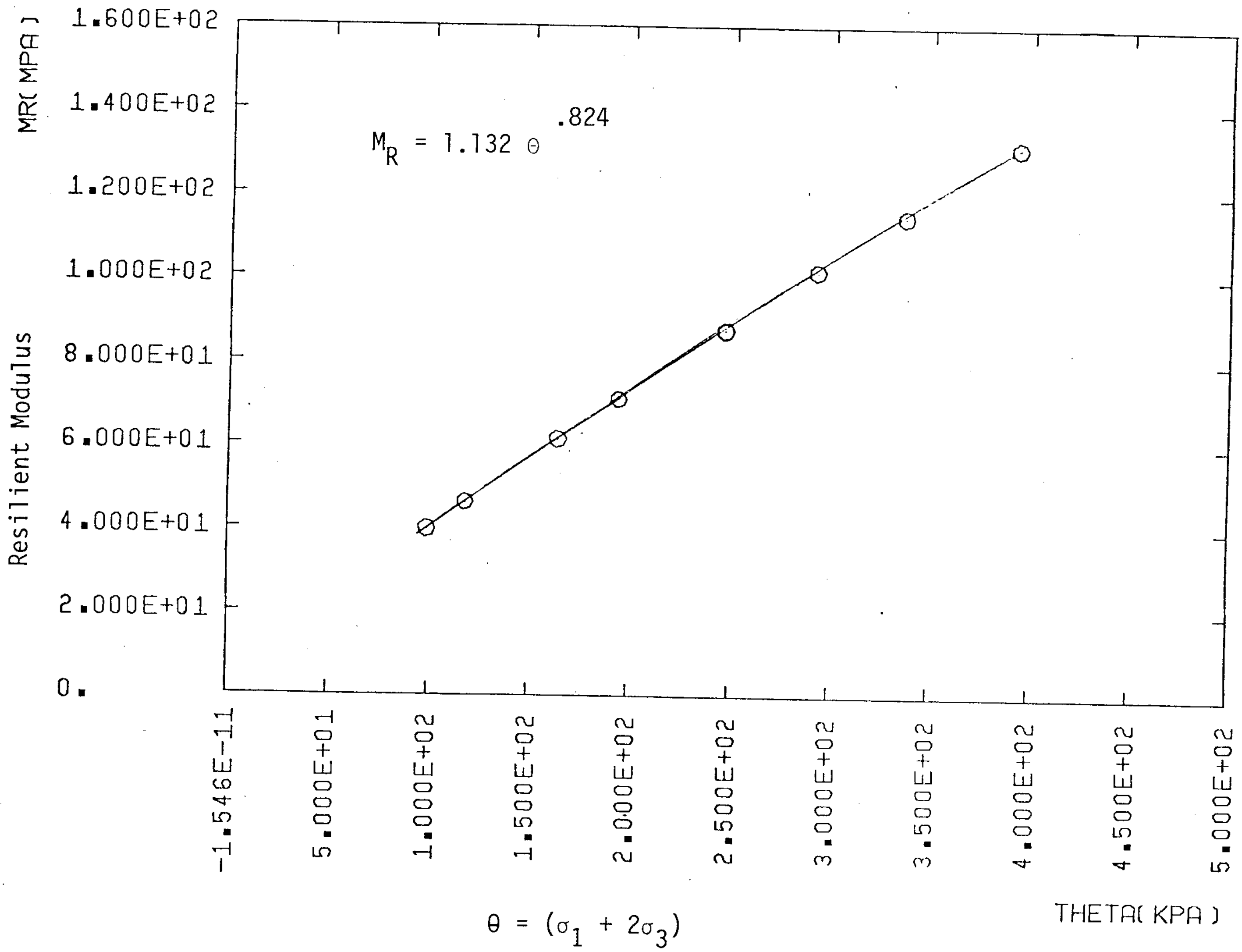

FIGURE 4-11b - Resilient Modulus (M_R) as a Function of Θ
Crushed Limestone Specimen (SC#19) Static Case

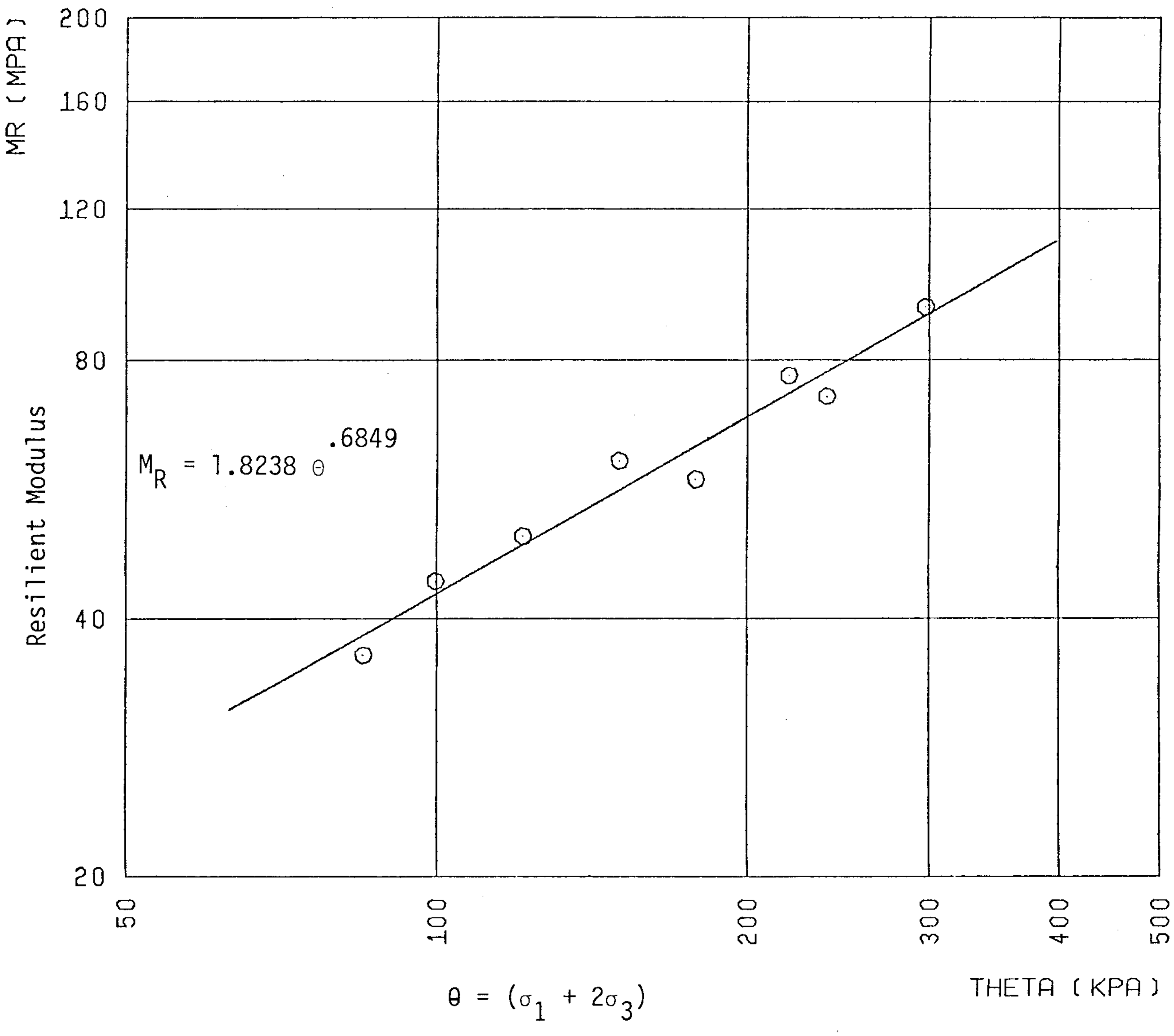

FIGURE 4-12a - Resilient Modulus (M_R) as a Function of the Sum of the Principal Stresses (θ)
Natural Gravel Specimen (SG#16), Dynamic Case

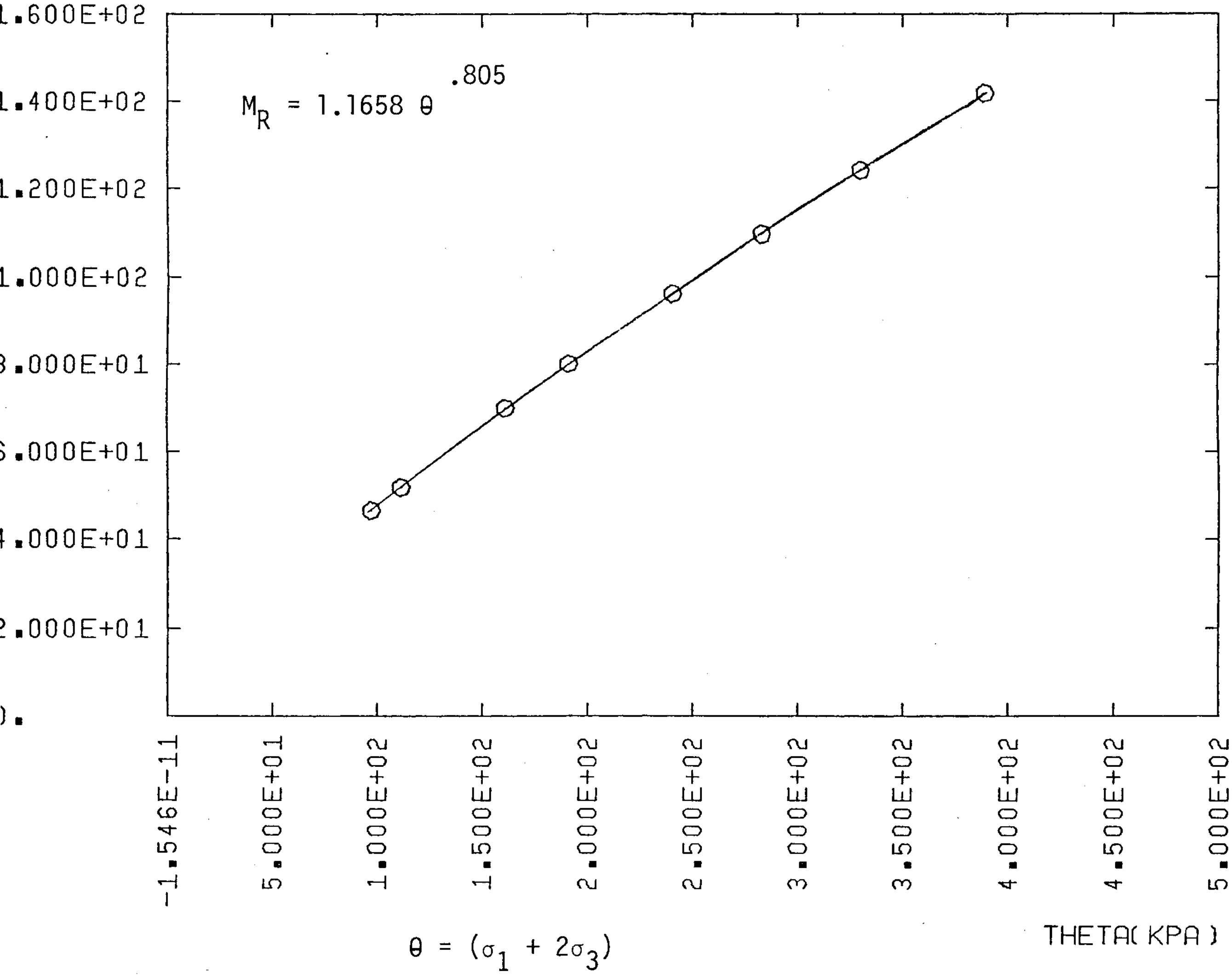

FIGURE 4-12b - Resilient Modulus (M_R) as a Function of θ
Natural Gravel Specimen (SG#16) Static Case

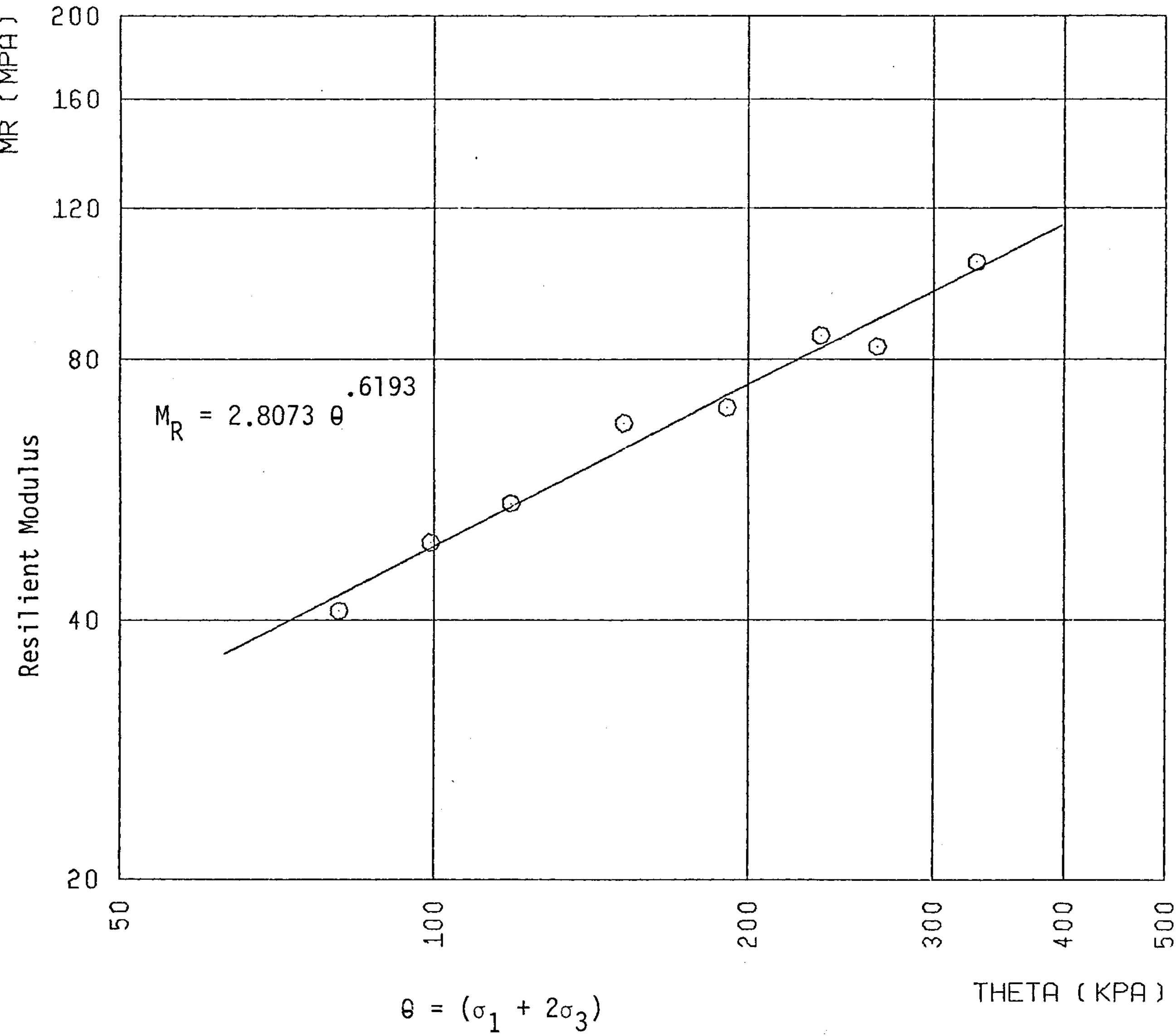

FIGURE 4-13a - Resilient Modulus (M_R) as a Function of the Sum of the Principal Stresses
Blend Specimen (SC-G#21), Dynamic Case

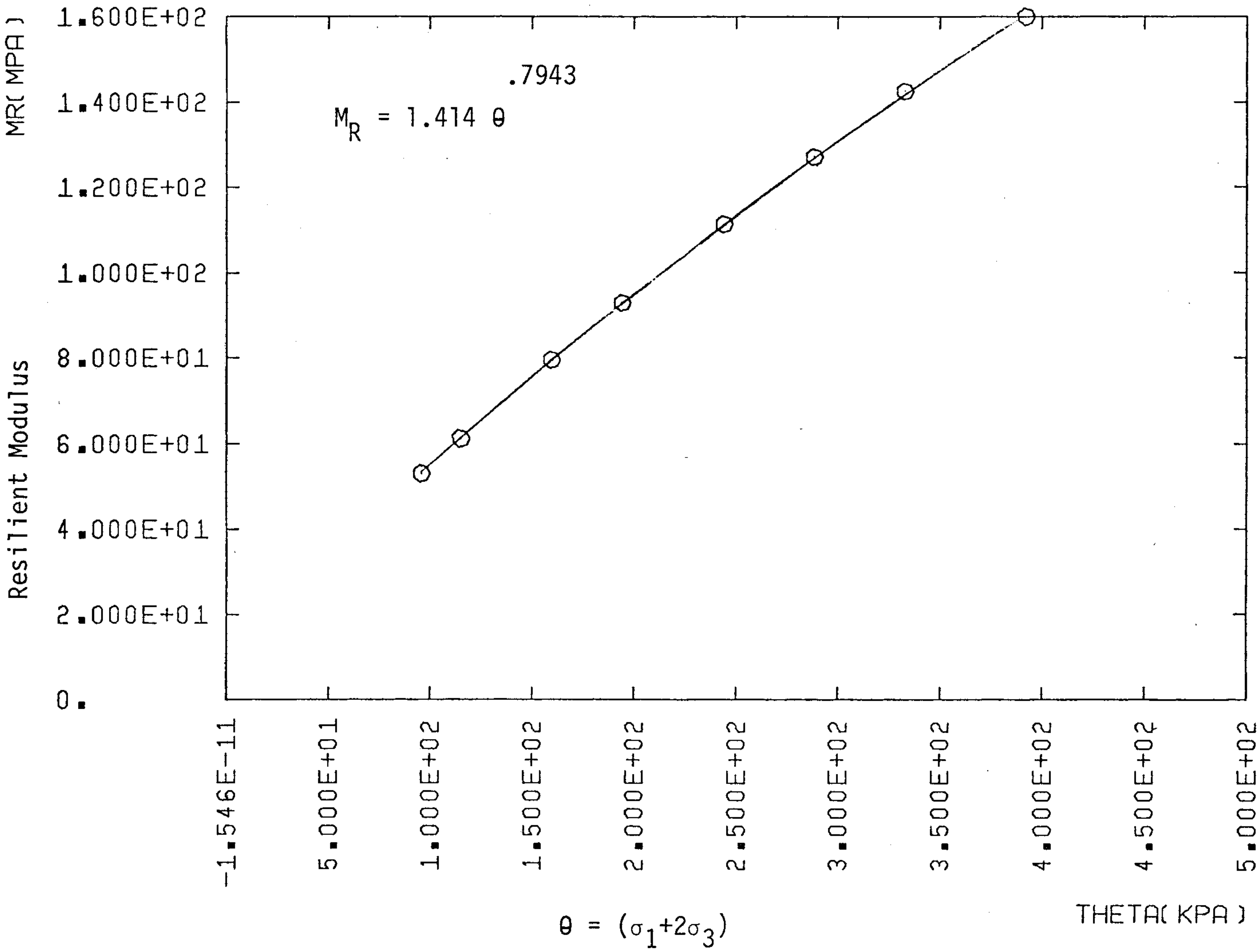

FIGURE 4-13b - Resilient Modulus (M_R) as a Function of θ

Crushed Limestone Specimen (SC-G#21), Static Case

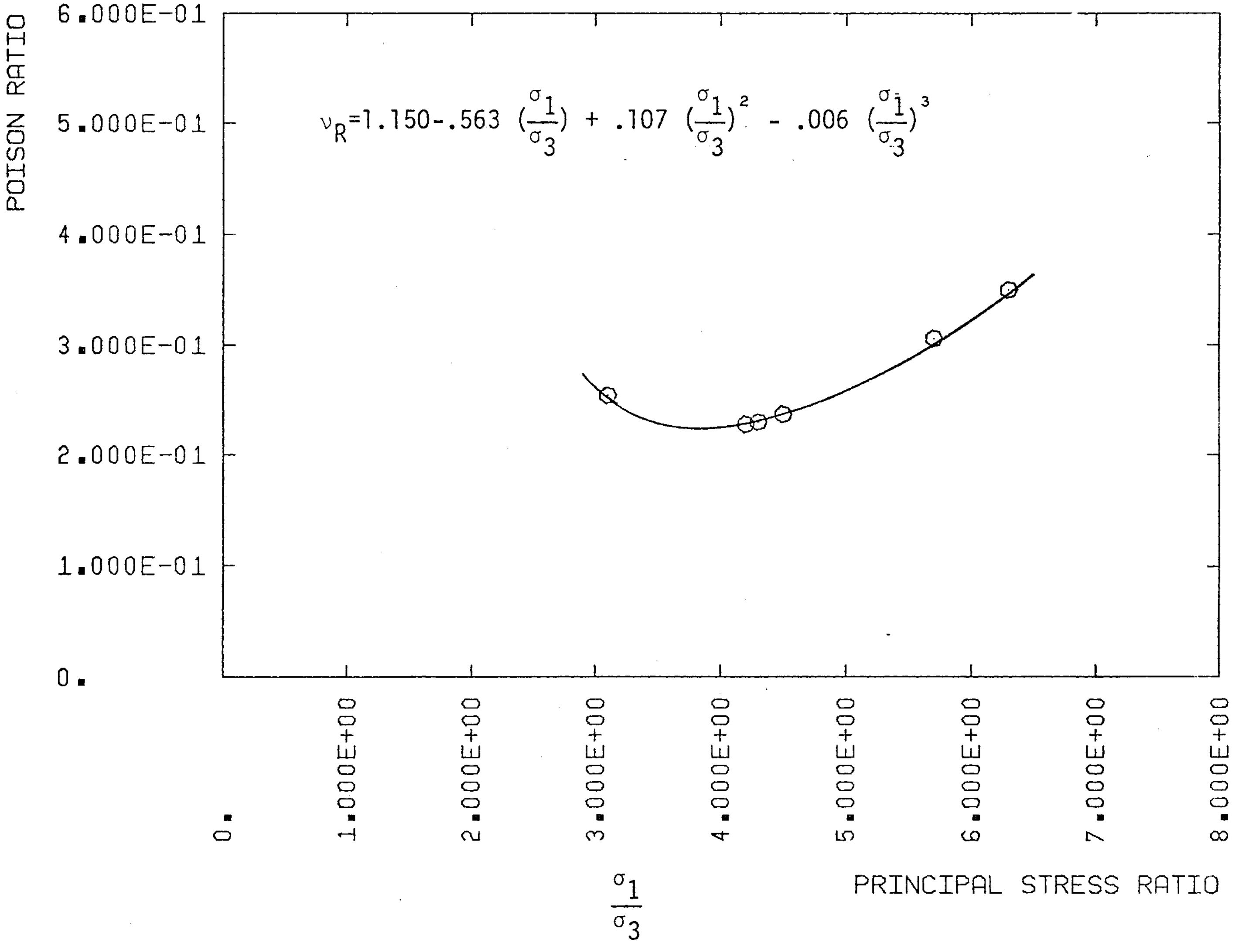

FIGURE 4-14 - Resilient Poisson's Ratio (ν_R) as a Function of Principal Stress Ratio Crushed Limestone Specimen (SC#19)

4.2.2 Comparison of Results with Different Types of Granular Materials

Figures 4-15 through 4-20 show the effects of different aggregate types on the resilient modulus of the granular material specimens. The dynamic test data in Figure 4-15 show that the crushed limestone is associated with higher M_R values, the blended material with intermediate values, and the natural gravel with somewhat lower values. The values throughout the entire range of θ in the static test (Figure 4-16) show that the materials ,ranked in order of somewhat decreasing stiffness are, the blended material, crushed limestone, and natural gravel. From this figure, the values of the M_R of both the blended and crushed stone are very close. The reason why the crushed limestone shows a slightly lower M_R value than the blended material is the higher degree of saturation for the crushed limestone. In general, the crushed limestone was "stiffer" than the gravel. This was also true in California Bearing Ratio testing. Table 4-3 gives the CBR values of crushed limestone, blended and natural gravel material which are 112, 105 and 44, respectively. This CBR data confirms trends incorporated in many empirical designs, and semi-rational designs such as the AASHTO layer coefficients.

Similar observations can be made over the full range of various granular materials considered. Figures 4-17 and 4-18 show the materials ranked in the order of decreasing stiffness in both static and dynamic testing cases for a unsaturated-drained state, respectively. Figure 4-17 shows that in the static, unsaturated drained state, the materials are ranked in the order of decreasing stiffness, crushed limestone; blended

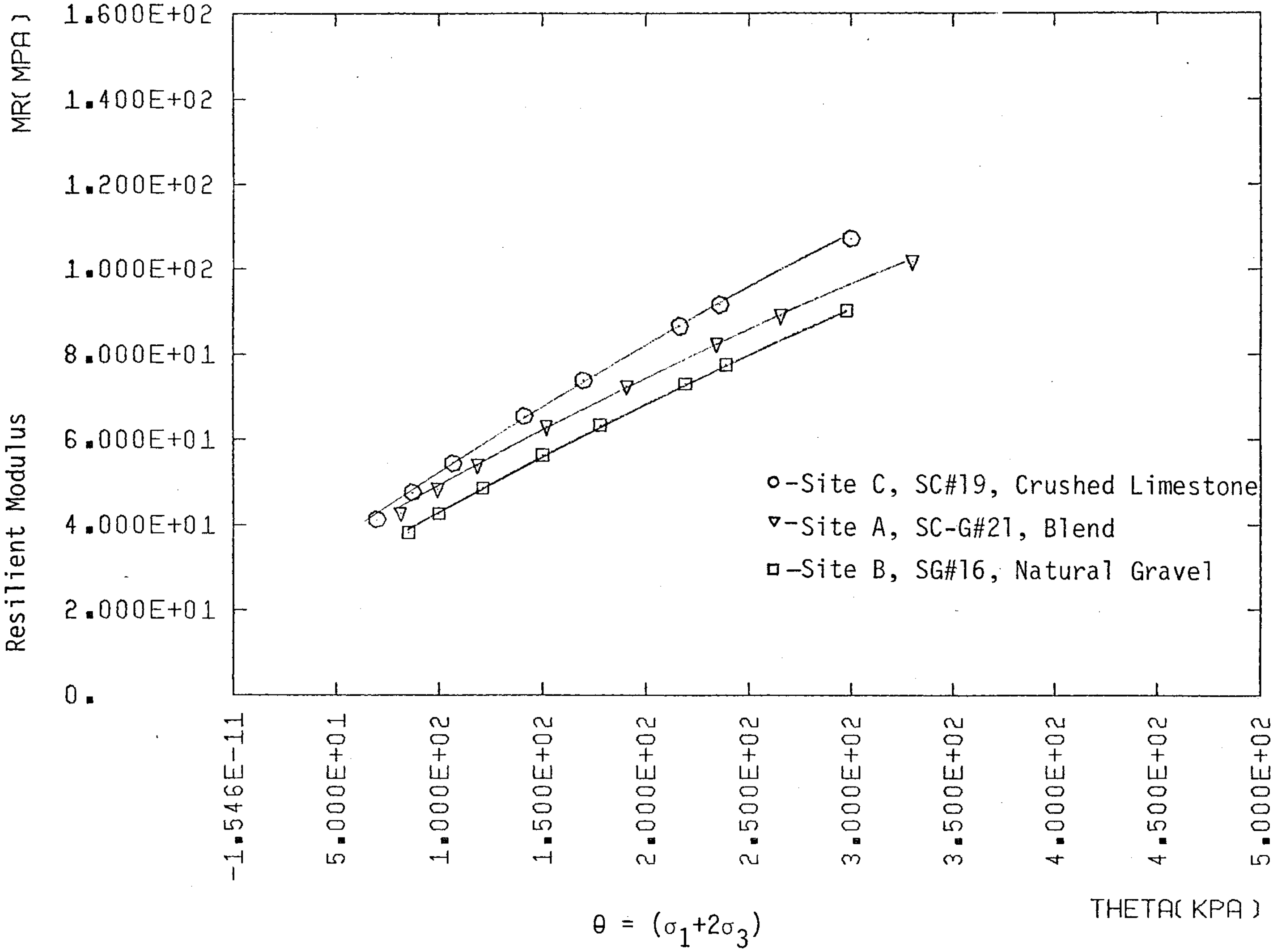

FIGURE 4-15 - Comparison of Typical Result of Resilient Modulus (M_R) With Different Types of Granular A Materials Crushed Limestone Specimen, Blend and Natural Gravel (SC#19, SC-G#21 and SG#16),(Dynamic Case)

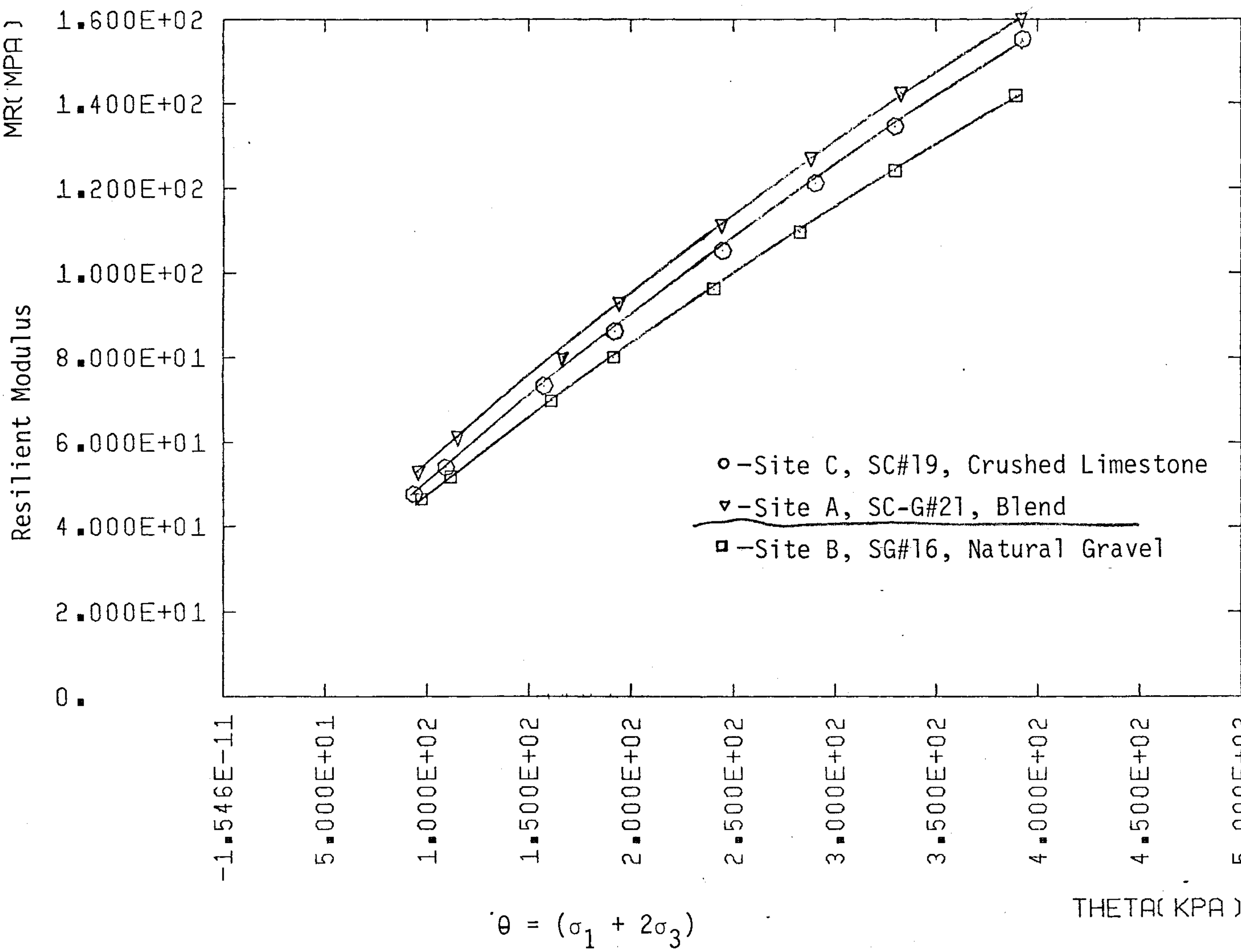

FIGURE 4-16 - Comparison of Typical Result of Resilient Modulus (M_R)
With Different Types of Granular A Materials
Crushed Limestone, Blend and Natural Gravel
(SC#19, SC-G#21 and SG#16),(Static Case)

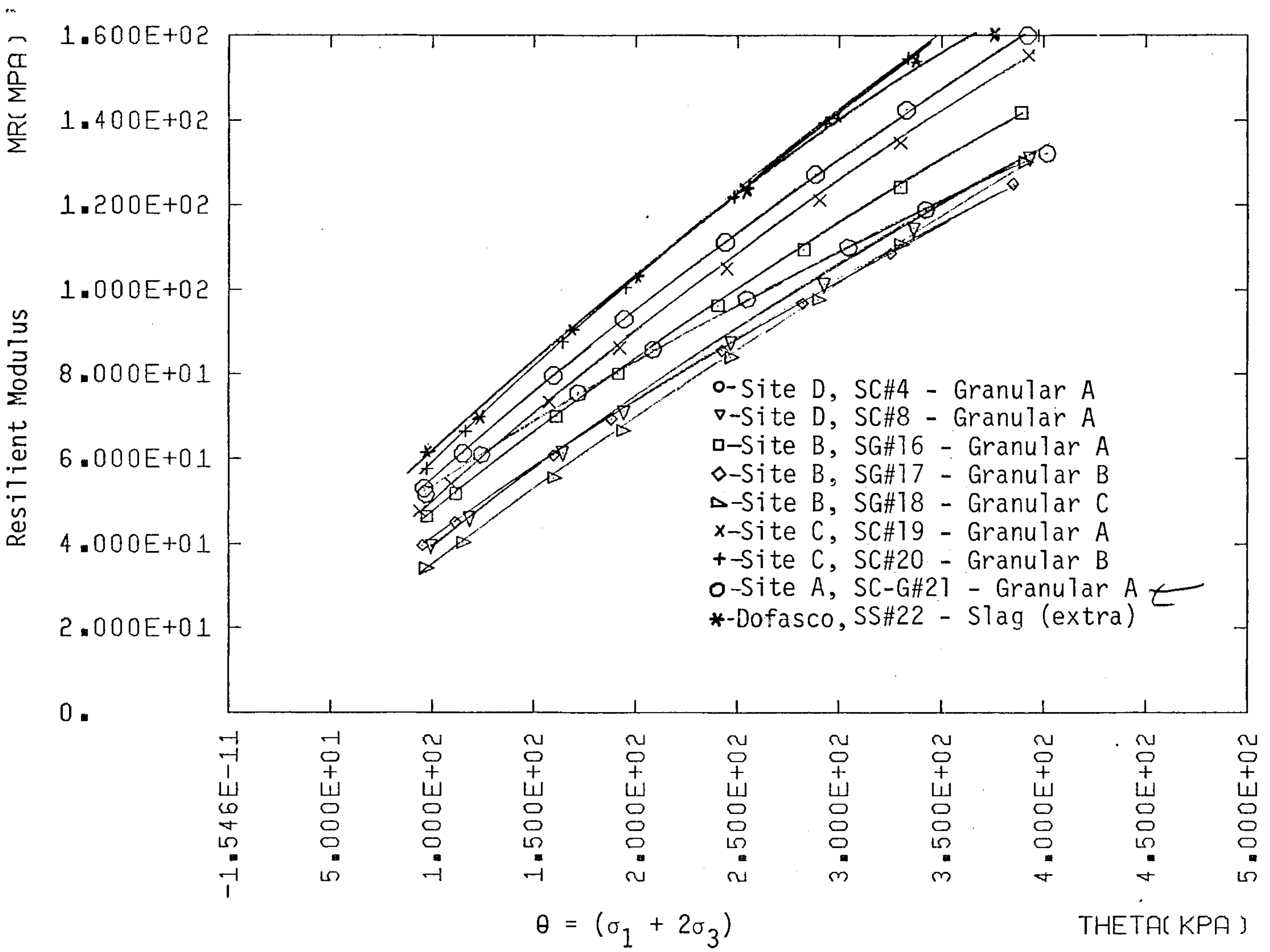

FIGURE 4-17 - Typical Results of Resilient Modulus (M_R) With Different Types of Granular Material in Unsaturated-Drained State (Static Case)

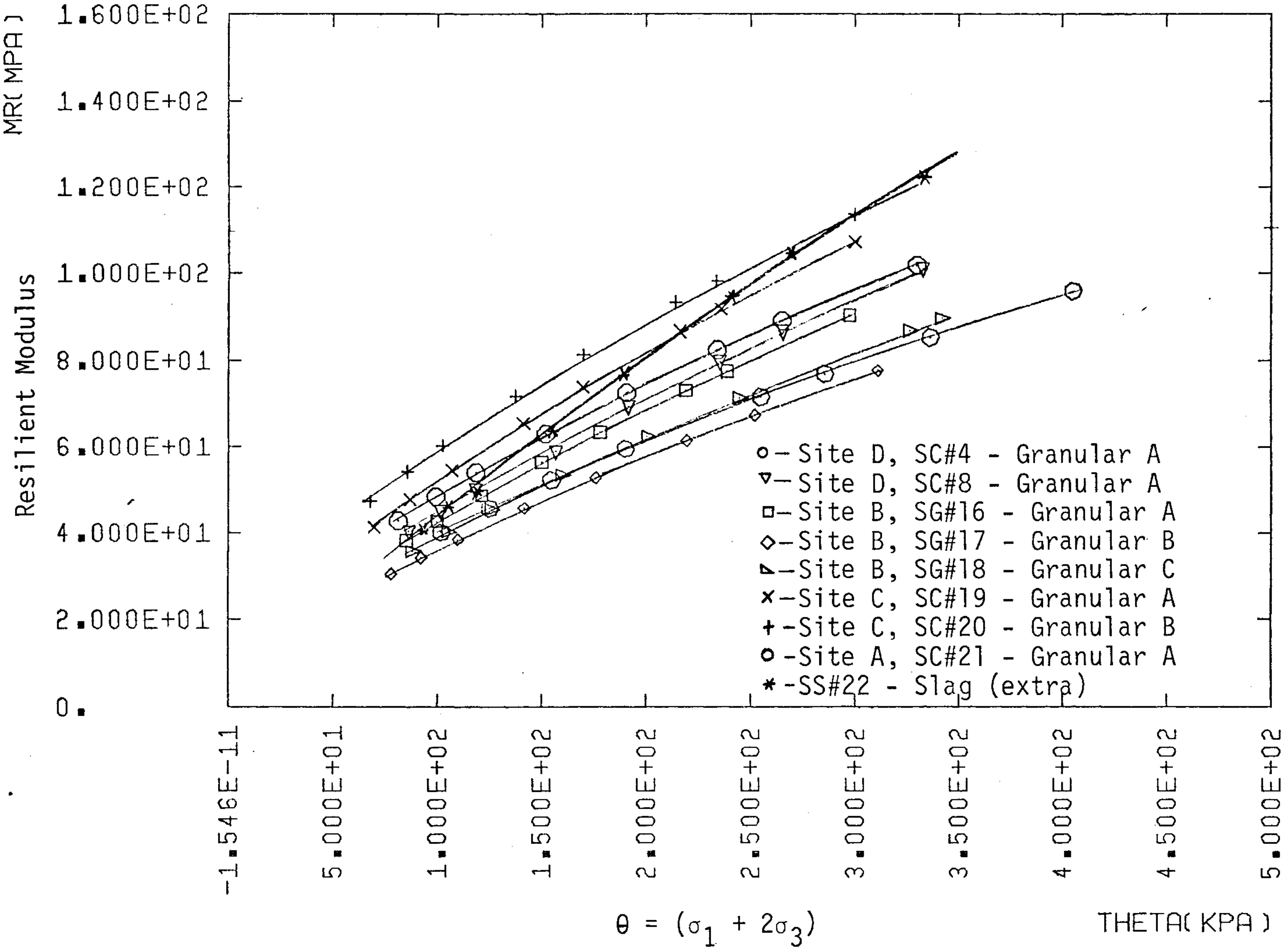

FIGURE 4-18 - Typical Results of Resilient Modulus (M_R) With Different Types of Granular Material in U-D State, (Dynamic Case)

TABLE 4-3

COMPARISON OF CBR AND M_R FOR DIFFERENT TYPES OF GRANULAR A MATERIAL

Location	Material Type	CBR	Resilient Modulus, MPa			
			σ_1 = 83 kPa	σ_3 = 21 kPa	σ_1 = 276 kPa	σ_3 = 69 kPa
			Dynamic	Static	Dynamic	Static
Site C	Crushed Limestone	112	50.490	56.730	108.080	150.890
Site B	Natural Gravel	44	42.660	51.724	90.196	141.789
Site A	Blend Materials	105	49.084	61.977	103.868	155.490

material, and natural gravel. On the other hand, although the results show that the Granular B crushed limestone (SC-20) M_R is slightly higher than the Granular A crushed limestone (SC-19), the moduli of Granular A are actually higher than those of Granular B when prepared under the same conditions (removing the particles whose size is greater than 19 mm (3/4") sieve number). The dynamic test data in Figure 4-18 show that the slag is associated with higher M_R values than the crushed limestone, the blended material and the natural gravel with somewhat lower value.

Figures 4-19 and 4-20 show the influence of the different drainage states for the same specimen (SC-8) in both the static and dynamic cases. The static test data in Figure 4-19 show that the unsaturated drained and undrained states are associated with a higher value of M_R than are the saturated (only partially in practice) drained and undrained states. Figure 4-20 for the dynamic loading case shows the different drainage states are ranked in the order of decreasing stiffness: unsaturated drained, saturated drained (not 100% saturation); unsaturated undrained; and saturated undrained (not 100% saturated). However, while the trend is as anticipated, the M_R for each case is not significantly different since 100% saturation was not achieved. However, the trends do indicate the potential stiffness loss with saturation.

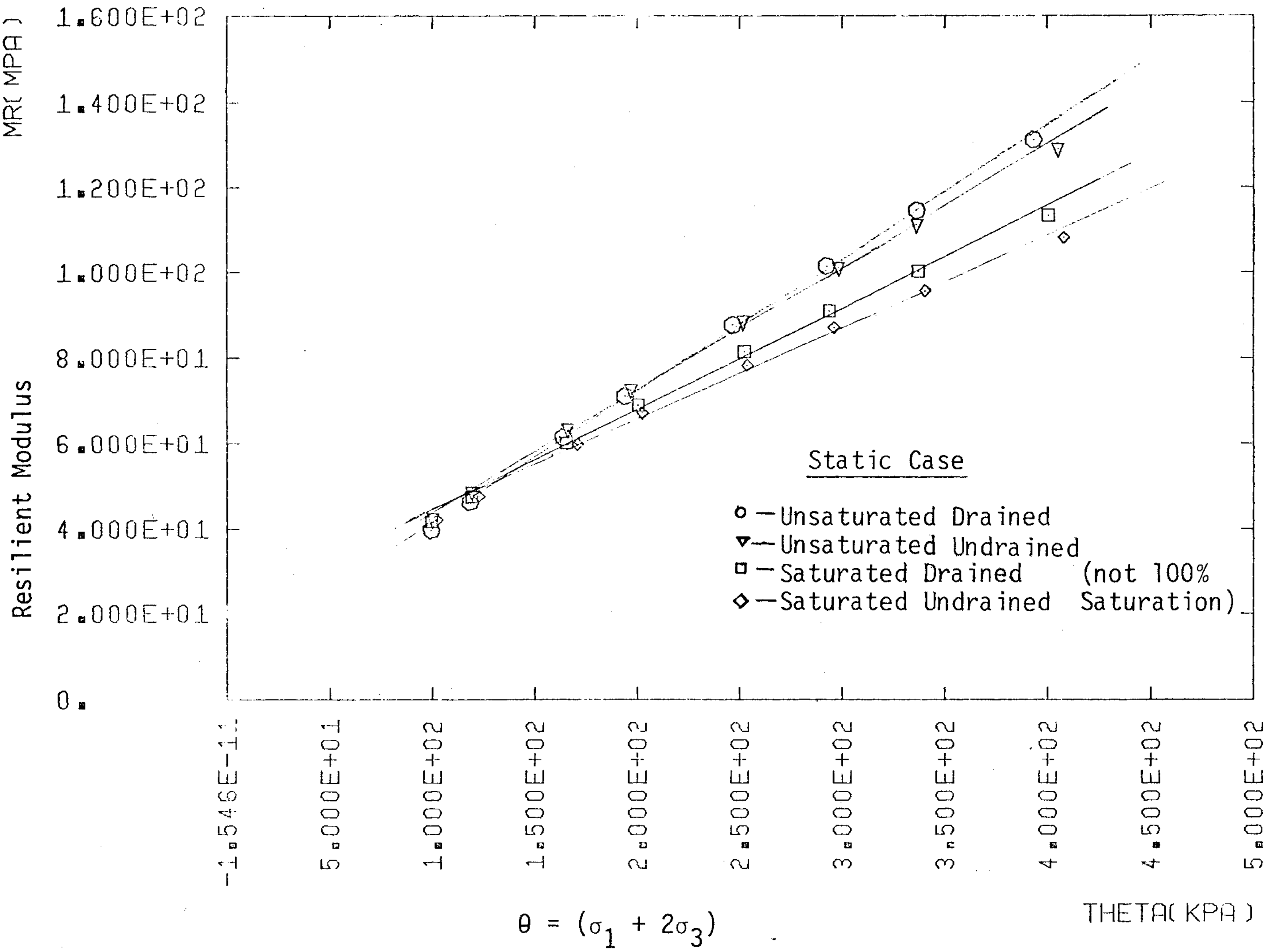

FIGURE 4-19 - Comparison of Typical M_R Results For Different Drainage State for Granular "A" Material - Crushed Limestone (SC-8, Static Case)

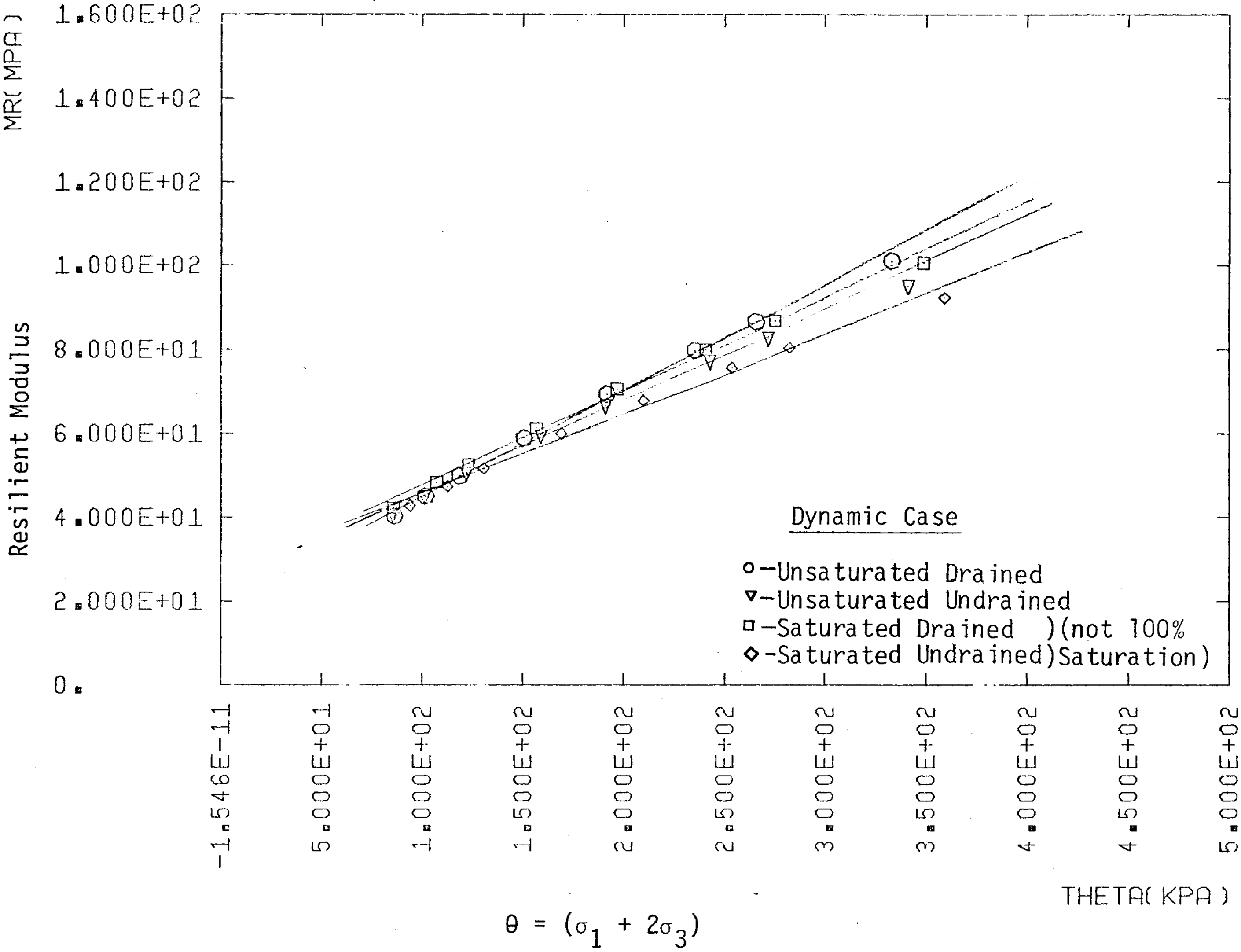

FIGURE 4-20 - Comparison of Typical M_R Results With Different Drainage Status for Granular "A" Material Crushed Limestone (SC-8, Dynamic Case)

In general, the aggregate grading only has a small effect on the resilient modulus. In this study, the influence of aggregate gradation was examined through the results summarized in Figure 4-21. Examination of Granular A - natural gravel material - was conducted in 4 different tests, with the preservation of the natural fines (4.5% passing 75 μm (#200) of the material in Test 1 (SG-12), the extraction of fines from the material in Test 2 (SG-13), the preservation of 5% fines content in Test 3 (SG-14) and the preservation of 10% fines content in Test 4 (SG-15). The resilient modulus increases slightly with increased fines content. Such an observation also holds true in the examination of the dynamic case.

In addition, results of the two types of test (constant and variable confining pressure) conducted on the crushed limestone and gravel materials indicate that the static case yields slightly higher values of M_R throughout the range of θ values than the dynamic case. The static test as plotted tends to "overestimate" the resilient modulus more than the dynamic test. The magnitude of the difference between the results of these tests depends upon the initial values of θ for which the values of M_R are calculated. It follows that differences in the results may or may not be significant to the pavement response to loading. The modulus throughout the granular layers is determined from the existing state of stress[23].

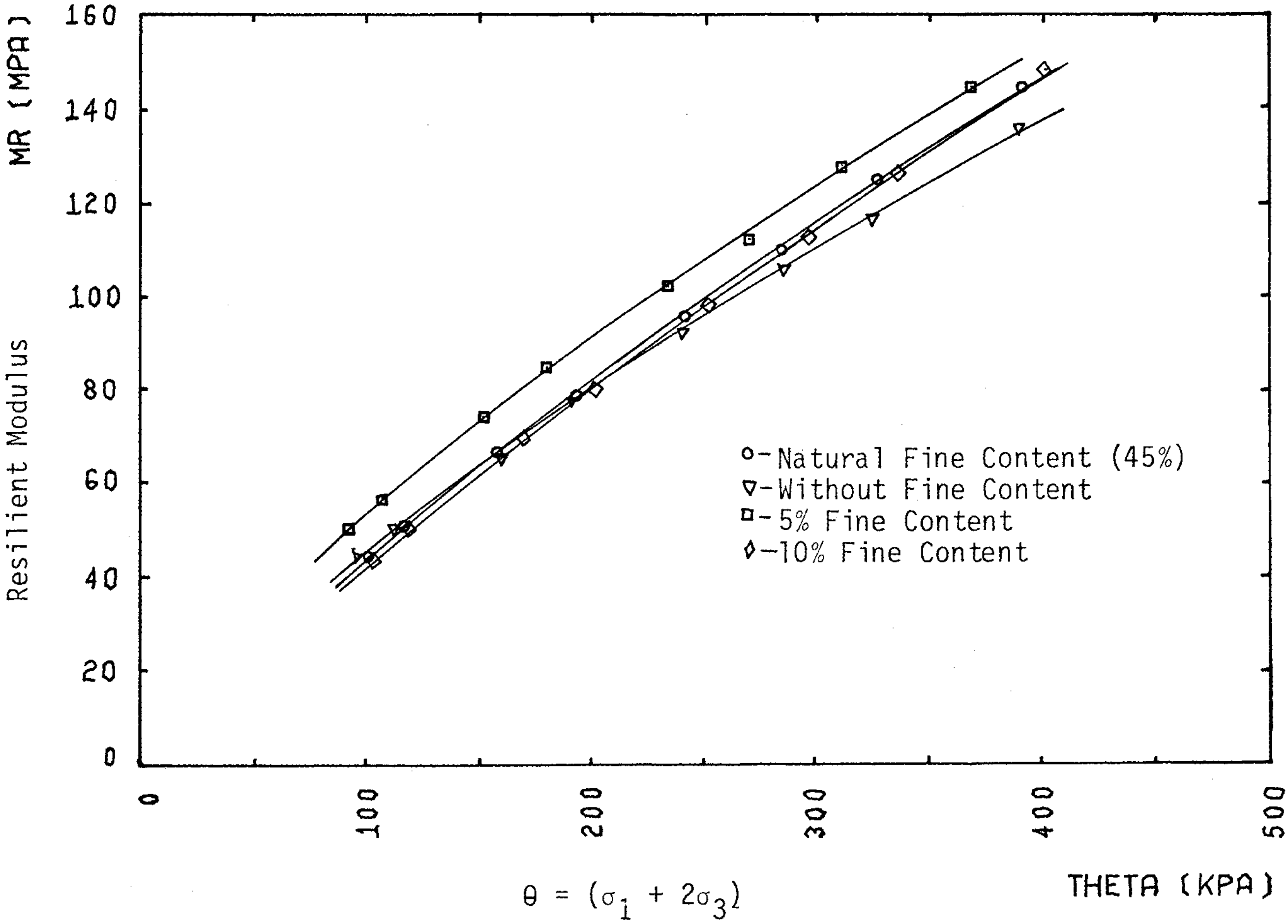

FIGURE 4-21 - Comparison of Typical Results for Resilient Modulus (M_R) with Different Aggregate Gradings (SG-12,SG-13,SG-14 and SG-15) Static Case

4.2.3 Comparison of Permeability Testing and CBR Test Results for Different Types of Granular Materials

Low, representative gradients of 0.3 were used for each permeability test specimen. For each material, two tests were run under the same conditions with the degree of saturation measured after the excess water was drained. The results of the permeability tests that were completed for the four different granular materials location are summarized in Table 4-4.

In general, higher permeability materials in granular pavement layers serve to prevent saturation and consequent strength loss. Table 4-5 clearly summarizes and describes the relationships between permeability, California Bearing Ratio (CBR) and resilient moduli for the aggregates tested. The Granular B and C permeabilities were somewhat lower, indicating a drainage disadvantage, and as indicated previously, somewhat lower stiffnesses.

4.3 SUBGRADE TESTING RESULTS

It was considered desirable to evaluate the resilient properties of a wide range of typical Ontario subgrade soils incorporated into the Ministry's OPAC system as outlined in Section 3.1.1. Before resilient modulus testing, general soil testing was completed on these subgrade soils as a logical starting point. Typical gradations and subgrade soil properties are given in Figure 4-22 and Table 4-6

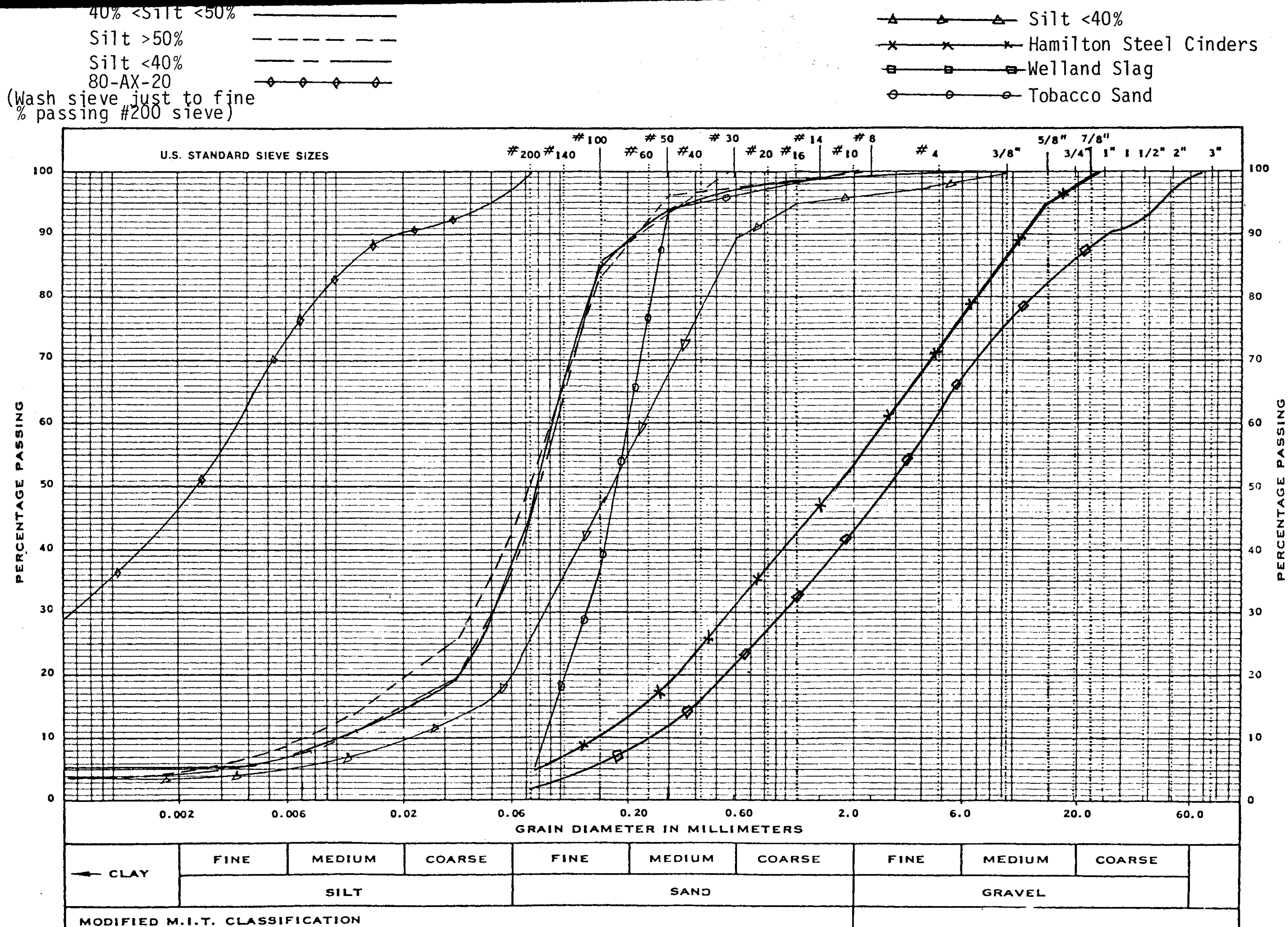

FIGURE 4-22 - MECHANICAL ANALYSIS

TABLE 4-4

PERMEABILITY OF SELECTED GRANULAR A, B AND C MATERIALS DETERMINED THROUGH THE USE OF LOW HYDRAULIC GRADIENTS ($i \cong 0.35$)

Site	Sample No.	Granular Type	Degree of Saturation	Specific Gravity	Dry Unit Weight kg/m³	k Average Permeability Coefficient cm/sec
D	SC#4	A	73	2.85	2310	1.23×10^{-3}
D	SC#5	A	78	2.86	2246	9.06×10^{-2}
D	SC#6	A	77	2.85	2284	5.97×10^{-2}
D	SC#7	A	72	2.79	2295	1.35×10^{-3}
D	SC#8	A	68	2.85	2420	3.54×10^{-2}
D	SC#9	A	71	2.85	2444	3.41×10^{-2}
D	SC#10	A	77	2.85	2440	1.2×10^{-3}
D	SC#11	A	75	2.85	2454	1.26×10^{-4}
B	SG#12	A	74	2.79	--	6.23×10^{-3}
B	SG#13	A	78	2.77	2358	8.58×10^{-2}
B	SG#14	A	77	2.78	2331	6.8×10^{-3}
B	SG#15	A	75	2.77	2326	7.96×10^{-3}
B	SG#16	A	75	2.78	2358	3.24×10^{-2}
B	SG#17	B	58	2.76	2098	2.8×10^{-4}
B	SG#18	C	80	2.76	2243	4.2×10^{-5}
C	SC#19	A	70	2.85	2267	3.3×10^{-3}
C	SC#20	B	59	2.85	2337	4.8×10^{-3}
A	SC#21	A	62	2.87	2273	6.25×10^{-3}
Dofasco	SS#22	A	50	2.93	--	3.0×10^{-3}

TABLE 4-5

SUMMARY OF TEST RESULTS FOR GRANULAR MATERIALS

Sample No.	Material	Degree of Saturation	Specific Gravity	Permeability ($i \cong 0.35$)	CBR	Modified AASHTO T180			Resilient Modulus (MPa)							
									σ_1=83 kPa (12 psi) σ_3=21 kPa (3 psi)				σ_1=276 kPa (40 psi) σ_3=69 kPa (10 psi)			
		Sr	GS	k cm/sec	%	$\gamma_{d(max)}$ kg/m³	ω_{opt} %	*	U-D	U-U	S-D	S-U	U-D	U-U	S-D	S-U
SC#4	Crushed Limestone, Upper Level (with natural fines) △D Canada Crushed G."A"	73	2.85	1.23×10^{-3}	80	2310	6.3	Dy	48.618	52.285	53.584	52.341	95.415	91.214	-	100.795
								St	56.629	60.252	59.019	63.498	136.142	132.204	130.413	125.788
SC#5	Crushed Limestone, Upper Level (without fines) △D G."A"	78	2.86	9.06×10^{-2}	104	2246	6.3	Dy	45.724	42.979	48.037	48.883	91.598	87.922	95.726	95.726
								St	57.485	50.123	42.770	50.164	119.041	111.677	130.769	106.630
SC#6	Crushed Limestone, Upper Level (with 5% fines) △D G."A"	77	2.85	5.97×10^{-2}	65	2284	6.0	Dy	39.970	40.919	44.310	44.666	80.021	77.610	86.525	89.470
								St	48.606	46.561	50.376	49.175	52.019	66.771	78.689	78.599
SC#7	Crushed Limestone, Upper Level (with 10% fines) △D G."A"	72	2.79	1.35×10^{-3}	75	2295	5.4	Dy	47.116	48.853	53.002	52.25	100.77	95.394	105.044	101.111
								St	61.344	62.410	59.789	61.261	146.834	140.988	147.808	131.049
SC#8	Crushed Limestone; Lower Level (with natural fines) △D G."A"	68	2.85	3.54×10^{-2}	64	2420	5.5	Dy	46.343	46.712	50.313	48.516	101.339	97.485	102.467	93.304
								St	49.877	50.086	50.542	49.588	130.755	128.943	117.897	110.194
SC#9	Crushed Limestone, Lower Level (without fines) △D G."A"	71	2.85	3.41×10^{-2}	73	2444	5.7	Dy	39.014	36.228	38.666	35.971	85.743	82.016	87.295	80.423
								St	47.434	42.835	45.489	36.9	134.739	120.030	134.497	100.966
SC#10	Crushed Limestone, Lower Level (with 5% fines) △D G."A"	77	2.85	1.2×10^{-3}	48	2440	5.8	Dy	40.934	42.867	40.583	44.137	88.283	33.325	89.059	90.49
								St	47.385	53.499	50.432	43.649	126.062	124.827	117.575	104.683

NOTES: Tests 1 to 3 were for Preliminary Tests (i.e., stress repetitions, duration, etc.)

* Dynamic Case - Variable Confining Pressure Test
Static Case - Constant Confining Pressure Test

** Extra Test

U-D --- Unsaturated Drain Test
S-U --- Saturated Undrain Test
△ --- See Figure 3-1 for Location

TABLE 4-5 - Cont'd

Sample No.	Material	Degree of Saturation Sr	Specific Gravity GS	Permeability ($i \cong 0.35$) k cm/sec	CBR %	Modified AASHTO T180 $\gamma_{d(max)}$ kg/m³	Modified AASHTO T180 ω_{opt} %	*	Resilient Modulus (MPa) σ_1=83 kPa (12 psi), σ_3=21 kPa (3 psi) U-D	U-U	S-D	S-U	σ_1=276 kPa (40 psi), σ_3=69 kPa (10 psi) U-D	U-U	S-D	S-U
SC#11	Crushed Limestone, Lower Level (with 10% fines) △D G."A"	75	2.85	1.26×10^{-4}	49	2454	5.0	Dy	53.836	45.192	45.767	46.092	80.707	79.492	96.889	86.974
								St	48.596	44.451	42.835	43.504	116.371	134.600	106.085	106.263
SC#12	Natural Gravel (Semi Crushed Pit Run) (with natural fines) △B Consolidated Sand and Gravel Co. G."A"	74	2.79	6.23×10^{-3}	36			Dy	46.891	48.575	56.350	49.784	108.455	103.086	87.618	79.491
								St	53.556	53.084	59.485	35.338	151.690	136.634	122.474	81.043
SG#13	Natural Gravel (without fines) △B G."A"	78	2.77	8.58×10^{-2}	42	2358	6.6	Dy	42.384	42.271	45.494	43.891	94.121	90.556	94.876	94.876
								St	49.472	46.643	49.101	44.584	137.164	124.004	141.667	123.453
SG#14	Natural Gravel (with 5% fines) △B G."A"	77	2.78	6.8×10^{-3}	38	2331	5.3	Dy	48.993	46.930	51.628	52.283	99.951	97.634	105.919	108.807
								St	57.611	53.633	58.164	47.594	142.163	143.352	144.655	133.980
SG#15	Natural Gravel (with 10% fines) △B G."A"	75	2.77	7.96×10^{-3}	35	2326	5.4	Dy	49.877	55.728	56.528	52.365	118.585	118.001	118.548	107.842
								St	53.056	55.984	56.117	49.383	147.433	142.251	153.729	125.012
SG#16	Natural Gravel (with natural fines) △B G."A"	75	2.78	3.24×10^{-2}	44	2358	6.5	Dy	44.228	43.643	50.065	44.611	92.187	88.393	101.265	92.610
								St	53.341	48.987	56.627	49.619	142.106	127.882	148.697	124.470
SG#17	Natural (with natural fines) △B G."B"	58	2.76	2.8×10^{-4}	42	2098	6.6	Dy	35.069	37.017	44.451	44.867	80.400	75.444	86.542	84.624
								St	44.867	47.325	47.885	45.505	123.068	116.919	130.841	124.485

TABLE 4-5 Cont'd

Sample No.	Material	Degree of Saturation Sr	Specific Gravity GS	Permeability (i ≅ 0.35) k cm/sec	CBR %	Modified AASHTO T180 $\gamma_{d(max)}$ kg/m³	Modified AASHTO T180 ω_{opt} %	*	Resilient Modulus (MPa) σ_1=83 kPa (12 psi) σ_3=21 kPa (3 psi) U-D	U-U	S-D	S-U	σ_1=276 kPa (40 psi) σ_3=69 kPa (10 psi) U-D	U-U	S-D	S-U
SG#18	Natural Gravel (with natural fines) B G."C"	80	2.76	4.2×10^{-5}	10	2243	6.8	Dy	41.720	43.910	48.005	50.345	94.54	97.31	101.268	102.473
								St	42.870	46.580	50.726	50.065	127.86	124.19	133.540	124.612
SG#19	Crushed Limestone (with natural fines) C Canada Crushed Co. G."A"	70	2.85	3.3×10^{-3}	112	2267	6.7	Dy	50.490	48.080	54.869	56.340	108.080	107.420	108.524	111.450
								St	56.730	54.060	58.674	49.300	150.890	147.680	149.853	123.550
SG#20	Crushed Limestone (with natural fines) C G."B"	59	2.85	4.8×10^{-3}	132	2337	5.9	Dy	55.017	52.535	58.546	57.152	116.165	111.245	117.258	117.132
								St	68.592	64.079	65.920	55.181	168.968	164.114	161.057	145.400
SG#21	Blend, (Crushed Stone & Natural Gravel Mix) A T.C.G. Materials Co. G."A"	62	2.87	6.25×10^{-3}	105	2273	7.1	Dy	49.084	48.140	50.008	50.698	103.868	99.371	101.285	99.159
								St	61.977	54.554	57.422	52.182	165.490	148.506	150.320	133.588
** SG#22	Air Cooled Slag Dofasco	50	2.93	3.0×10^{-3}	-	--	-	Dy	48.303	51.754	56.987	56.315	116.616	115.308	121.952	123.238
								St	66.134	66.794	66.951	63.273	175.100	165.191	170.236	168.546

TABLE 4-6

PROPERTIES OF TEST SPECIMENS

Specimen Number	Material	Maximum Dry Unit Weight kg/m^3	Optimum Moisture %	Degree of Saturation %	Specific Gravity
A	SILT <40%	2100	9.3	19.5	2.79
B	40% <SILT <50%	1812	11.4	20.6	2.72
C	SILT >50%	1887	10.8	20.3	2.73
D	LACUSTRINE CLAY (MTC 80-AX-20)	1685	21	35.4	3.0
E	LEDA CLAY	-	-	-	-
F	TOBACCO SAND	1674	14.3	-	-
G	WELLAND SLAG	1384	14	19.5	2.79
H	HAMILTON STEEL CINDERS	2155	10.5	21.8	2.91

TABLE 4-7

SUMMARY OF TEST RESULTS FOR SUBGRADE MATERIALS

No	MATERIAL		W %	RESILIENT MODULUS (kPa) σ_3=0 kPa, σ_1=20.7kPa (=3 psi)	RESILIENT MODULUS (kPa) σ_3=0 kPa, σ_1=41.4kPa (=6 psi)	RESILIENT MODULUS (kPa) σ_3=20.7kPa (=3 psi), σ_1=41.4kPa (=6 psi)	RESILIENT MODULUS (kPa) σ_3=20.7kPa (=3 psi), σ_1=62.1kPa (=9 psi)	CBR-100% AASHTO T99 Unsoaked %	CBR-100% AASHTO T99 Soaked %	COMPACTION AASHTO T99 γ_d(max.) kg/m³	COMPACTION AASHTO T99 W(opt.) %	Specific Gravity Gs	Degree of Saturation Sr%
H	Hamilton Steel Cinders	-2%	8.5	79.071	105.715	80.406	98.629	42	38	2154.7	10.5	2.91	21.8
		Opt.	10.5	86.975	115.241	93.183	104.230						
		+2%	12.5	69.298	80.514	131.665	139.342						
B	40%<silt<50%	-2%	9.4	25.071	23.757	23.150	23.697	20	2	1811.9	11.4	2.72	20.6
		Opt.	11.4	19.895	24.031	26.666	32.399						
		+2%	13.4	17.100	24.500	39.300	36.800						
A	Silt<40%	-2%	7.3	10.420	13.175	11.817	14.004	3	2	2100.2	9.3	2.79	19.5
		Opt.	9.3	8.433	11.190	13.385	12.722						
		+2%	11.3	7.876	-	9.470	-						
F	Tobacco Sand	-2%	12.3	11.895	-	13.033	11.429	2	18	1674.1	14.3	-	-
		Opt.	14.3	13.973	15.609	18.876	21.085						
		+2%	16.3	21.492	23.272	62.158	59.647						
C	Silt>50%	-2%	8.8	22.970	22.276	-	-	26	2	1887.2	10.8	2.73	20.3
		Opt.	10.8	18.440	21.015	27.885	27.429						
		+2%	12.8	21.500	25.400	31.000	34.300						
G	Welland Slag	-2%	-	-	-	-	-	33	31	1384.1	14.0	2.79	19.5
		Opt.	14.0	26.632	34.944	27.156	35.557						
		+2%	16.0	22.409	31.612	21.911	28.637						
D	MTC-80-AX-20 Clay	-2%	-	10.640	9.082	16.580	11.251	8	4	1685.3	21.0	3.0	35.4
		Opt.	9.1	28.000	16.400	26.700	-						
		+2%	-	-	-	-							
E	Leda Clay		σ_1=6.9kPa 4.608		σ_1=20.7kPa 4.922	σ_1=41.4kPa (=6 psi) 7.257		2	-	-	-	-	-

TABLE 4-8

TYPICAL DESIGN VALUES FOR ONTARIO CONSTRUCTION MATERIALS

	Material Type		Permeability (i ≅0.35) K cm/sec	CBR (Soaked) %	Poisson's Ratio ν_R	Dynamic M_R (MPa) (Unsaturated Drained)	
						σ_1=47kPa σ_3=21kPa	σ_1=271kPa σ_3=69kPa
Base and Subbase	Granular A	crushed stone	7.0×10^{-2}	95	0.30	41	108
		gravel	1.0×10^{-3}	42	0.30	40	100
	Granular B	crushed stone	4.0×10^{-3}	130	0.32	45	110
		gravel	2.0×10^{-4}	40	0.32	35	89
	Granular C	gravel	1.0×10^{-5}	?	0.33	35	89
	Slag A	-	3.0×10^{-3}	-	0.22	42	121
Subgrade	-		-	-	-	σ_1=21kPa σ_3=0 kPa	σ_1=62kPa σ_3=21kPa
	40% <silt <50%		-	2	0.35	20	32
	Silt <40%		-	2	0.35	9	13
	Silt >50%		-	2	0.35	19	28
	MTC80-AX-20 Clay		-	4	0.35	28	-
	Leda Clay		-	2	0.35	(σ_1=69kPa) 5	(σ_3=42kPa) 7
	Tobacco Sand		-	18	0.35	14	21
	Welland Slag		-	31	0.35	27	36
	Hamilton Steel Cinders		-	38	0.35	87	104

respectively. From this data, strategies were developed for making specimens that closely approximated compacted subgrades in the field. A summary of the soil testing data and resilient modulus results are given in Table 4-7.

4.4 SUMMARY OF TYPICAL DESIGN VALUES

The typical design values in Table 4-8 are suggested from the overall testing program. These results reflect the M_R and ν_R values observed at the lowest and highest stress level applied. It should be noted that the dynamic condition represents a repetitive loading situation (i.e., most likely to occur in field).

CHAPTER 5

SUMMARY AND CONCLUSIONS

5.1 SUMMARY

In the course of this study, the resilient modulus and resilient Poisson's ratio for a number of granular aggregates and representative subgrades soils were determined through repeated-loading triaxial tests in the laboratory. These materials were:

1. Crushed Limestone
   - Granular A
   - Granular B
2. Gravel
   - Granular A
   - Granular B
   - Granular C
3. A Blend of Crushed Limestone and Natural Gravel
   - Granular A
4. Subgrade soils typical to Southern Ontario.

A number of other parameters, notably permeability, were also determined where applicable.

Two types of repeated-load triaxial tests were applied to each of the materials.

1. Dynamic Confining Pressure Test - Chamber pressure varied simultaneously with the axial stress.

2. Static Confining Pressure Test - Chamber pressure held constant during application of the axial stress.

For both types of test, the predictive equations for the resilient modulus of the specimen were developed through a regression analysis of the test data. A highly significant correlation was found to exist between the state of stress in the specimen and the resilient parameters.

5.2 CONCLUSIONS

The major conclusions derived from the results of this study are:

1. The testing variable that most significantly affected the resilient response of the granular specimens was the applied state of stress (confining pressure). The stress dependent nature of the resilient parameters is characterized by the predictive equations for resilient modulus (M_R):

$$M_R = k_1 \, \theta^{k_2} \tag{2-4}$$

or

$$M_R = k_1' \, \sigma_3^{k_2'} \tag{2-3}$$

where: θ is the sum of the three principal stresses; and,

k_1, k_2, k_1' and k_2' are constants which result from the regression analysis of the test data.

Significantly, the "θ" equation for M_R yielded higher correlation coefficients and lower standard errors than the equation where M_R is based on σ_3. There is considerable inconsistency in the results of the σ_3 equation because it fails to account for the effects of the axial stress on M_R.

2. The resilient modulus increases slightly as the axial stress and principal stress ratio increase.

3. The state of stress is the most significant factor that affects the resilient properties of granular materials. Other less important factors are the degree of saturation, aggregate type, gradation and density.

4. The pulse duration of 0.1 second with a frequency of 20 cycles per minutes was satisfactory to determine the resilient modulus or resilient Poisson's ratio.

5. Aggregate gradation was shown to have only a small effect on the modulus. In general, the resilient modulus slightly increased with increased fines content.

6. Comparing the unsaturated and saturated state of the specimen, the resilient modulus decreased with increasing saturation.

7. Using higher permeability granular materials serves to avoid saturation and consequent strength loss.

8. For most applications, the effect of confining pressure in subgrade soils can be disregarded, but resilient properties of cohesive soils are greatly dependent on the magnitude of the deviator stress (repeated axial stress).

REFERENCES

1. Warren, H., and Dieckmann, W.L. "Numerical Computation of Stresses and Strains in a Multiple-Layered Asphalt Pavement System", California Res. Corp., Richmond, California, September, 1963.

2. Peutz, M.G.F., Jones, A., and Van Kempen, H.P.M. "Computer Program Bistro-Layered Systems Under Normal Surface Loads", Shell-Laboratorium, Amsterdam.

3. De Jong, D.L., Peutz, M.G.F., Korswagen, A.R., "Computer Program Bisar-Layered System Under Normal and Tangential Surface Loads", Shell-Laboratorium, Amsterdam, External Report, AMSR.0006.73.

4. The Asphalt Institute, "Computer Program Supplement to Full-Depth Asphalt Pavements for Air Carrier Airport," Manual Series No. 11A (MS-11A).

5. Gonsalves, Stanislaus E.M., "Determining the Resilient Modulus and Dynamic Poisson's Ratio of Asphaltic Concrete", Master of Engineering Thesis, McMaster University, Hamilton, Ontario, 1978.

6. Lee, M.A., "Resilient Modulus and Dynamic Poisson's Ratio of Asphaltic Concrete Mixes", Master of Engineering Thesis, McMaster University, Hamilton, Ontario, December 1976.

7. Cedergren, H.R., "Drainage of Highway and Airfield Pavements", John Wiley & Sons., Inc., New York, 1974.

8. The Asphalt Institute, "Drainage of Asphalt Pavement Structures", Manual Series No. 15 (MS-15), May 1966.

9. Jung, F.W., and Phang, W.A., "Elastic Layer Analysis Related to Performance in Flexible Pavement Design", Ministry of Transportation and Communications, Ontario, March 1975.

10. Carey, W.N. and Irick, P.E., "The Pavement Servicibility-Performance Concept", H.R.B. Bulletin, No. 250, 1960.

11. Pell, P.S., and Brown, S.F. "The Characteristics of Materials for the Design of Flexible Pavement Structures", Proc. Third Int. Conf. on the Struct. Des. of Asph. Pvts., London, England, 1972.

12. Pell, P.S., and Cooper, K.E. "The Effect of Testing and Mix Variables on the Fatigue Performance of Bituminous Materials", Proc. Assoc. Asph. Paving Technologists, 1975.

13. Dorman, G.M., and Metcalf, C.T. "Design Curves for Flexible Pavements Based on Layered System Theory", H.R.B. Record, No. 71, 1964.

14. Sargious, M., "Load Equivalency Factors for Highway Flexible Pavements", Pavement and Surfacings for Highway and Airports, Applied Science Publishers Ltd., London, 1975.

15. Westmann, R.A., "Stress Analysis by Finite Elements", Highway Research Record No. 228, 1968.

16. Seed, H.B., Mitry, F.G., Monismith, and Chan, C.K., "Prediction of Flexible Pavement Deflections from Laboratory Repeated Load Tests", National Co-operative Highway Research Program Report No. 35, 1967.

17. Hicks, R.G., "Factors Influencing the Resilient Properties of Granular Materials", Ph.D., of Engineering Thesis. University of California, Berkeley, 1970.

18. Dehlen, G.L. "The Effect of Non-Linear Material Response on the Behaviour of Pavements Subjected to Traffic Loads," Ph.D., Dissertation, University of California, Berkeley, 1969.

19. Haynse, J.H. and Yoder, E.J., "Effects of Repeated Loading on Gravel and Crushed Stone Base Material used in the AASHO Road Test," Highway Research Board, Record 39, 1963.

20. Kallas, B.F. and Riley, J.C., "Mechanical Properties of Asphalt Pavement Materials," Proceedings, Second International Conference on the Structure Design of Asphalt Pavements, Ann Arbor, 1967.

21. Thompson, O.O., "Evaluation of Flexible Pavement Behaviour with Emphasis on the Behavior of Granular Layers," Ph.D., Thesis, University of Illinois, Urbana, 1969.

22. Allen, J.J., "The Effects of Non-Constant Lateral Pressures on the Resilient Response of Granular Materials", Ph.D., Thesis. University of Illinois at Urbana-Champaign, May 1973.

23. Allen, J.J., and Thompson, M.R., "Significance of the Variable Confining Pressure Triaxial Test".

24. Kasianchuk, D.A., "Fatigue Considerations in the Design of Asphalt Concrete Pavements," Ph.D., Dissertation, University of California, Berkeley, 1968.

25. Emery, J.J., and Lee, M.A., "Permeability of Granular Base and Subbase Materials". Construction Materials Laboratory, Department of Civil Engineering and Engineer Mechanics, McMaster University, March 1979.

26. Yoder, E.J., and Witizak, M.W., "Principles of Pavement Design" Second edition, Wiley, New York, 1975.

27. Monismith, C.L., Seed, H.B., Mitry, F.G., and Chan, C.K., "Prediction of Pavement Deflections from Laboratory Tests" Virgina Highway Research Council, Department of Highways and the University of Virginia. Charlottesville, Virginia, August, 1967.

28. Jone, M.P., and Witczak M.N., "Subgrade Modulus on the San Diego Test Road" Transportation Research Record 641, Washington, D.C., 1977.

29. Nair, K. and C-Y Chang, "Flexible Pavement Design and Management" National Academy of Engineering 1973, p. 62-78.

30. Johnson, T.C., Cole, D.M. and Chamberlain, E.J., "Influence of Freezing and Thawing on the Resilient Properties of a Silt Soil Beneath an Asphalt Concrete Pavement", CRREL Report 78-23, U.S. Army Corps of Engineers, Hanover, New Hampshire.

31. Chou, Y.T., "Engineering Behaviour of Pavement Materials. State of the Art,", Report No. FAA-RD-77-37 Wes TRS-77-9. U.S. Army Engineer Waterways Experiment Station Soils and Pavement Laboratory, Final Report, February 1977.

32. Thompson, M.R. and Robnett, Q.L., "Final Report Resilient Properties of Subgrade Soils", UILU-ENG-76-2009, University of Illinois, Urbana, Illinois, June 1976.

33. Majidzadeh, K., Guirguis, H.R., and Joseph, G.S., "Fundamentals of Soil Compaction", Final Report EES 248, The Ohio State University, Columbus, Ohio 43210, June 1971.

34. Poulsen, J. and Stubstad, R.N., "Laboratory Testing of Cohesive Subgrade: Results and Implications Relative to Structure Pavement Design and Distress Models", The National Danish Road Laboratory, November 1977.

35. Cole, David M. "A Technique for Measuring Radial Deformation During Repeated Load Triaxial Testing", Canadian Geotechnical Journal Vol. 15, Aug. 1978, p. 426-429.

36. Transportation Research Board, NRC, "Test Procedures for Characterizing Dynamic Stress-Strain Properties of Pavement Materials" Special Report 162, Washington, D.C., 1975.

37. Dunlop, W.A. "Deformation Characteristics of Granular Materials Subjected to Rapid Repetitive Loading." Research Report 27-4, Texas Transportation Institute, 1966.

38. Chou, Y.T., "Engineering Behaviour of Pavement Materials Stage of the Art" U.S. Army Engineer Waterways Experiment Station Soil and Pavements Laboratory, February 1977.

APPENDIX

```
      PROGRAM TST (INPUT,OUTPUT,TAPE5=INPUT,TAPE6=OUTPUT)
      DIMENSION A(200),B(200)
      READ(5,1)C,RAD
C****WHERE C = WIDTH OF STRIP,RAD = RADIUS OF SPECIMEN ************************
    1 FORMAT(2F10.5)
      R = 0.01
C****WHERE R = DISTANCE FROM CENTRE OF DISK **********************************
      DR = 0.02
      DELA = 0.0
      DELB = 0.0
      ALPHA = C/(2.0*RAD)
      SN = SIN(2.0*ALPHA)
      CS = COS(2.0*ALPHA)
      TN = TAN(ALPHA)
      I = 0
      J = 0
    3 I = I+1
      J = J+1
      TOPA = (1.0-(R**2)/(RAD**2))
      BOTA = 1.0+2*(R**2)/(RAD**2)*CS+(R**4)/(RAD**4)
      TOPB = (1.0-(R**2)/(RAD**2))
      BOTB = (1.0+(R**2)/(RAD**2))
      A(I) = (TOPA/BOTA)*SN*DR
      B(J) = (ATAN((TOPB/BOTB)*TN))*DR
      DELA = DELA + A(I)
      DELB = DELB + B(J)
      R = R+ 0.02
      IF(R.GT.RAD)GOTO4
      GOTO3
    4 WRITE(6,5)C,RAD
    5 FORMAT(1H ,*WIDTH OF STRIP = *,1X,F10.5,1H ,*RADIUS = *,1X,F10.5)
      WRITE(6,2)DELA,DELB
    2 FORMAT(1H ,*DELA = *,1X,F12.8,1H ,*DELB = *,1X,F12.8)
      STOP
      END
```

APPENDIX A

COMPUTER PROGRAMME FOR CALCULATING DELA & DELB

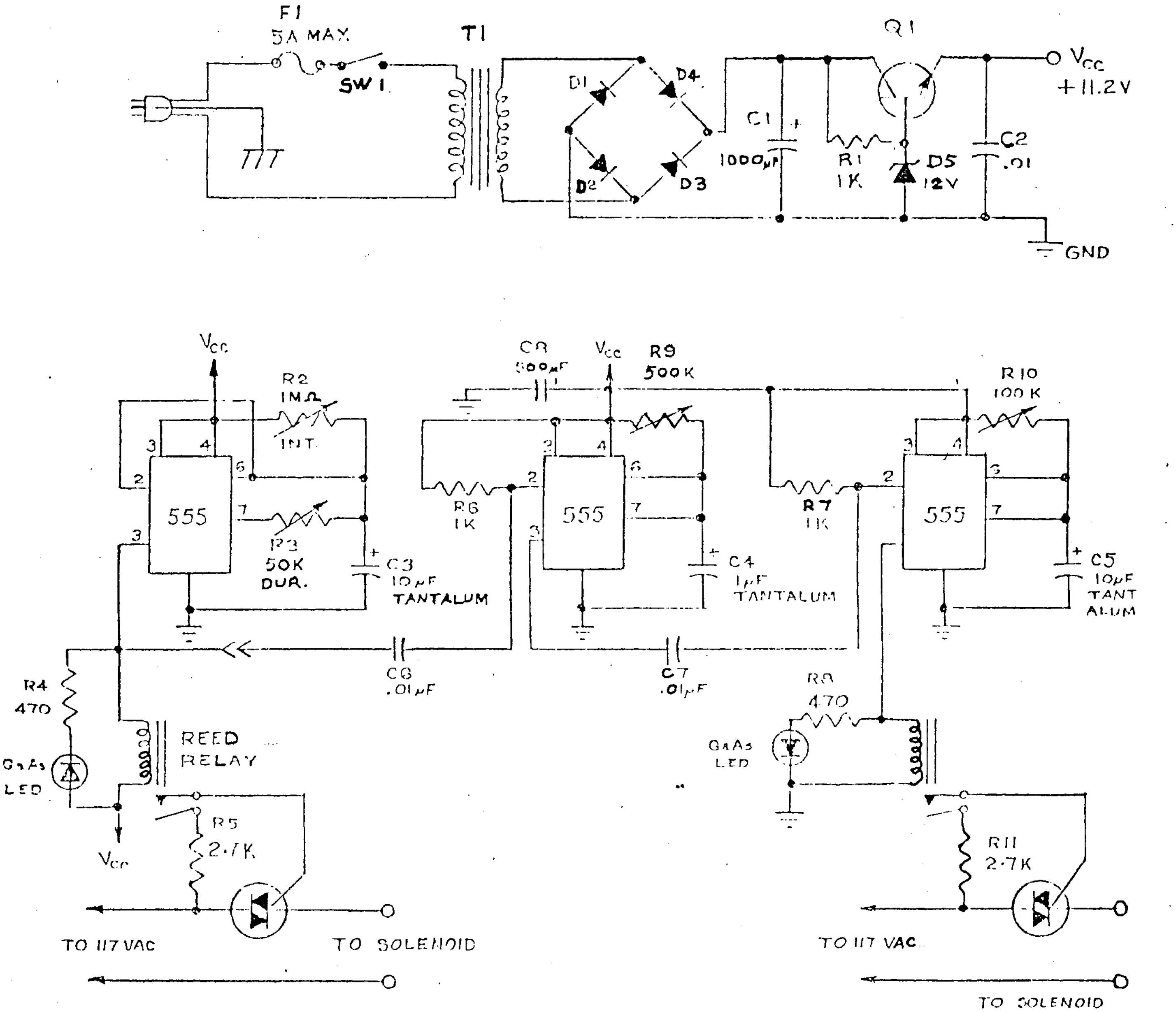

FIGURE A.1: CIRCUIT DIAGRAM FOR MAIN AND PHASE LAG TIMERS

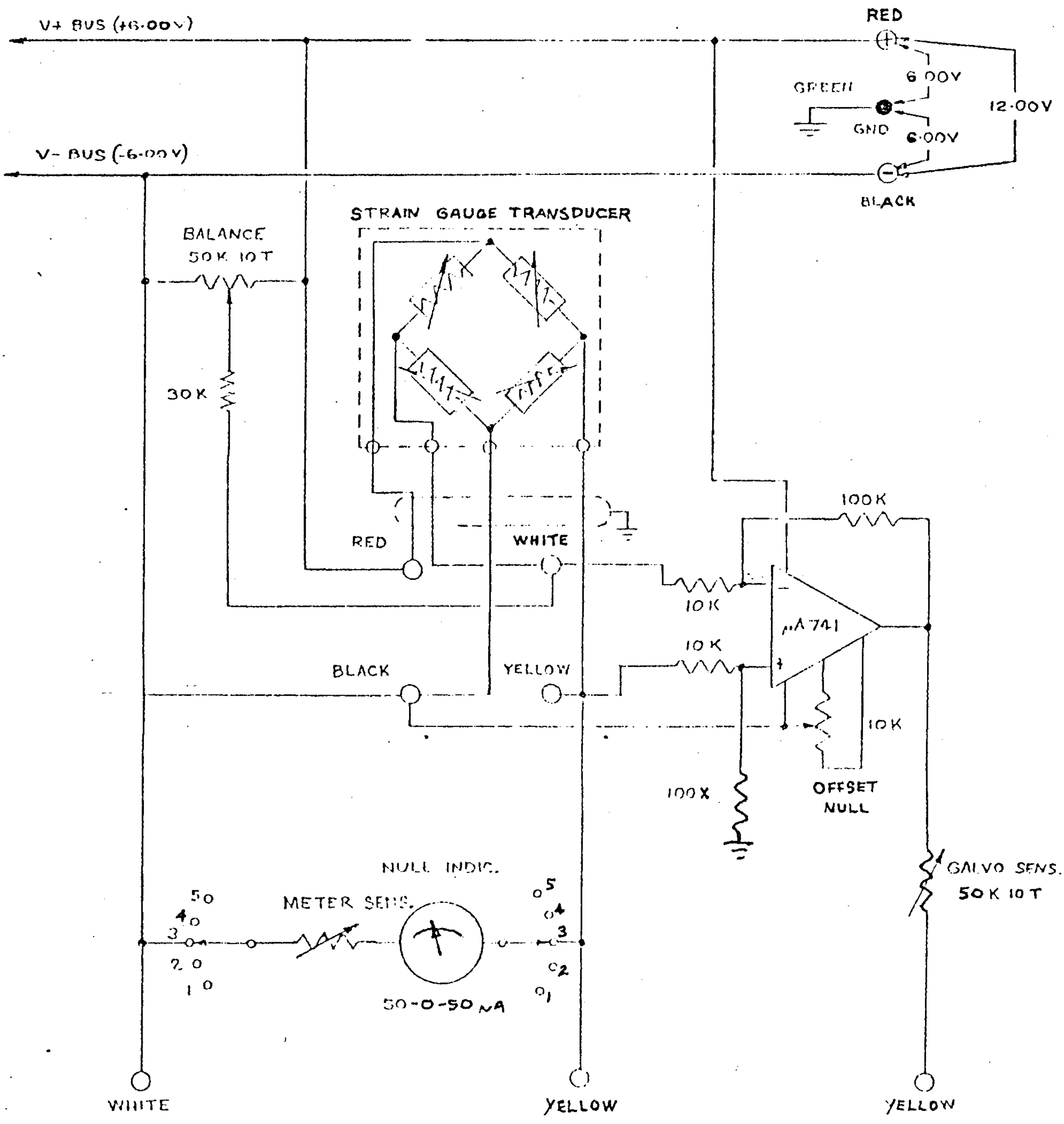

FIGURE A.2: DIAGRAM OF TYPICAL AMPLIFIER CIRCUIT FOR 5-CHANNEL AMPLIFIER